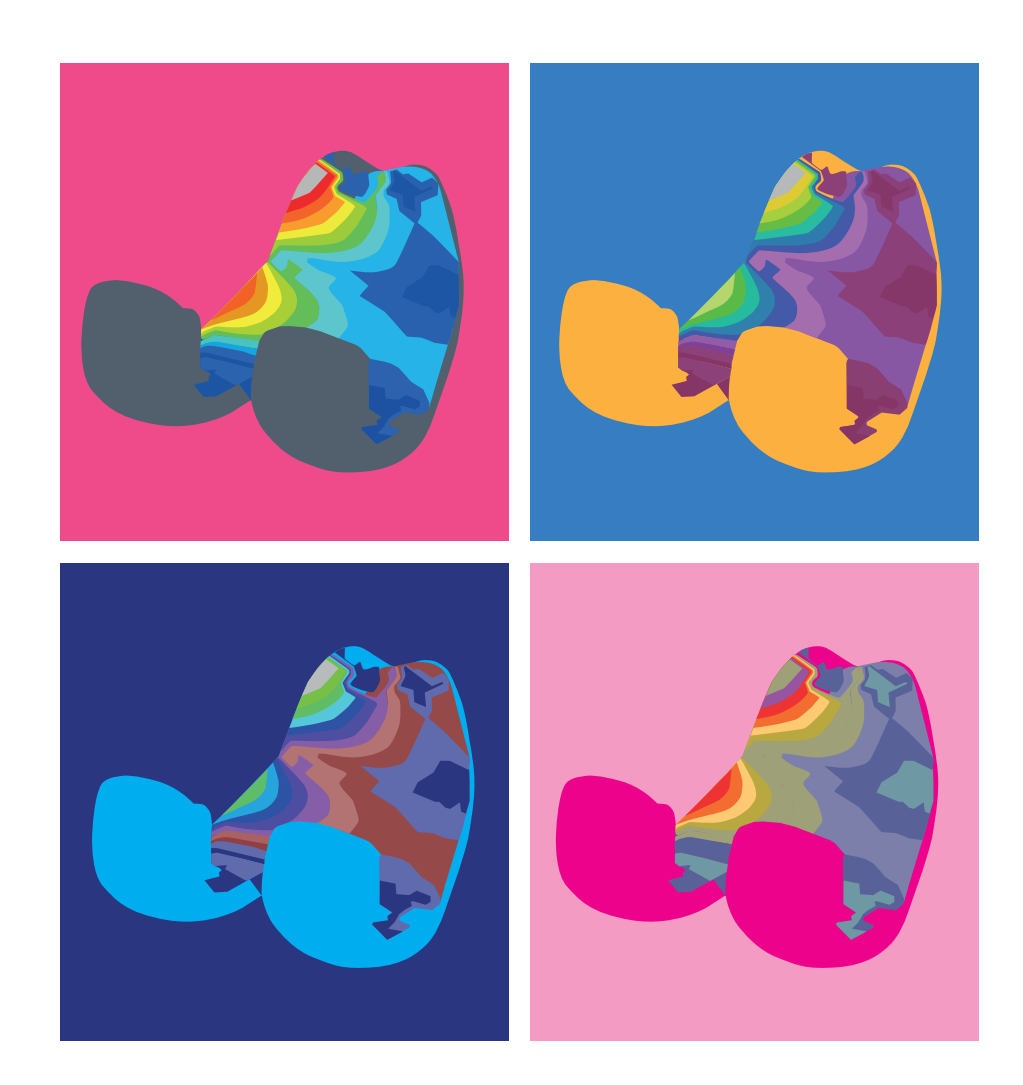
The PEEK performance

Analysis of the primary fixation of a novel cementless knee implant



Cornelia Elisabeth Post

RADBOUD UNIVERSITY PRESS

Radboud Dissertation Series

The PEEK performance Analysis of the primary fixation of a novel cementless knee implant **Cornelia Elisabeth Post**

Author: Corine Post

Title: The PEEK performance

Radboud Dissertations Series

ISSN: 2950-2772 (Online); 2950-2780 (Print)

Published by RADBOUD UNIVERSITY PRESS Postbus 9100, 6500 HA Nijmegen, The Netherlands www.radbouduniversitypress.nl

Design: Proefschrift AIO | Guus Gijben Cover: Proefschrift AIO | Guntra Laivacuma

Printing: DPN Rikken/Pumbo

ISBN: 9789493296602

DOI: 10.54195/9789493296602

Free download at: www.boekenbestellen.nl/radboud-university-press/dissertations

© 2024 Corine Post

RADBOUD UNIVERSITY PRESS

This is an Open Access book published under the terms of Creative Commons Attribution-Noncommercial-NoDerivatives International license (CC BY-NC-ND 4.0). This license allows reusers to copy and distribute the material in any medium or format in unadapted form only, for noncommercial purposes only, and only so long as attribution is given to the creator, see http://creativecommons.org/licenses/by-nc-nd/4.0/.

The PEEK performance

Analysis of the primary fixation of a novel cementless knee implant

Proefschrift

ter verkrijging van de graad van doctor aan de Radboud Universiteit Nijmegen op gezag van de rector magnificus prof. dr. J.M. Sanders, volgens besluit van het college voor promoties in het openbaar te verdedigen op

> donderdag 14 november 2024 om 12.30 uur precies

door

Cornelia Elisabeth Post
geboren op 8 juni 1993
te Hilversum

Promotor:

Prof. dr. ir. N.J.J. Verdonschot

Copromotoren:

Dr. ir. D.W. Janssen Dr. ir. T. Bitter

Manuscriptcommissie:

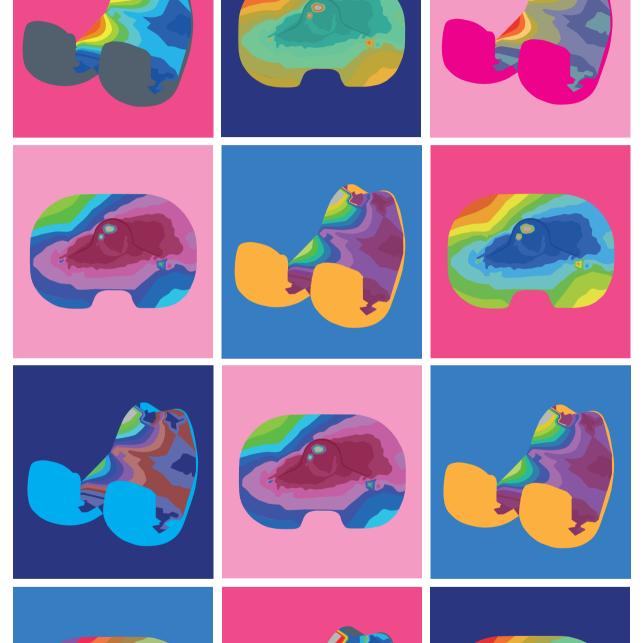
Prof. dr. ir. S.C.G. Leeuwenburgh

Prof. dr. P.C. Jutte (Universitair Medisch Centrum Groningen)

Prof. dr. ir. G.J. Verkerke (Universitair Medisch Centrum Groningen)

Table of contents

Chapter 1 General introduction and Thesis outline	7
Chapter 2 A FE study on the effect of interference fit and coefficient of friction on the micromotions and interface gaps of a cementless PEEK femoral component	19
Chapter 3 The sensitivity of the stiffness and thickness of a titanium inlay in a cementless PEEK femoral component to the micromotions and bone strain energy density	37
Chapter 4 The primary stability of a cementless PEEK femoral component is sensitive to BMI: a population-based FE study	53
Chapter 5 The sensitivity of the micromotions of a cementless PEEK tibial component to the interference fit and coefficient of friction	71
Chapter 6 The effect of patient related factors on the primary fixation of PEEK and titanium tibial components: a population-based FE study	85
Chapter 7 Summary and General discussion	103
Chapter 8 Nederlandse samenvatting	113
Appendix Research Data Management PhD Portfolio Curriculum Vitae Dankwoord	119



Chapter 1

General introduction and Thesis outline

Osteoarthritis

Osteoarthritis (OA) is a common disease of the joints in which the articular cartilage and subsequently the bone degenerates. It can be caused by ageing, overweight, lack of exercise, or following a traumatic incident [1]. OA causes pain and functional disability, and therefore has a significant effect on the quality of life [2]. OA generally is a multi-joint disease, with the knee joint being affected in around 80 percent of the cases [1] (Figure 1-1). Due to a combination of a population that is ageing and an increase in obesity, the incidence of OA has been rising over the past years and will continue to increase coming decades. Recent numbers show that, worldwide, around 250 million people are suffering from knee OA [3].



Figure 1-1. Healthy knee (left) and knee with osteoarthritis (right) [4].

Total knee arthroplasty

Total knee arthroplasty (TKA) is the most commonly used surgical treatment in patients suffering from advanced OA. The main objective of TKA is to relieve pain and to restore function of the knee joint by replacing the damaged articular surfaces of the distal femur and proximal tibia by femoral and tibial prosthetic components. The TKA usually consists of three components: a metal femoral component, a metal tibial tray and a polyethylene tibial insert that functions as bearing surface. A patellar button is optionally inserted to replace the damaged patellar cartilage (Figure 1-2).



Figure 1-2. Knee joint with total knee arthroplasty [5].

The success rate and clinical outcomes of TKA are usually very high. However, around 20% of the patients are dissatisfied after a total knee arthroplasty [6]. Nowadays, the main reasons for a revision TKA surgery are aseptic loosening and infection [7]. Other causes of TKA failure are instability and (patellofemoral) pain [7]. One of the potential causes of aseptic loosening is a lower bone density in the periprosthetic regions (Figure 1-3). Since bone remodels based on the forces acting on the bone, a reduction of the force acting on the bone will result in a lower bone density, according to Wolff's law [8]. The phenomenon in which the normal loading conditions in the knee are disturbed after TKA is called periprosthetic stress-shielding. Stress-shielding is caused by the high stiffness of the metal implant, which effectively shields the underlying bone from stresses of joint loading. Additionally, this phenomenon adversely affects the success of performing revision surgery. Due to the bone resorption caused by stress-shielding, the bone is less suitable for proper bone ingrowth on the implant interface. Therefore, early failure of the revision TKA may be caused.



Figure 1-3. Periprosthetic bone resorption after TKA [9].

Implant materials

CoCr and Titanium

During the past few centuries, numerous designs, techniques and materials have been developed to improve the TKA procedure. Current TKA components are usually made of metal alloys, such as cobalt-chrome (mainly used for the femoral component) or titanium (mainly used for the tibial component). Tibial inserts are mainly made of ultra high molecular weight polyethylene (UHMWPE). The quality of these UHMWPE tibial inserts has improved immensely over time due to better production and sterilisation methods. The CoCr to UHMWPE combination is considered a successful bearing coupling combination. However, one of the drawbacks of using CoCr is that it could potentially lead to metal sensitive reactions in the patient. Additionally, the high stiffness of CoCr leads to more stress-shielding compared to materials with a lower stiffness.

PEEK

Polyetheretherketone (PEEK) is a polymer with an increasing number of applications in the orthopaedic field due to its biocompatible and durable material properties (Table 1-1). One of the first applications of PEEK is as material for an isoelastic femoral stem to fulfil the need for hip implants with stiffness properties similar to bone [10-12]. Other medical applications of PEEK are spine cages, craniomaxillofacial implants and suture anchors [13-15]. PEEK also has become of interest for both the femoral and tibial component (Figure 1-4). PEEK has multiple potential advantages as application for TKA components (Table 1-1). At first, a PEEK TKA implant may be a solution for patients having a metal hypersensitivity as it provides a fully metalfree solution. Furthermore, diagnosis of the failing TKA may be improved as metal artefacts using imaging modalities as CT or MRI are avoided [16]. In addition, from a biomechanical point of view, the use of PEEK may reduce stress-shielding, as it has stiffness properties in the range of human bone [17, 18]. More explicitly, the elastic modulus of PEEK is 30 times smaller than the elastic modulus of titanium and 60 times smaller than the elastic modulus of CoCr (Table 1-1).



Figure 1-4. PEEK-OPTIMA[™] femoral component [19].

	DEEK	T'	C - C
	PEEK	Titanium	CoCr
Elastic modulus	3.6 GPa	113 GPa	210 GPa
Plain radiograph contrast	Radiolucent	Radiopaque	Radiopaque
CT studies	Compatible	May cause artifacts	May cause artifacts
MRI studies	Compatible	May cause artifacts	May cause artifacts
Cost of manufacturing	High costs and complexity of manufacturing	Low	Low
Thermoformability		Thermoformability allowing alteration of the shape to fit the normal contour of the bone	Thermoformability allowing alteration of the shape to fit the normal contour of the bone
Allergies	None reported	Metal allergy	Metal allergy

Table 1-1. Comparison of PEEK vs. Titanium vs. CoCr as biomaterial for orthopaedic implants [10].

Cemented vs cementless fixation

Fixation of TKA components can be achieved by using bone cement, in which the fixation is achieved by cement in between the implant and bone, or by a cementless, press-fit fixation, in which the long-term fixation is achieved by bone growing on- and into the implant surface (also known as osseointegration). Currently, the majority of TKA procedures are often performed using a cemented fixation, although cementless fixation is gaining popularity since it provides a more biological fixation [20]. Cementless fixation is mainly used for specific patient categories, i.e., young, physically active, or obese patients, in which cemented fixation has a high failure rate [21]. In cementless fixation a biological bond is created at the implant-bone interface, which has the potential to offer a lifelong fixation, while a cemented fixation by definition degenerates due to fatigue failure or cement fracture leading to gross loosening.

Primary fixation of cementless implants

Interference fit

To achieve an adequate long-term fixation, a stable primary fixation is required to facilitate osseointegration. The primary fixation is obtained during the implantation by compressive and shearing forces at the bone-implant interface. The compressive forces are generated at the interface by the so-called interference fit. During surgery the bone is cut slightly larger than the implant. The interference fit is referred to the dimensional difference between the implant and bone. During implantation, this interference fit causes compressive forces at the implant-bone interface. The pressfit fixation of the femoral component is obtained by cutting the distal side of the femur slightly larger than the internal implant dimensions. On the tibial side, the primary fixation is often achieved by changing the coating thickness.

The optimal interference fit is highly dependent on the specific knee implant design and the implant stiffness and has therefore been widely investigated in multiple studies for currently used metal knee implants [22, 23]. However, it is unknown whether this value needs to be adapted for PEEK knee implants, although it is expected that the lower stiffness of PEEK requires a different interference fit. Therefore, one of the objectives of this thesis was to evaluate the effect of varying the interference fit on the primary fixation of a cementless PEEK femoral and tibial component and compare this effect with a conventional cementless CoCr femoral component and cementless titanium tibial component.

Frictional properties

Friction at the interface causes shear forces that eventually provide a stable primary fixation. The shear forces depend on the coefficient of friction, which are largely defined by the roughness characteristics of the implant surface [24]. The shear forces are also influenced by the implant stiffness, as stiffer implants will provide higher compressive forces with the same interference fit. There are multiple possibilities to adapt the frictional properties of knee implants as these properties are greatly dependent on the implant design and implant material. The optimal coefficient of friction value for cementless PEEK knee implants is, however, currently unknown. Therefore, one of the objectives of this thesis was to evaluate the effect of varying the coefficient of friction on the primary fixation of a cementless PEEK femoral and tibial component and compare this effect with a conventional cementless CoCr femoral component and cementless titanium tibial component.

Micromotions

To quantify the primary fixation of knee implants, the relative shearing motions between the bone and the implant, and (dynamic) gaps at the interface can be quantified. The motions in the shearing direction are called the micromotions. After proper primary fixation, the bone will start growing in- and onto the implant surface after a few weeks to months. Several studies have reported that micromotion values of below 40 µm have been reported as favouring osseointegration [25]. During the implantation of the knee implant as well as during repeatable loading of the knee joint, motions in the direction normal to the implant interface may also occur. This may cause cyclic opening and closing of gaps at the bone-implant interface. When these motions become too large, the bone may be unable to bridge the boneimplant gap, inhibiting the bone ingrowth. Moreover, due to the opening and closing of the interface, fluid flow including transport of debris may occur, which can result in inflammation, osteolysis and loosening of the implant [26, 27].

This paragraph highlights the importance of the primary fixation for the overall success of knee implants. Therefore, one of the main objectives of this thesis was to investigate whether it is possible to obtain a same degree of primary stability with a PEEK knee implant as a CoCr and titanium knee implant.

Finite element analysis

Finite element (FE) studies can be used to evaluate the primary fixation by simulating micromotions at the bone-implant interface under varying conditions. One single FE model can be created with varying parameters on the design of the implant to test the influence of design-related parameters. On the other hand, population-based FE can be performed to obtain more information on outliers and risk factors within a population. Population-based analysis provide the opportunity to evaluate the effect of variability in patient characteristics, such as age, gender and BMI. Additionally, a population of FE models inherently includes variations in bone geometry, bone quality and loading conditions. As these characteristics may have implications for the primary fixation, it is essential to evaluate the primary fixation of TKA components in a population to obtain more robust results. Therefore, our objective was to investigate whether a knee implant with a new implant material (PEEK) would perform as robust in a full patient cohort as CoCr and titanium knee implants perform. Moreover, we wanted to identify the most critical patient characteristics for obtaining a proper primary fixation of cementless knee components. Fast computational methods and workflows are essential requirements to create a population of FE models.

Thesis outline

The aim of this thesis is to investigate the primary fixation of a cementless PEEK knee implant. The primary fixation can be influenced by multiple implant design related factors and patient characteristics. The outcomes of the studies in this thesis give a first insight into the application of cementless PEEK knee components in clinical practise. Chapters 2, 3 and 4 of this thesis study PEEK femoral components, while chapters 5 and 6 investigate PEEK tibial components.

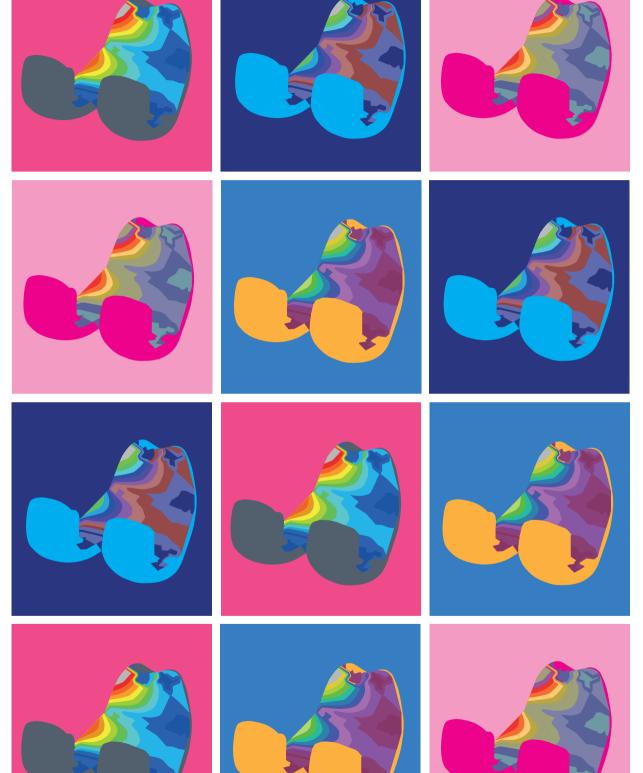
In **chapter 2**, the sensitivity of micromotions and gapping of a cementless PEEK femoral component to the interference fit and coefficient of friction was defined and compared with a cementless CoCr femoral component. Based on the findings of chapter 2, chapter 3 investigates the addition of a titanium inlay on the inner surface of a cementless PEEK femoral component. This titanium inlay may improve the primary fixation of cementless PEEK femoral components without losing its favourable characteristics of the reduction in stress-shielding compared to a conventional cementless CoCr femoral component. Therefore, the objective of this study was to investigate the effect of thickness and stiffness of a titanium inlay on the primary fixation, quantified by the micromotions, and on stressshielding, quantified by the strain energy density. Since the single-patient models of chapter 2 and 3 may not be representative of a whole population, we describe in chapter 4 a population study on the primary fixation of a cementless PEEK femoral component using an automated workflow. In this chapter we investigated the effect of simulated implant material (PEEK vs CoCr) on femoral micromotions within a population and whether these micromotions are influenced by gender, age and BMI and if there is a difference in response between PEEK and CoCr material.

In chapter 5, the influence of variations in interference fit and coefficient of friction on the primary fixation of a cementless PEEK tibial component is investigated. Finally, chapter 6 describes a population study on the primary fixation of a cementless PEEK tibial component. The same automated workflow of chapter 4 was used to create the models. In this chapter we investigated the effect of simulated implant material (PEEK vs titanium) on tibial micromotions within a population and whether these micromotions are influenced by gender, age and BMI and if there is a difference in response between PEEK and titanium material. Finally, the general results of this thesis are summarized and discussed in **chapter 7**. Additionally, these findings are associated with the clinical practise and the limitations of the methods applied in this thesis are discussed. Finally, future recommendations are described.

References

- Vos, T., C. Allen, and M. Arora, Global, regional, and national incidence, prevalence, and years lived with disability for 310 diseases and injuries, 1990-2015: a systematic analysis for the Global Burden of Disease Study 2015. Lancet, 2016. 388(10053): p. 1545-1602.
- Hunter, D.J. and S. Bierma-Zeinstra, Osteoarthritis. Lancet, 2019. 393(10182): p. 1745-1759. 2
- Vos, T., et al., Years lived with disability (YLDs) for 1160 seguelae of 289 diseases and injuries 1990-2010: a systematic analysis for the Global Burden of Disease Study 2010. Lancet, 2012. 380(9859): p. 2163-96.
- Figure 1-1. https://www.thepodiatryclinics.co.uk/blogs/does-running-or-jogging-helpsosteoarthritis-or-is-it-bad-for-knees.
- Figure 1-2. https://www.orthopediezuidlimburg.nl/knieprothese/. 5.
- 6. Price, A.J., et al., Knee replacement. Lancet, 2018. 392(10158): p. 1672-1682.
- 7 Australian Orthopaedic Association National Joint Replacement Registry - Hip, Knee & Shoulder Arthroplasty 2022 Annual Report. 2022.
- Huiskes, R., et al., Adaptive bone-remodeling theory applied to prosthetic-design analysis. Journal of Biomechanics, 1987. 20(11-12): p. 1135-1150.
- 9. Figure 1-3. https://orthoinfo.aaos.org/en/treatment/revision-total-knee-replacement/.
- 10. Mbogori, M., et al., Poly-Ether-Ether-Ketone (PEEK) in orthopaedic practice- A current concept review. Journal of Orthopaedic Reports, 2022. 1: p. 3-7.
- 11. Trebse, R., et al., Poor results from the isoelastic total hip replacement: 14-17-year follow-up of 149 cementless prostheses. Acta Orthop, 2005. 76(2): p. 169-76.
- 12. Huiskes, R., H. Weinans, and B. van Rietbergen, The Relationship Between Stress Shielding and Bone Resorption Around Total Hip Stems and the Effects of Flexible Materials. Clin Orthop Relat Res, 1992. 274: p. 124 - 134.
- 13. Kurtz, S.M., PEEK Biomaterials Handbook. 2012.
- 14. Chamberlain, K.A., et al., Wear properties of poly-ether-ether-ketone bearing combinations under zero and cross shear kinematics in total knee arthroplasty. J Biomed Mater Res B Appl Biomater, 2019. 107(2): p. 445-453.
- 15. Kurtz, S.M. and J.N. Devine, PEEK biomaterials in trauma, orthopedic, and spinal implants. Biomaterials, 2007. 28(32): p. 4845-69.
- 16. Nishio, F., et al., Radiopaque properties of polyetheretherketone crown at laboratory study. J Oral Biosci, 2023. 65(3): p. 253-258.
- 17. de Ruiter, L., et al., A preclinical numerical assessment of a polyetheretherketone femoral component in total knee arthroplasty during gait. J Exp Orthop, 2017. 4(1): p. 3.
- 18. Rankin, K.E., et al., Does a PEEK Femoral TKA Implant Preserve Intact Femoral Surface Strains Compared With CoCr? A Preliminary Laboratory Study. Clin Orthop Relat Res, 2016. 474(11): p. 2405-2413.
- 19. Figure 1-4. https://invibio.com/en/news/2021/first-peek-knee.
- 20. Swedish Knee Arthroplasty Register. 2019.
- 21. Uivaraseanu, B., et al., Highlighting the advantages and benefits of cementless total knee arthroplasty (Review). Exp Ther Med, 2022. 23(1): p. 58.
- 22. Sanchez, E., et al., No effect in primary stability after increasing interference fit in cementless TKA tibial components. J Mech Behav Biomed Mater, 2021. 118: p. 104435.

- 23. Sanchez, E., et al., The effect of different interference fits on the primary fixation of a cementless femoral component during experimental testing. J Mech Behav Biomed Mater, 2021. 113: p.
- 24. de Vries, E., et al., Predicting friction at the bone Implant interface in cementless total knee arthroplasty. J Mech Behav Biomed Mater, 2022. 128: p. 105103.
- 25. Engh, C.A., et al., Quantification of Implant Micromotion, Strain Shielding, and Bone Resorption With Porous-Coated Anatomic Medullary Locking Femoral Prostheses. Clin Orthop Relat Res, 1992. 285: p. 13-29.
- 26. Peters, P.C., et al., Osteolysis after Total Knee Arthroplasty without Cement. Journal of Bone and Joint Surgery, 1992: p. 864 - 876.
- 27. Du, Z., Z. Zhu, and Y. Wang, The degree of peri-implant osteolysis induced by PEEK, CoCrMo, and HXLPE wear particles: a study based on a porous Ti6Al4V implant in a rabbit model. J Orthop Surg Res, 2018. 13(1): p. 23.



Chapter 2

A FE study on the effect of interference fit and coefficient of friction on the micromotions and interface gaps of a cementless PEEK femoral component

Corine Post, Thom Bitter, Adam Briscoe, Nico Verdonschot, Dennis Janssen

Published in Journal of Biomechanics: https://doi.org/10.1016/j.jbiomech.2022.111057

Abstract

The use of a more compliant material, such as polyetheretherketone (PEEK), for a cementless femoral component is a potential solution to prevent aseptic loosening caused by peri-prosthetic stress-shielding. Long-term fixation of a cementless femoral component is achieved by a proper primary fixation of the bone-implant interface, which is influenced by the interference fit and frictional properties of the implant surface. This computational study investigates the sensitivity of micromotions and interface gaps of a cementless PEEK femoral component to the interference fit and coefficient of friction. 24 finite element models of the femur and femoral component were created with variations in implant material, interference fit and coefficient of friction. Peak loads of a jogging activity were applied on the models. Micromotions and interface gaps were both sensitive to the interference fit, coefficient of friction and implant material. Besides the implant material, the micromotions and interface gaps of the implant were most sensitive to the interference fit. Compared to the cobalt-chrome (CoCr) femoral component, the PEEK femoral component generated higher micromotions and interface gaps when equal interference fit and friction values were applied. However, increasing the interference fit and friction of the PEEK component resulted in micromotion values comparable with the CoCr component. This result leads to possibilities using cementless PEEK femoral components.

Introduction

Total knee arthroplasty (TKA) is a widely performed procedure to restore the knee joint after chronic knee disorders such as osteoarthritis. Despite the high success rates, aseptic loosening remains a problem for more than 30% of the patients having a single-stage revision operation according to the National Joint Registry of the United Kingdom 2021 [1]. One problem affecting long-term survival of TKA is stress-shielding of the peri-prosthetic bone [2]. Stress-shielding is the disturbance of the normal loading conditions in the knee after TKA, causing loss of bone stock around the knee implant, which eventually can result in aseptic loosening. One potential solution to prevent peri-prosthetic stress-shielding is the use of more compliant materials, such as polyetheretherketone (PEEK-OPTIMA™) [3]. PEEK already has some orthopaedic applications in the spine and cranio-maxillofacial surgery due to its biocompatible and durable material characteristics and due to its low indication for metal hypersensitivity [4, 5]. As the stiffness of PEEK is more similar to the stiffness of bone, the implantation of a PEEK implant may result in a more physiological distribution of the loads in the knee compared to conventional cobalt-chrome alloy (CoCr) femoral components [6].

While the majority of the femoral TKA components currently are fixated using bone cement, cementless femoral TKA has gained popularity over the last decades [7]. To achieve a long-term fixation of a cementless knee implant, a proper primary fixation of the bone-implant interface is of major importance. The primary fixation is obtained by the formation of compressive forces and subsequent shearing forces at the bone-implant interface during implantation. These compressive and shearing forces can be influenced by multiple factors, such as the interference fit, and the frictional properties of the implant surface. The interference fit refers to the dimensional difference between the prepared bone cuts and the implant. In cementless TKA, the femoral bone is cut slightly larger than the internal implant dimensions, resulting in a press-fit fixation after implantation. The coefficient of friction is determined by the roughness of the implant surface. In combination with the press-fit compressive forces, the roughness of the interface therefore affects the resistance to shear forces at the implant-bone interface, and thus plays a major role in the primary fixation of cementless TKA components.

The two most important parameters to quantify the primary fixation of a knee implant are the relative shearing motions between the bone and the implant, and (dynamic) gaps at the interface. Shearing motions parallel to the interface, also referred to as micromotions, below a threshold of 40 µm have been reported as favouring osseointegration [8]. Additionally, too large micromotions will result in the formation of fibrous connective tissue, which inhibits osseointegration.

During the implantation and cyclic loading of the knee joint, also relative displacements in the direction perpendicular to the interface may occur, causing opening and closing of gaps at this interface. When these motions in the normal direction become too large, bone is unable to bridge the bone-implant gap [9]. Moreover, cyclic opening and closing of the implant-bone interface may result in fluid flow and debris transport into the interface, potentially leading to inflammatory reactions, osteolysis and implant loosening [10, 11].

The use of a more flexible material such as PEEK for a femoral component may have implications for implant-bone micromotions and the potential opening and closing of the interface gaps. It is therefore important to investigate the optimal values of the interference fit and coefficient of friction. Consequently, the first objective of this study was to define the sensitivity of micromotions, gapping and gap volume change of a cementless PEEK femoral component to the interference fit and coefficient of friction and to compare these outcomes to a cementless CoCr femoral component, using finite element (FE) simulations. In addition, based on this sensitivity analysis, we assessed which parameter values of the interference fit and coefficient of friction of a cementless PEEK femoral component will result in a similar biomechanical behaviour as a cementless CoCr femoral component.

Materials and methods

3D models of the femur and femoral component were created based on previously developed 3D bone models [12]. The 3D model of the femur was created by segmenting cadaveric CT-data of a right femur (62 years, male) using medical imaging software (Mimics 14.0, Materialise, Leuven, Belgium). The CAD model of a size C cementless femoral knee implant was provided by the manufacturer (Freedom knee, Maxx Orthopedics, Norristown, PA, USA). The femoral bone cuts were prepared based on the inner surface of the femoral component using modelling software (SimLab 2019.1, Altair Engineering, Troy, MI, USA). The correct placement of the femoral component was confirmed by an experienced orthopaedic surgeon. FE mesh models were created using meshing software (HyperMesh 2017, Altair Engineering, Troy, MI, USA). Tetrahedral elements with an edge size of 2.5 mm were used for the implant and bone meshes, based on previous mesh convergence

studies [12]. This resulted in 67,948 elements for the femur and 16,255 elements for the femoral implant.

To account for permanent deformation of the bone resulting from the press-fit fixation, bone was modelled as an elastic-plastic material [12]. The assignment of the material properties of the bone was performed using a calibration phantom (0, 50, 100, 200 mg/ml calcium hydroxyapatite, Image Analysis), which was scanned along with the cadaveric limb. Using this calibration phantom, the Hounsfield Units of the CT scan were converted to calcium values. Subsequently, these calcium values were converted to the Young's modulus, which is specifically for this bone in a range of 0–19 GPa [13]. Typical Young's modulus values for trabecular and cortical bone are in a range of 5–20.5 GPa [14].

The implant was modelled as an elastic isotropic material. The Young's modulus for PEEK was assumed to be 3.7 GPa as provided by the manufacturer. To compare the results to the currently used knee implant systems, models with the material properties of CoCr alloy (210 GPa) were also created.

A single-sided touching contact algorithm was applied to model the interaction between the femur and the implant. The friction was modelled using a Coulomb bilinear (displacement) friction model. Three different values for the coefficient of friction were analysed to evaluate the extreme and average coefficient of friction values [15].

The interference fit was defined through the contact algorithm and applied at the anterior, posterior, distal, and chamfer sides of the bone-implant interface. Based on common values of current TKA systems, the interference fit values were taken in a range from 250 to 1000 µm, with the latter representing an extreme interference fit value [16, 17]. The interference fit was linearly increased during a simulated implantation phase, in 50-120 increments. Subsequent to this implantation phase, the loads were applied during the loading phase. The interference fit was kept constant at the maximum value during the loading phase.

The proximal side of the femur was completely constrained in all directions. Two axial point loads were applied on the medial and lateral condyles, representing the tibiofemoral contact forces. The loads were derived from a jogging activity of the Orthoload dataset, taken at the peak load during the activity [18]. The jogging activity was chosen as the most demanding loading condition from the dataset, which combined with the frictional implant-bone interface represented the worst-case scenario for the implant comparisons. The division of the axial load into the medial and lateral loads was calculated using the medial force ratio, also taken from Orthoload [19]. The loads were applied in an incremental manner, using six increments to go from an unloaded situation to the maximal load, and six increments to go back to the unloaded situation, resulting in 12 increments in total for one loading cycle. To allow for (numerical) settling, the loading cycles were repeated four times for each model, with the results being taken from the final (fourth) cycle [12].

The two implant material models were simulated with all variations of interference fit and coefficient of friction values, resulting in 24 FE models in total (Figure 2-1). All 24 FE models were analysed using linear analyses (MSC.Marc2018, MSC. Software Corporation, Santa Ana, CA, USA).

As outcome measures for the 24 simulations, we calculated the relative motion between the implant and bone in the shear direction, referred to as micromotions, and the relative motion in the normal direction, referred to as the gap.

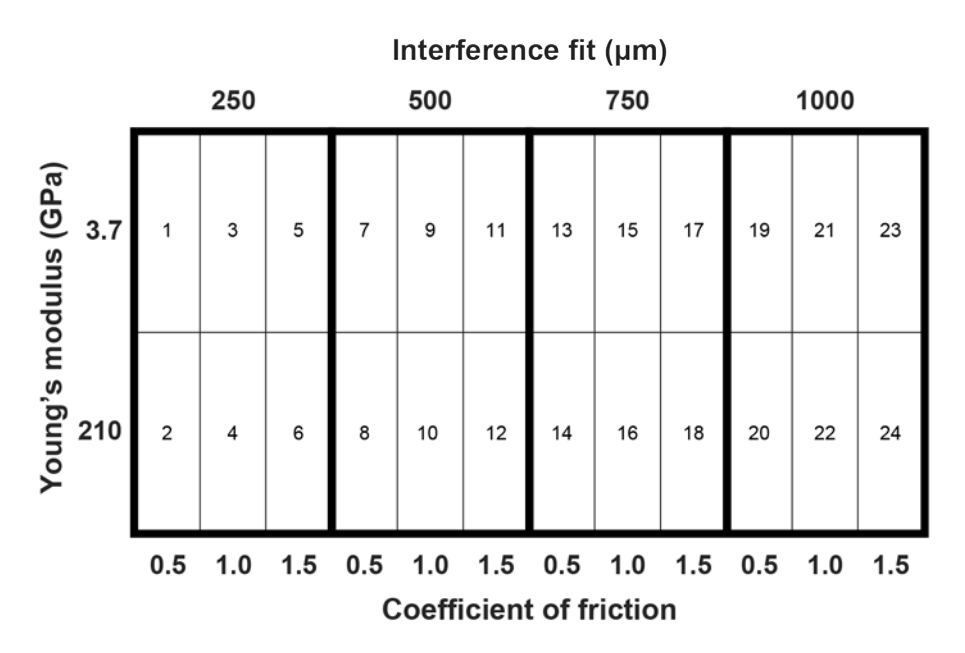


Figure 2-1. Variable values of the 24 FE models.

Micromotions

The micromotions were defined as the relative displacements between the implant and the bone. For each contact node on the implant interface, the corresponding closest contact face of the bone was detected. The relative motion in the shear direction between the implant contact node and the bone contact face was calculated as the largest possible distance during the loading cycle. Areas of the pegs and those areas that had a large normal gap, for example due to overhang at the anterior flange, were excluded from the presented results. For each simulation, the 95th percentile of the maximum resulting micromotions was obtained. The resulting micromotions are defined as the largest displacement of an implant contact node during a full loading cycle. The maximum resulting micromotion value was equal to the maximum value of the resulting micromotions at a specific moment in time, determined amongst all included implant contact nodes. The 95th percentile of the maximum resulting micromotions was taken to remove the nodes which potentially represented outliers.

Interface gaps

By monitoring the displacement of the implant relative to the bone in the direction perpendicular to the interface, the effects of the design parameters on gapping at the interface were quantified. We calculated the maximum absolute gap, being the largest distance between the implant and bone, but also determined the change in this gapping distance multiplied by the nodal surface area, which represented the dynamic change in volume between the implant and the bone, referred to as the gap volume change.

The absolute gap and gap volume change were visualized at the interface of the implant and calculated to facilitate a quantitative comparison between the different model configurations. The interference fit applied through the contact algorithm created an artificial gap, and was therefore subtracted from the interface gap values.

Statistical analyses

Pearson correlations were obtained to evaluate statistical significance of the interactions between the micromotions and interface gaps and the interference fit, coefficient of friction and implant material. A linear regression analysis was performed in which micromotions, actual gap, and gap volume change were taken as dependent variables, and interference fit, coefficient of friction and implant material as independent variables.

Results

Micromotions

Distinct differences were seen in the micromotion distributions between the PEEK and CoCr models. Both PEEK and CoCr models with an interference fit of 250 µm showed the largest resulting micromotions at the medial side of the anterior flange (Figure 2-2 A-D). The posterior condyles also showed relatively large resulting micromotions, while the smallest resulting micromotions were found at the distal side. The PEEK and CoCr models with an interference fit of 1000 um showed the highest micromotions at the medial side of the implant interface (Figure 2-2 E-H).

Micromotions depended on interference fit, coefficient of friction and implant material. The largest maximum resulting micromotions (92.7 µm) occurred in the PEEK model with low interference fit and low coefficient of friction (Figure 2-3). Increasing the interference fit and coefficient of friction resulted in lower resulting micromotions. The resulting micromotions were mainly sensitive to the implant material (r = -0.732) and less sensitive to the interference fit (r = -0.460) and coefficient of friction (r = -0.262). All three correlations were statistically significant (p < 0.05).

Interface gaps

The gap distributions were similar after the implantation phase and the 4th loading cycle for both PEEK and CoCr models (Figure 2-4 A-D), although the gap values were much lower in the CoCr models. The highest actual gaps were found at the anterior flange for all models, under all conditions.

The largest actual gap can be found at the PEEK model with a high interference fit and low coefficient of friction (Figure 2-5). Interface gaps depended on the interference fit, coefficient of friction and implant material. Increasing the interference fit resulted in an increasing actual gap for the PEEK models. However, the CoCr models showed a decrease of the actual gap when increasing the interference fit from 250 um to 750 um. The CoCr models with an interference fit of 1000 µm showed an increase of the actual gap compared to the CoCr models with an interference fit of 500 µm and 750 µm. Only weak correlations were found between the gap and the interference fit (r = 0.314) and between the gap and coefficient of friction (r = -0.149). The CoCr models resulted in smaller gaps than the PEEK models, with the gap being most sensitive to the implant material (r = -0.856). Only the correlations between the implant material and the gap and the interference fit and the gap were statistically significant correlations (p < 0.05).

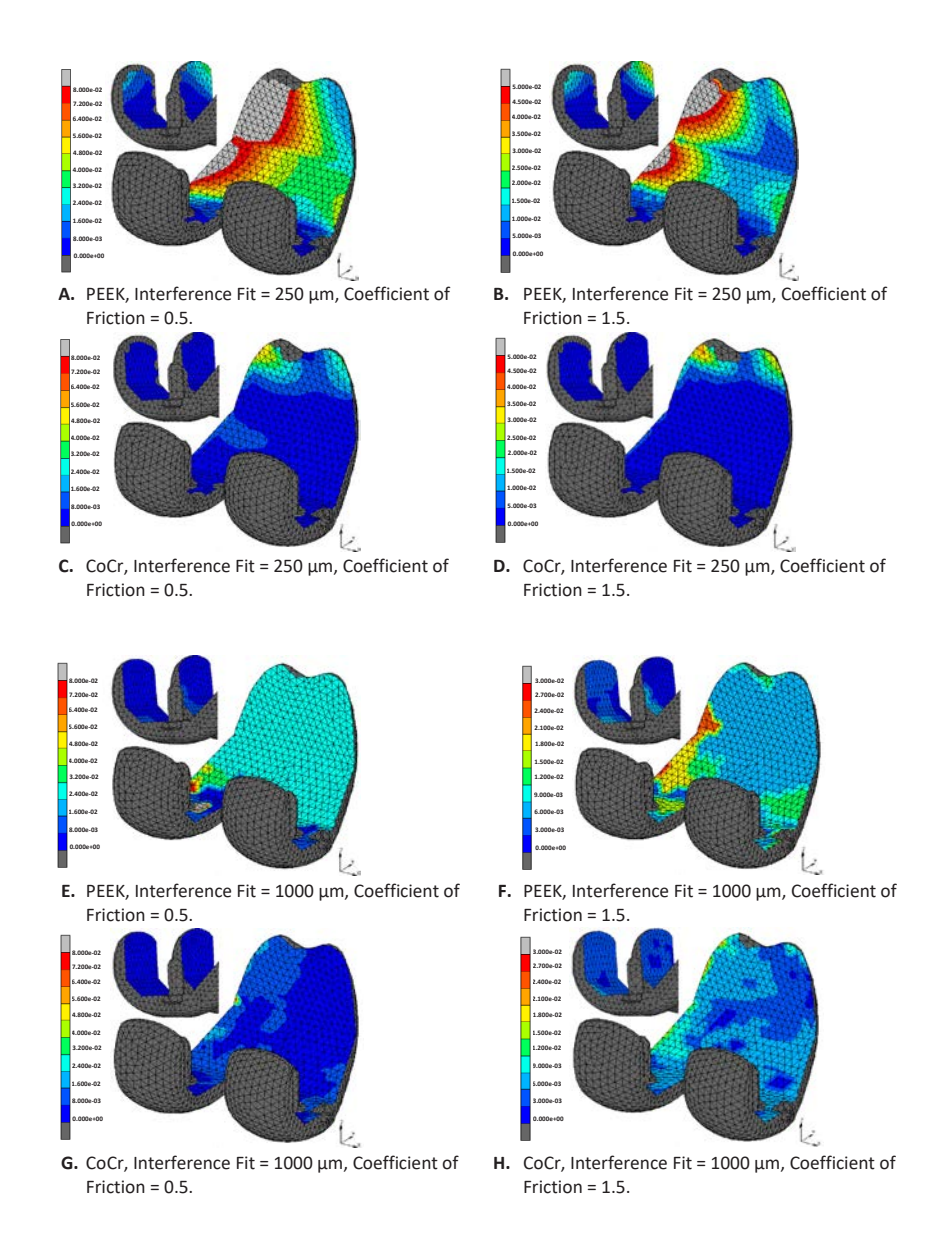


Figure 2-2. Resulting micromotion (mm) distribution at the implant interface after the 4th loading cycle. Notice that the colour scale representing the micromotion values differs per column.

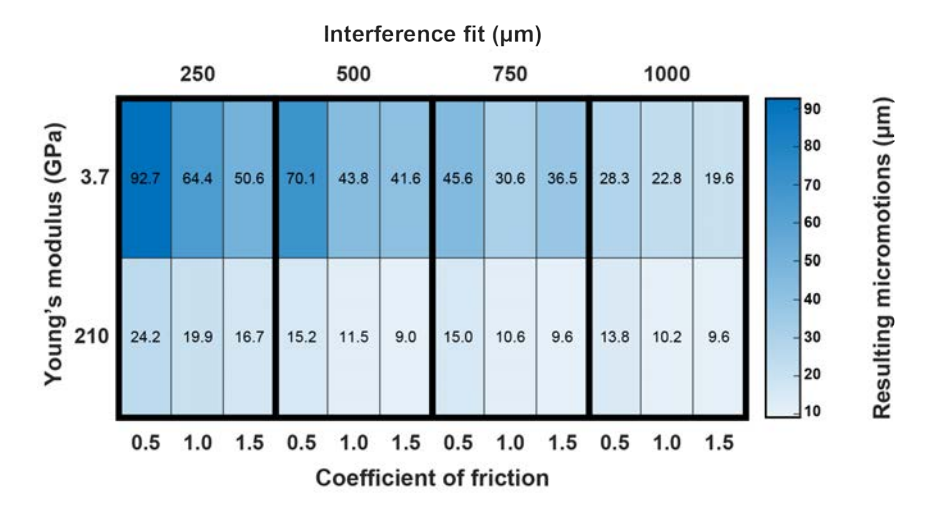


Figure 2-3. Heatmap of the 95th percentile of the maximum resulting micromotions (µm) on the implant interface after the 4th loading cycle.

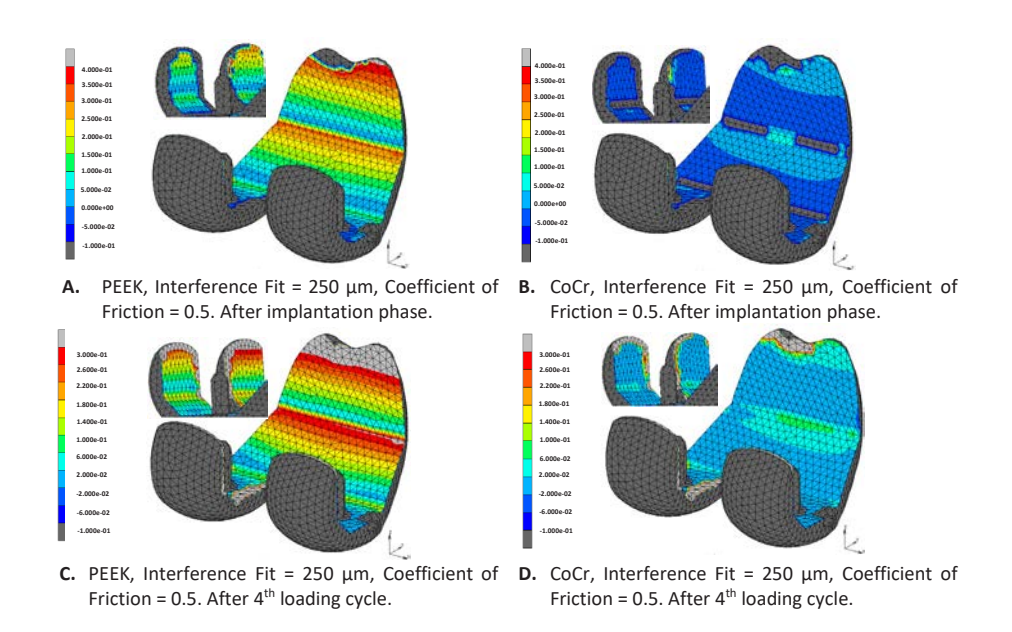


Figure 2-4. Distribution of the actual gap (mm) between the bone and the implant at the implant interface. Notice that the colour scale representing the actual gap values differs per row.

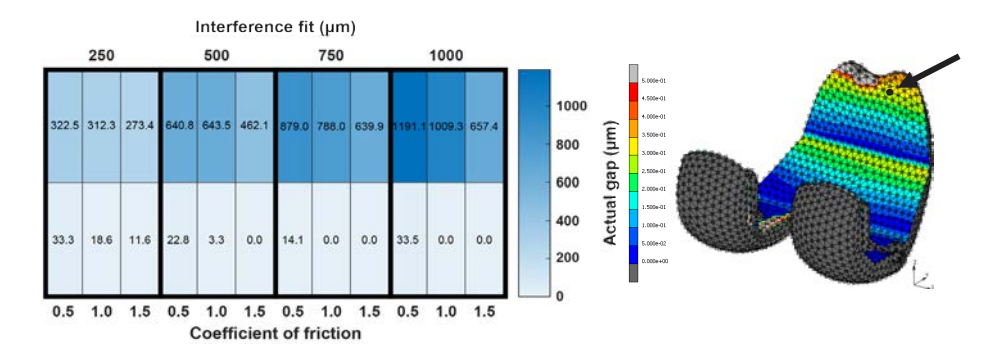


Figure 2-5. Heatmap of the actual gap (µm) of one node at the anterior flange after the 4th loading cycle.

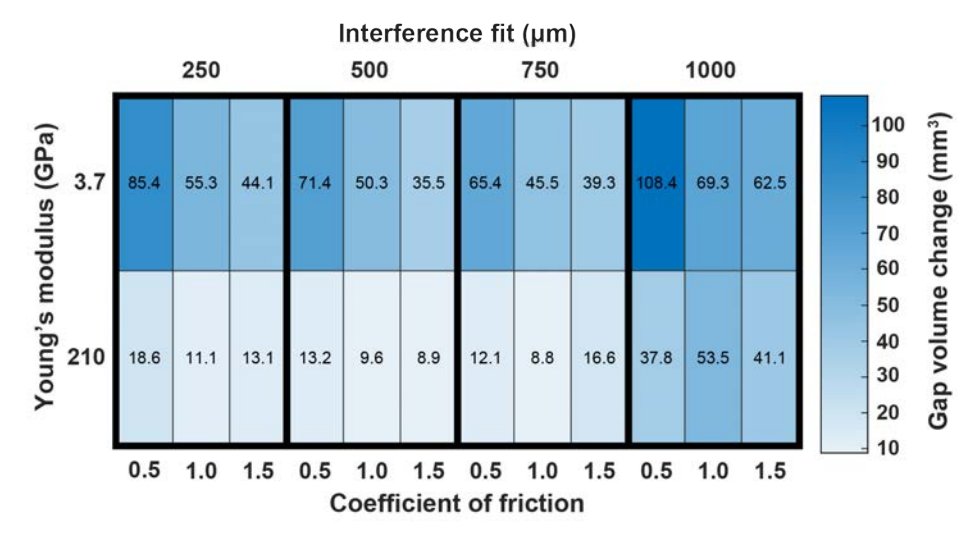


Figure 2-6. Heatmap of the gap volume change (mm³) between the implant and the bone on the implant interface after the 4th loading cycle.

Increasing the coefficient of friction resulted in a lower gap volume change for all values of interference fit and for both PEEK and CoCr models. The CoCr models gave lower gap volume change results than the PEEK models. The gap volume change depended on the interference fit, coefficient of friction and implant material. The effect of the interference fit and coefficient of friction on the gap volume change was relatively limited. The largest gap volume change was found at the PEEK model with a high interference fit and low coefficient of friction (Figure 2-6). Increasing the interference fit resulted in lower gap volume change values until the interference fit of 750 µm. The PEEK and CoCr models with an interference fit of 1000 µm showed the highest values of gap volume change. Only weak correlations were found between the gap volume change and the interference fit (r = 0.302) and between the gap volume change and coefficient of friction (r = -0.288). The CoCr models resulted in lower gap volume change values than the PEEK models, with gap volume change being most sensitive to the implant material (r = -0.759). All three correlations were statistically significant (p < 0.05).

Discussion

This study investigated the sensitivity of micromotions, gapping and gap volume change of a cementless PEEK femoral component to the interference fit and coefficient of friction and compared these outcomes to a cementless CoCr femoral component. Additionally, based on this sensitivity analysis, this study investigated which values of interference fit and coefficient of friction of a cementless PEEK femoral component would result in similar biomechanical behaviour as a cementless CoCr femoral component. All outcome measures seemed to be sensitive to the investigated parameters, although the implant material had the largest effect. When applying equal values for the interference fit and coefficient of friction. the PEEK femoral component generated higher micromotions and interface gaps compared with the CoCr femoral component. By adapting the interference fit and coefficient of friction, micromotion, and gap values can be obtained that should facilitate proper osseointegration of a cementless PEEK femoral component. The micromotion values of the PEEK femoral component using a high interference fit are similar as the micromotion values of the CoCr femoral component in standard conditions, using a low interference fit and low coefficient of friction. However, a too high interference fit is unfavourable as this might result in bone fractures due to too high compressive forces. Therefore, it could be possible to achieve an equal level of osseointegration with a cementless PEEK femoral component as compared to that with a cementless CoCr femoral component. Optimal values of interference fit are dependent on the specific implant design and therefore further analysis on the optimal interference fit for this specific implant design is necessary.

Only few studies have investigated the primary fixation of cementless femoral knee components [12, 20, 21]. The introduction of new implant materials such as PEEK demands extensive research methods for indicating sufficient implant fixation. Some studies have been looking into PEEK as a material for femoral components [6, 22, 23]. However, there are no studies that have investigated the effect of the interference fit and coefficient of friction on the primary fixation of a PEEK cementless femoral component. Therefore, we compared the results of our study to other studies that have analysed the primary fixation of cementless femoral knee components. The micromotion distributions at the implant interface are similar to the micromotion distributions found by Berahmani et al. [12]. This study also found the largest micromotions at the anterior flange. The maximum resulting micromotion values are in the same range as the maximum resulting micromotion values found during this study (20–70 μm).

In the current study, we created FE models combining variations of interference fit, coefficient of friction and implant material. We found that the micromotions and gapping of the implant are, besides the implant material, most sensitive to the interference fit. The importance of the effect of the interference fit on the micromotion prediction was also underlined by Abdul-Kadir et al. who found that the interference fit value has a major influence on the micromotions and thus on the primary fixation of the bone-implant interface [24].

Currently, there is paucity of knowledge about the gapping motion of the femoral component. There are only few studies that have investigated the interface gaps and the effect on bone ingrowth [9, 25]. The implications of the gap volume change could be very important since opening and closing of the implant can result in fluid flow around the bone-implant interface. This could potentially lead to metal or polyethylene wear debris particle transport, resulting in osteolysis and finally aseptic loosening [10, 26-28]. Therefore, gapping should be included when investigating the primary fixation of cementless femoral components.

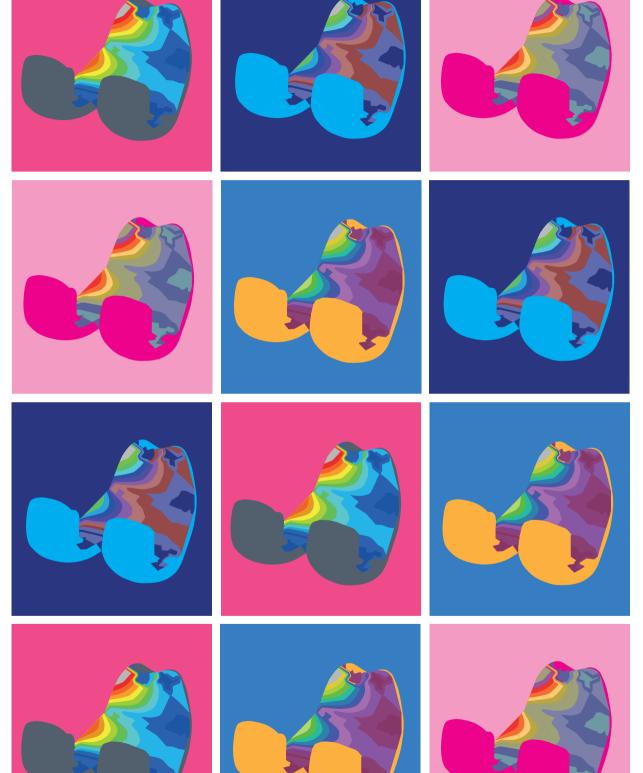
In this study, some limitations could be improved in further research. One limitation is that we did not model viscoelastic behaviour of the bone. This is an important characteristic for investigating the primary fixation of cementless implants as viscoelastic behaviour of the bone would reduce the press-fit forces due to the interference fit that are acting on the implant [29]. For future research, this could be improved by creating a more physiological model including the viscoelastic behaviour of the bone. A second limitation is the FE model of Berahmani et al. 2016 on which our FE model is based. The FE model of Berahmani et al. 2016 is validated for a maximum interference fit of 300 µm while we are in this study interested in a larger range of interference fit with a maximum value of 1000 µm. Another limitation of this study is the loading which was applied to the models. Although literature shows that simplifications of peak loading conditions can be applied to evaluate the implant fixation of cementless femoral components, more physiological loading conditions need to be tested for more robust models [12]. Particular attention needs to be paid to more demanding, deep-flexion activities such as stair climbing or a squat motion. For such activities the inclusion of the patellofemoral contact force is essential, which may be even more important for a PEEK femoral component. Current loads were based on the Orthoload database, which unfortunately does not provide these patellofemoral loads. We therefore chose the most demanding loading configuration at smaller flexion angles (i.e., jogging), in which patellofemoral forces are expected to be small. Another limitation of this study was the use of one single femur with an optimal alignment of the femoral component resulting in an optimal bone-implant interface. Varying the femoral size, geometry and bone density might lead to different results which emphasizes the benefit of performing population studies [30].

To conclude, the PEEK femoral component generated higher resulting micromotions and interface gaps compared with the CoCr femoral component when equal interference fit and friction values were applied. However, by increasing the interference fit and frictional properties of the PEEK design, micromotions were similar as found with the CoCr design in standard conditions. This finding opens the possibility to apply PEEK femoral components in TKA utilizing cementless fixation. We would recommend further evaluation to assess the optimal combination of friction and interference fit in mechanical experiments, and finite element experiments that incorporate more physiological loading conditions and variations of femoral bone characteristics to investigate interface micromotions of a cementless PEEK femoral component.

References

- 1. National Joint Registry 18th Annual Report 2021. 2021.
- 2. de Ruiter, L., et al., The Effects of Cyclic Loading and Motion on the Implant-Cement Interface and Cement Mantle of PEEK and Cobalt-Chromium Femoral Total Knee Arthroplasty Implants: A Preliminary Study. Materials (Basel), 2020. 13(15).
- 3 Koh, Y.G., et al., Total knee arthroplasty application of polyetheretherketone and carbon-fiberreinforced polyetheretherketone: A review. Mater Sci Eng C Mater Biol Appl, 2019. 100: p. 70-81.
- Chamberlain, K.A., et al., Wear properties of poly-ether-ether-ketone bearing combinations under 4. zero and cross shear kinematics in total knee arthroplasty. J Biomed Mater Res B Appl Biomater, 2019. 107(2): p. 445-453.
- Kurtz, S.M. and J.N. Devine, PEEK biomaterials in trauma, orthopedic, and spinal implants. Biomaterials, 2007. 28(32): p. 4845-69.
- de Ruiter, L., et al., The mechanical response of a polyetheretherketone femoral knee implant under a deep squatting loading condition. Proc Inst Mech Eng H, 2017. 231(12): p. 1204-1212.
- Robertsson, O., et al., Annual Report Swedish Knee Arthroplasty Register. 2019. 7.
- Engh, C.A., et al., Quantification of Implant Micromotion, Strain Shielding, and Bone Resorption With Porous-Coated Anatomic Medullary Locking Femoral Prostheses. Clin Orthop Relat Res, 1992. 285: p. 13-29.
- Tarala, M., D. Janssen, and N. Verdonschot, Toward a method to simulate the process of bone ingrowth in cementless THA using finite element method. Med Eng Phys, 2013. 35(4): p. 543-8.
- 10. Du, Z., Z. Zhu, and Y. Wang, The degree of peri-implant osteolysis induced by PEEK, CoCrMo, and HXLPE wear particles: a study based on a porous Ti6Al4V implant in a rabbit model. J Orthop Surg Res, 2018. 13(1): p. 23.
- 11. Peters, P.C., et al., Osteolysis after Total Knee Arthroplasty without Cement. Journal of Bone and Joint Surgery, 1992: p. 864 - 876.
- 12. Berahmani, S., et al., FE analysis of the effects of simplifications in experimental testing on micromotions of uncemented femoral knee implants. J Orthop Res, 2016. 34(5): p. 812-9.
- 13. Keyak, J.H., et al., Predicting proximal femoral strength using structural engineering models. Clin Orthop Relat Res, 2005(437): p. 219-28.
- 14. Keyak, J.H. and Y. Falkinstein, Comparison of in situ and in vitro CT scan-based finite element model predictions of proximal femoral fracture load. Med Eng Phys, 2003. 25(9): p. 781-787.
- 15. Berahmani, S., et al., An experimental study to investigate biomechanical aspects of the initial stability of press-fit implants. J Mech Behav Biomed Mater, 2015. 42: p. 177-85.
- 16. Sanchez, E., et al., The effect of different interference fits on the primary fixation of a cementless femoral component during experimental testing. J Mech Behav Biomed Mater, 2021. 113: p.
- 17. Berahmani, S., et al., Evaluation of interference fit and bone damage of an uncemented femoral knee implant. Clin Biomech (Bristol, Avon), 2018. 51: p. 1-9.
- 18. Bergmann, G., et al., Standardized loads acting in knee implants. PLoS One, 2014. 9(1): p. e86035.
- 19. Kutzner, I., et al., Mediolateral force distribution at the knee joint shifts across activities and is driven by tibiofemoral alignment. Bone Joint J, 2017. 99-B(6): p. 779-787.

- 20. Berahmani, S., D. Janssen, and N. Verdonschot, Experimental and computational analysis of micromotions of an uncemented femoral knee implant using elastic and plastic bone material models. J Biomech, 2017. 61: p. 137-143.
- 21. Conlisk, N., et al., The influence of stem length and fixation on initial femoral component stability in revision total knee replacement. Bone Joint Res, 2012. 1(11): p. 281-288.
- 22. Rankin, K.E., et al., Does a PEEK Femoral TKA Implant Preserve Intact Femoral Surface Strains Compared With CoCr? A Preliminary Laboratory Study. Clin Orthop Relat Res, 2016. 474(11): p. 2405-2413.
- 23. Wang, J.P., et al., Structural stability of a polyetheretherketone femoral component-A 3D finite element simulation. Clin Biomech (Bristol, Avon), 2019. 70: p. 153-157.
- 24. Abdul-Kadir, M.R., et al., Finite element modelling of primary hip stem stability: the effect of interference fit. J Biomech, 2008. 41(3): p. 587-94.
- 25. Tarala, M., D. Janssen, and N. Verdonschot, Balancing incompatible endoprosthetic design goals: a combined ingrowth and bone remodeling simulation. Med Eng Phys, 2011. 33(3): p. 374-80.
- 26. Hirakawa, K., et al., Relationship Between Wear Debris Particles and Polyethylene Surface Damage in Primary Total Knee Arthroplasty The Journal of Arthroplasty, 1999. 14(2): p. 165-171.
- 27. Nine, M.J., et al., Wear Debris Characterization and Corresponding Biological Response: Artificial Hip and Knee Joints. Materials (Basel), 2014. 7(2): p. 980-1016.
- 28. Stratton-Powell, A.A., et al., The Biologic Response to Polyetheretherketone (PEEK) Wear Particles in Total Joint Replacement: A Systematic Review. Clin Orthop Relat Res, 2016. 474(11): p. 2394-2404.
- 29. Popescu, R., E.G. Haritinian, and S. Cristea, Relevance of Finite Element in Total Knee Arthroplasty - Literature Review. Chirurgia (Bucur), 2019. 114(4): p. 437-442.
- 30. Anijs, T., et al., Population-based effect of total knee arthroplasty alignment on simulated tibial bone remodeling. J Mech Behav Biomed Mater, 2020. 111: p. 104014.



Chapter 3

The sensitivity of the stiffness and thickness of a titanium inlay in a cementless PEEK femoral component to the micromotions and bone strain energy density

Corine Post, Thom Bitter, Adam Briscoe, Nico Verdonschot, Dennis Janssen

Published in Medical Engineering & Physics: https://doi.org/10.1016/j.medengphy.2023.104072

Abstract

Polyetheretherketone (PEEK) has been proposed as alternative material for total knee arthroplasty implants due to its low stiffness, which may reduce stressshielding. In cementless fixation, a proper primary fixation is required for long-term fixation. Previous research showed that the lower stiffness of a cementless PEEK femoral component results in larger micromotions at the implant-bone interface compared to a cobalt-chrome femoral component. A titanium inlay on the PEEK implant surface may improve the primary fixation while maintaining the favourable stiffness properties. Therefore, the effect of thickness and stiffness of a titanium inlay on the primary fixation and stress-shielding was investigated. A finite element model of the femur and femoral component was created with five titanium inlay variants. The micromotions and strain energy density (SED) were quantified as outcome measures. The distal thin - proximal thick variant showed the largest resulting micromotions (51.2 µm). Relative to the all-PEEK femoral component, the addition of a titanium inlay reduced the micromotions with 30% to 40% without considerably affecting the stress-shielding capacity (strain energy difference of 6% to 10%). Differences in micromotions (43.0 - 51.2 um) and SED between the variants were relatively small. In conclusion, the addition of a titanium inlay could lead to a reduction of the micromotions without substantially affecting the SFD distribution.

Introduction

While traditional total knee arthroplasty (TKA) components are made of metal alloys such as cobalt-chrome or titanium, high-grade plastics such as ultra high molecular weight polyethylene (UHMWPE) and polyetheretherketone (PEEK) have been proposed as alternative implant materials. PEEK has a lower stiffness than traditional metal alloys, which has the potential benefit of reduced stressshielding [1]. Stress-shielding could on the long-term lead to loss of bone stock and consequently bone fracture and aseptic loosening of the femoral component [2].

Recent computational studies of cemented femoral components using finite element (FE) analysis show that a PEEK implant leads to a stress distribution in the bone that more closely resembles the situation before prosthesis implantation [1, 3, 4]. These studies demonstrate that the reduction in stress-shielding for a PEEK femoral component is substantial compared to conventionally used cobalt-chrome alloy (CoCr) femoral components.

While previous studies focused on cemented femoral TKA reconstructions, there is also an interest in cementless fixation via bone ingrowth of PEEK implants, as the survival time of cemented TKA is generally thought to be limited [5-7]. Primary fixation is crucial to ensure a long-term survival of cementless implants. A recent study, however, concluded that a cementless PEEK femoral component leads to larger micromotions at the implant-bone interface compared to a cementless CoCr femoral component [8]. Large micromotions may lead to the formation of a soft tissue layer at the interface, inhibiting long-term fixation through osseointegration.

To improve the primary fixation of cementless femoral components a titanium coating on the inner implant interface can be used [9]. Porous titanium has been widely used for facilitating bone ingrowth and is therefore widely used in cementless implants. A titanium coating can be used to optimize the frictional properties of the coating that is in contact with the bone, but by increasing the coating thickness also the structural stiffness of the implant can be adapted. This in turn influences the press-fit fixation and the micromotions at the interface. The titanium coating can be integrated in the PEEK implant through an inlay that is incorporated in the injection moulding process. However, the optimal thickness and stiffness of such an inlay for a press-fit PEEK femoral component is unknown. A too thick inlay would result in the implant losing its potential bone saving capacity, while a too thin inlay would result in no reduction of the micromotions. An implant with an inlay with variable thickness might enhance the primary stability as well as preserving the reducing stress-shielding capacity of the PEEK component. Such variations are quite difficult to investigate in an experimental set-up. Computational modelling, however, provides the opportunity to isolate and simulate the effect of inlay variations on the primary stability.

Therefore, the objective of the current study was to investigate the effect of thickness and stiffness of a titanium inlay on the primary fixation, quantified by the micromotions, and on stress-shielding, quantified by the strain energy density (SED), using finite element analysis.

Materials and Methods

A FE model of the femur with a femoral component including a titanium inlay was created. Three different inlay thickness variants named thin, medium and thick were considered (Figure 3-1). To define the structural stiffness of the titanium inlays, the three different thickness variants were tested in physical three-point bending tests. Subsequently, the thickness and stiffness characteristics of the three inlay variants were used in the FE model.

Titanium inlavs

Five samples of each inlay variant were obtained to define the material properties using a three-point bending test. Each inlay consisted of a solid core and two porous outer layers sintered together (Table 3-1).



Figure 3-1. Thin, medium and thick inlay.

Titanium inlay type	Global thickness (mm)	Thickness solid core (mm)
Thin	1.50	0.25
Medium	1.70	0.50
Thick	2.20	1.00

Table 3-1. Characteristics of the three inlay variants

Experimental three-point bending tests

Three-point bending experiments were performed in an MTS machine (MTS Systems Corporation, Eden Prairie, Minnesota, USA) with a custom-made set-up consisting of a load applicator and two supports, all with a radius of 2 mm. Three-point bending experiments were performed to determine the stiffness properties of the corresponding titanium inlay variant that will be used in the FE models. Before the three-point bending tests, the inlays were milled, painted with white paint and marked with three red dots to facilitate measurement of the deflection using digital image correlation (DIC) (Figure 3-2). DIC measurements were used to quantify the small displacements of the inlay instead of the MTS displacements, to avoid measurement errors due to plastic deformation of the porous outer layers. We performed a sensitivity analysis which showed a precision of 95% for the Young's modulus of the whole system. A 3D printed tool was used to position the inlay on the supports.



Figure 3-2. Overview of the titanium inlay including supports and load applicator. The red dots are indicated with black circles.

At the start of the experiment, the load applicator was positioned on the inlay. Subsequently, one sample was used to define the maximum displacement in the elastic region, in displacement increments of 1.0 mm. Subsequently, all samples were tested at a rate of 2.0 mm/min until the maximum displacement in the elastic region was achieved. A force-displacement curve was created to calculate the average representative Young's modulus per sample (Equation 3-1). This equation is typically used for a homogeneous material. Although the physical inlays are not homogeneous, it was modelled as a homogeneous material in the FE model. The displacement of the left and right dot was subtracted from the displacement of the central dot. As a final result, the average representative Young's modulus of all five samples was taken for the three inlay types.

$$\frac{dP}{dw_0} = \frac{48EI}{L^3}$$
$$I = \frac{a^3b}{12}$$

Equation 3-1. The gradient between the applied force P and the central displacement w_0 was used to define the average representative Young's modulus E. I = second moment of area, L = support span, a =thickness inlay, b =width inlay.

FE model

The FE model of a femur implanted with a cementless femoral component from a previous study was used [8]. The CT-scan of a cadaveric right femur (62 years, male) was segmented to create the 3D model of the femur using medical imaging software (Mimics 14.0, Materialise, Leuven, Belgium). An average size C cementless femoral knee component was virtually implanted on the femur (Freedom knee, Maxx Orthopedics, Norristown, PA, USA). The alignment of the implant on the bone was verified by an experienced orthopaedic surgeon. The implant was aligned according to the mechanical alignment strategy. Subsequently, the femoral bone cuts were created corresponding to the internal implant interface using modelling software (SimLab 2019.1, Altair Engineering, Troy, MI, USA). Meshing software was used to create FE models of both the femur and femoral component consisting of linear tetrahedral elements with an edge size of 2.5 mm, based on previous mesh convergence studies (HyperMesh 2017, Altair Engineering, Troy, MI, USA) [10]. As a result, the femur consisted of 67,948 elements and 12,709 nodes and the femoral component of 16,255 elements and 3,883 nodes.

A calibration phantom (0, 50, 100, 200 mg/ml calcium hydroxyapatite, Image Analysis), scanned along the cadaveric femur, was used for assignment of the material properties for each bone element. The material properties were defined based on the conversion of the CT Hounsfield Units to calcium values. In a custom user subroutine, these calcium values were converted to the Young's modulus [11]. The bone was defined as an elastic-plastic material.

The implant was defined as an elastic isotropic material and assigned with a Young's modulus of 3.7 GPa for PEEK-OPTIMA™ given by the manufacturer (Invibio Ltd, Thornton Cleveleys, Lancashire, United Kingdom).

The titanium inlay was modelled using 3D shell elements with a zero thickness, and were fixed to the inner surface of the femoral component. Thickness and stiffness properties for the corresponding titanium inlay variant were subsequently assigned to the shell elements

The contact between the bone and the implant was modelled using a single-sided touching contact algorithm. The coefficient of friction was set for all variants at 0.5 to evaluate an average value of coefficient of friction [12]. A coulomb bilinear (displacement) friction model was used to define the friction.

The interference fit was numerically specified through the contact algorithm between the bone and the implant at the distal, anterior, posterior and chamfer sides and was only applied in the micromotion simulations and not in the SED simulations.

An interference fit value of 500 µm was chosen based on previous simulations [8]. The FE simulation was divided in an implantation phase and a loading phase. During the implantation phase, the interference fit was linearly increased until the maximum value in 50 increments. The loads were consecutively applied during the loading phase. During the loading phase, the maximum value of the interference fit was kept constant. The variation in inlay thickness did not influence the applied interference fit.

The models were subjected to a jogging loading configuration, which was chosen as a high-load activity for the evaluation of the primary fixation, and was taken from the Orthoload database [13]. The jogging loads were applied as two point loads at the centre of the medial and lateral femoral condyles in the axial direction, defining the tibiofemoral contact forces. Considering the frictionless contact, the anteroposterior and mediolateral components of the forces were assumed negligible. The axial force was separated into a medial and lateral axial force using the medial force ratio from the Orthoload database [14]. A quasi-static simulation was performed in which the loads were incrementally applied in a sequence of twelve increments. Six increments were used to move from the starting situation without loading to the maximum load, and six increments were used to move back to the situation without loads. This represented one loading cycle. Four loading cycles were simulated to allow the implant to settle (numerically). The results were taken from the final loading cycle [10]. As a constraint, a fixed displacement in all directions was applied on the proximal side of the femur.

Five different variations of FE models with a titanium inlay were analysed. The PEEK implant material model was first simulated with a uniform thin, medium, and thick titanium inlay. Additionally, two FE models with titanium inlay variants were created: a thin inlay at the anterior flange and posterior condyles, and a thick inlay distally and at the chamfers, and vice versa (Figure 3-3). The proximal and distal region were modelled with a different inlay thickness separately as previous researched showed that the anterior flange and posterior condyles are the regions with the largest micromotions [8, 10]. The strain values are, however, typically larger in the distal region than the proximal region of the femur [1]. Therefore, a thin inlay at the proximal region and a thick inlay at the distal region of the femoral component and vice versa were analysed.

As outcome measures the micromotions and strain energy for all simulations were calculated.

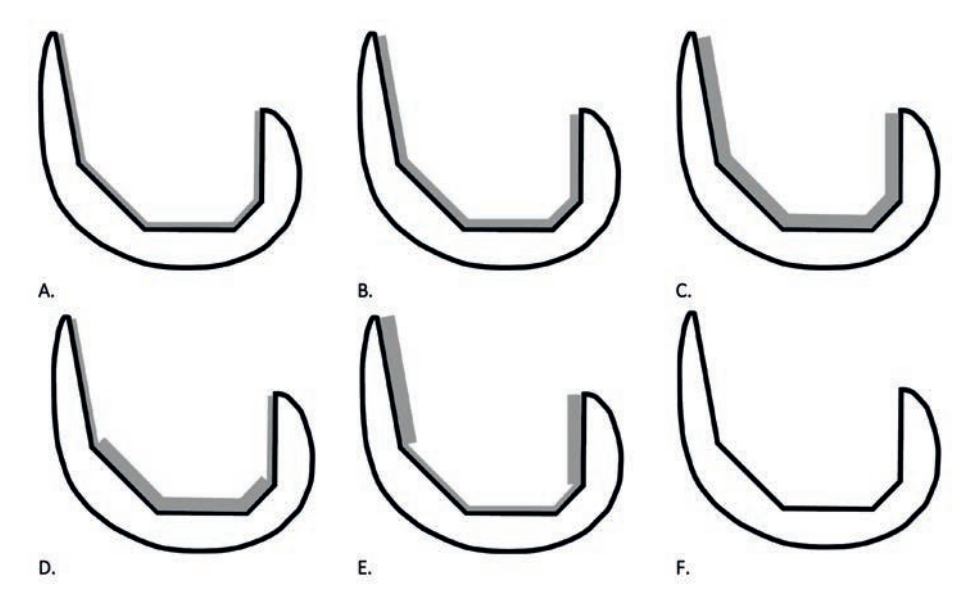


Figure 3-3. Titanium inlay variants. **A.** Uniform thin titanium inlay; **B.** Uniform medium titanium inlay; **C.** Uniform thick titanium inlay; **D.** Distal thick – proximal thin; **E.** Distal thin – proximal thick; **F.** All-PEEK femoral component without titanium inlay.

Micromotions

For quantification of the primary fixation, the micromotions, defined as the inplane relative displacements at the contact interface between the implant and the bone in the shearing direction, were defined. Therefore, the nodes on the implant interface were defined as well as the corresponding contact face on the bone interface. The largest distance in the in-plane direction between the contact node on the implant interface and the closest contact face on the bone was calculated for all nodes during the fourth loading cycle in the loading phase, defined as the resulting micromotions. The regions of the pegs and the regions having a large overhang, for example at the posterior condyles and anterior flange, were not included in the results. The 95th percentile of the maximum resulting micromotions was defined for each FE model. This value was defined to remove any possible micromotion outliers in the model

Strain energy

For the quantification of stress-shielding, the SED was calculated in each FE model. SED is an accepted stimulus for bone remodelling, with bone resorption being caused by a decrease in SED, relative to the reference case [15, 16]. The SED of the reconstruction with an all-PEEK femoral component without an inlay was taken as the reference case, in order to quantify the impact of the titanium inlay. The total strain energy was defined as the SED per element multiplied by the element volume, summed for the whole periprosthetic bone. The strain energy difference was defined as the total strain energy of the femoral reconstruction with the initial all-PEEK femoral component subtracted from the femoral reconstruction with the PEEK component with a titanium inlay. A negative strain energy difference leads to a decrease in strain energy compared to the femoral reconstruction with the all-PEEK femoral component which therefore has a negative impact on the bone remodelling. Regions of interest (ROI) were defined according to similar models from literature to identify the regions with the largest strain energy differences [1].

Results

Experimental three-point bending tests

As expected, the largest mean representative Young's modulus value was found for the thick titanium inlay (Table 3-2).

Titanium inlay type	Mean representative Young's modulus (GPa) (mean ± SD)	Global thickness (mm)
Thin	14.35 ± 0.3775	1.5
Medium	17.34 ± 1.1905	1.7
Thick	24.74 ± 1.7030	2.2

Table 3-2. Mean representative Young's modulus per Titanium inlay type

Micromotions

The addition of a titanium inlay reduced the micromotions with 30% to 40% compared to the all-PEEK femoral component. In all models the largest micromotion values were seen on the medial side of the anterior flange (Figure 3-4). After the all-PEEK femoral component, the distal thin – proximal thick variant showed the largest resulting micromotions (Table 3-3). The micromotion values at the distal and chamfer regions decreased with increasing inlay thickness and stiffness. A thick inlay at the distal and chamfer regions resulted in lower micromotions than a thin inlay at the distal and chamfer regions.

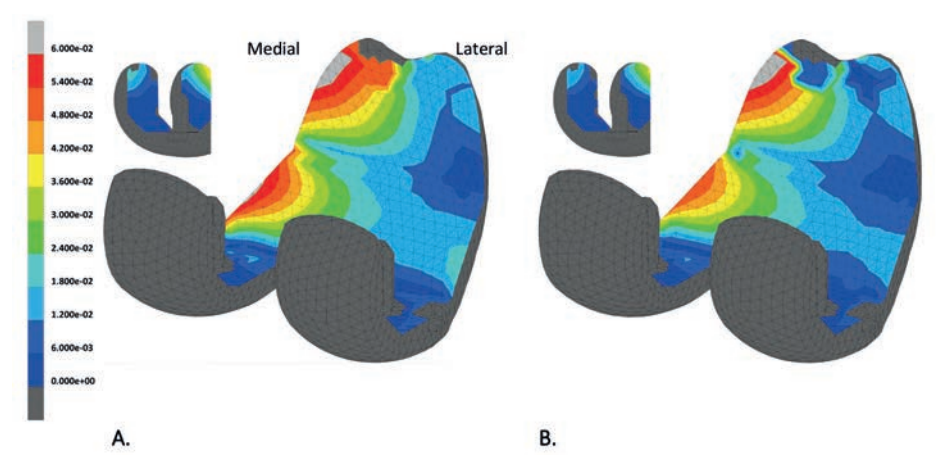


Figure 3-4. Resulting micromotion (mm) distribution at the implant interface after the 4th loading cycle. A. PEEK femoral component including uniform thin titanium inlay. B. PEEK femoral component including distal thick – proximal thin titanium inlay.

All-PEEK	Thin	Medium	Thick	Distal thick – proximal thin	Distal thin – proximal thick
69.5	51.0	48.9	49.8	43.0	51.2

Table 3-3. 95th percentile of maximum resulting micromotions (μm).

Strain energy density visualization

The SED decreased mainly in the distal region with the addition of an inlay (Figure 3-5). This decrease was more pronounced for the inlays with high stiffness and thickness values.

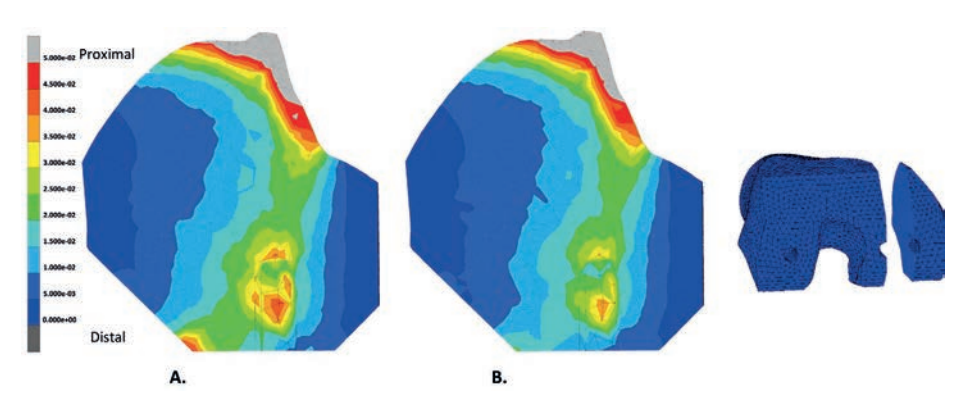


Figure 3-5. Total SED (MPa), cutting plane through the medial peg. A. All-PEEK femoral component without titanium inlay; B. PEEK femoral component with uniform thick titanium inlay.

Strain energy difference

The addition of a titanium inlay resulted in a decrease in the strain energy. For the total ROI, the difference in strain energy of the PEEK component including titanium inlay compared with the all-PEEK femoral component is 6% to 10%. The largest strain energy differences were found in the medial distal region, ROI 2 and ROI 4, for all inlay types. The largest strain energy differences compared to the all-PEEK femoral component were found for the thick inlay with a high stiffness and thickness (Figure 3-6).

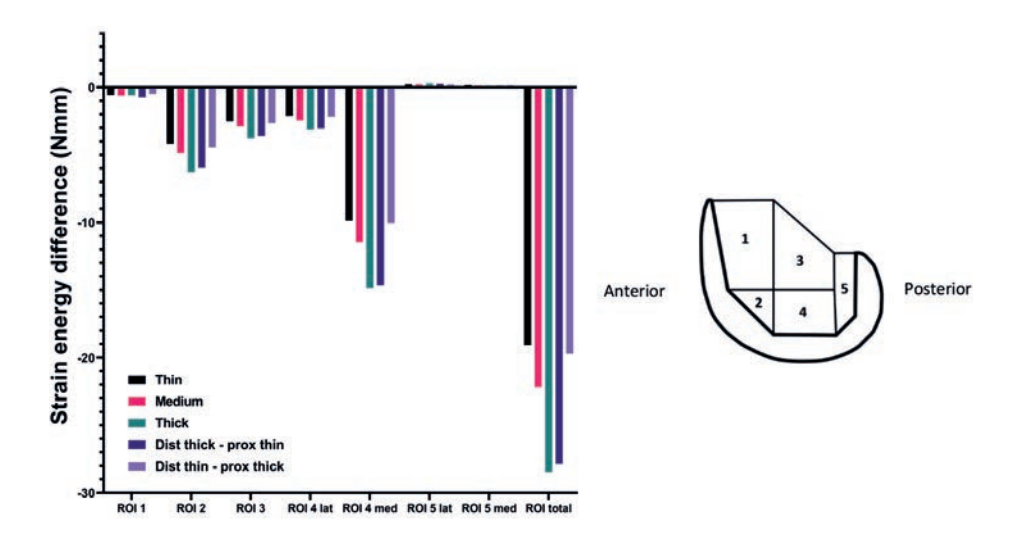


Figure 3-6. Strain energy difference (Nmm) per ROI for the three uniform titanium inlay types and two variants with respect to the all-PEEK femoral component without titanium inlay. The ROI total is the sum of the strain energy difference of all ROIs.

Discussion

The objective of the current study was to investigate the effect of the thickness and stiffness of a titanium inlay on the primary fixation, quantified by the micromotions, and on the stress-shielding, quantified by the SED, using FE models. Both outcome measures were sensitive to the presence of a titanium inlay, although the subsequent effects of the different variants investigated were relatively small.

De Ruiter et al. studied the stress-shielding of a cemented PEEK femoral component compared to the stress-shielding of a cemented CoCr femoral component [1]. Their study found that the strain patterns of the femur including a PEEK implant more closely resembles the intact femur than the femur including a CoCr implant. SED differences were more pronounced in the distal and anterior regions at the implant interface and less pronounced in the posterior region. This corresponds with the current results in which the largest strain energy differences were seen in the medial distal region. Similarly, in the current study a PEEK implant with a thick (and hence a stiff) titanium inlay resulted in a larger strain energy difference than a PEEK implant with a thin titanium inlay, although the differences in strain energy difference are small among the inlay variants.

The addition of a titanium inlay resulted in a decrease in the micromotions. The micromotion values of the cementless PEEK femoral component including titanium inlay variants that were investigated in the current study were in the same range as the micromotion values of cementless CoCr femoral components investigated previously (20 - 70 µm) [8]. Although, like the strain energy difference values, the differences in micromotion values among the inlay variants are small [10, 17]. However, the micromotion values found in the current study were all below the reported micromotion threshold for bone ingrowth (40 - 50 μ m) [18, 19].

Several studies reported on the use of a surface coating to improve osseointegration of cementless TKA components [9, 20]. The study of Aerts et al. investigated the effect of fibre size and porosity on the stiffness of a titanium fibre mesh [9]. As a conclusion, changing the stiffness could effectively be achieved by adapting the fibre size and porosity. The study of Ryu, et al. showed that a titanium porous coating is biocompatible to use as a surface coating of cementless TKA components [20]. Moreover, the contact area between the bone and the implant was larger for the sample including a titanium coating compared with the smooth sample without a coating. These studies suggest that the use of titanium coatings may improve the primary fixation of cementless TKA components. This was confirmed by our

study, showing decreased micromotion values in models including a titanium inlay compared with models without an inlay.

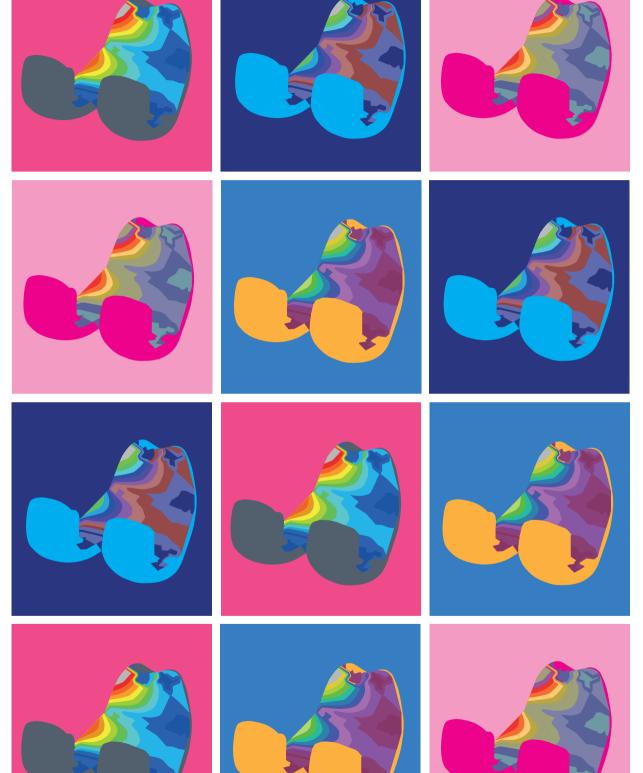
Our simulations showed that the addition of a titanium inlay resulted in a decrease in micromotion values, although the effect on the micromotions among the inlay variants is relatively small. This therefore allows for further design and development of a titanium inlay on the inner implant interface with an improved primary fixation of the femoral component as result. Especially the use of a thick inlay on the distal side reduces the micromotions and therefore the risk of poor primary fixation of the implant. Nonetheless, we would recommend further research with mechanical experiments to confirm the in this study simulated results. Additionally, the osseointegration of an implant including a titanium inlay may be investigated by assessing the osteoblast viability and the contact between the bone and the implant including a titanium inlay.

There are a few limitations in this study that could be improved in future research. The first limitation is that only one loading condition was investigated in this study, which also only included the tibiofemoral forces. Previous studies have shown that variations in loading conditions may influence the strain in the femur [3, 4]. Additionally, patellofemoral forces could also be of interest, particularly for a more flexible implant material such as PEEK. A second limitation is the alignment of the femoral component. Alignment variations influence the load transfer from femur to tibia, and therefore will also affect the strain distribution in the femur. Including loading configurations for more alignment conditions may therefore provide more robust results, although the relative results will not be influenced. Another limitation is that only one bone geometry with corresponding bone density distribution was analysed in this study. A population study including patient variations and surgical variations as cutting errors would result in models with varying bone density distributions and could therefore influence the SED in the bone models. Therefore, this study may be further assessed in a larger population of models. Another limitation is that the titanium inlay has been modelled as a solid layer in the FE models, while the inlay consists of a solid core layer and two porous outer layers sintered together. However, this was accounted for by modelling the average representative Young's modulus. Finally, the inlays were simulated with zero thickness elements, which would be different from the actual physical specimens. Although the structural stiffness (e.g., shell thickness) was incorporated in the FEA models, in the clinical or experimental situation the titanium inlay would have a physical thickness, which was not included. For implants with an inlay, it is the intention to maintain the same internal dimensions for the femoral component, which means the inlay would take up space of the PEEK material. However, due to the porous structure the inlay would also partially be infused with PEEK during the manufacturing. The effects of an infused titanium inlay on the structural stiffness should be further investigated to evaluate the primary stability of actual end products. In addition, since the porosity was not physically modelled in the models, any change in porosity or composition of the inlay would require additional experimental testing to ensure the structural stiffness (i.e., second moment of inertia) is correctly reflected by the shell elements.

In conclusion, adding an inlay the PEEK femoral component led to a decrease in micromotions when compared to the all-PEEK component. Only small differences were seen between the different inlay variations. Adding an inlay only had a minor effect on the SED distribution as compared to the all-PEEK implant, with the largest decrease seen in the most distal region.

References

- de Ruiter, L., et al., Decreased stress shielding with a PEEK femoral total knee prosthesis measured in validated computational models. J Biomech, 2021. 118: p. 110270.
- 2 Petersen, M.M., et al., Decreased bone density of the distal femur after uncemented knee arthroplasty. A 1-year follow-up of 29 knees. Acta Orthop Scand, 1996. 67(4): p. 339-44.
- de Ruiter, L., et al., The mechanical response of a polyetheretherketone femoral knee implant under 3. a deep squatting loading condition. Proc Inst Mech Eng H, 2017. 231(12): p. 1204-1212.
- 4. de Ruiter, L., et al., A preclinical numerical assessment of a polyetheretherketone femoral component in total knee arthroplasty during gait. J Exp Orthop, 2017. 4(1): p. 3.
- 5. Dalury, D.F., Cementless total knee arthroplasty. The Bone & Joint Journal, 2016. 98-B(7): p. 867-873.
- Meneghini, R.M. and A.D. Hanssen, Cementless Fixation in Total Knee Arthroplasty: Past, Present, 6. and Future. Journal of Knee Surgery, 2008. 21(4): p. 307-314.
- 7. Prudhon, J.L. and R. Verdier, Cemented or cementless total knee arthroplasty? - Comparative results of 200 cases at a minimum follow-up of 11 years. SICOT J, 2017. 3: p. 70.
- Post, C.E., et al., A FE study on the effect of interference fit and coefficient of friction on the micromotions and interface gaps of a cementless PEEK femoral component. J Biomech, 2022. 137: p. 111057.
- Aerts, E., et al., Porous titanium fiber mesh with tailored elasticity and its effect on stromal cells. J 9 Biomed Mater Res B Appl Biomater, 2020. 108(5): p. 2180-2191.
- 10. Berahmani, S., et al., FE analysis of the effects of simplifications in experimental testing on micromotions of uncemented femoral knee implants. J Orthop Res, 2016. 34(5): p. 812-9.
- 11. Keyak, J.H., et al., Predicting proximal femoral strength using structural engineering models. Clin Orthop Relat Res, 2005(437): p. 219-28.
- 12. Shirazi-Adl, A., M. Dammak, and G. Paiement, Experimental determination of friction characteristics at the trabecular bone/porous-coated metal interface in cementless implants. J Biomed Mater Res, 1993. 27(2): p. 167-75.
- 13. Bergmann, G., et al., Standardized loads acting in knee implants. PLoS One, 2014. 9(1): p. e86035.
- 14. Kutzner, I., et al., Mediolateral force distribution at the knee joint shifts across activities and is driven by tibiofemoral alignment. Bone Joint J, 2017. 99-B(6): p. 779-787.
- 15. Carter, D.R., D.P. Fyhrie, and R.T. Whalen, Trabecular bone density and loading history: regulation of connective tissue biology by mechanical energy. Journal of Biomechanics, 1987. 20(8): p. 785-794.
- 16. Huiskes, R., et al., Adaptive bone-remodeling theory applied to prosthetic-design analysis. Journal of Biomechanics, 1987. 20(11-12): p. 1135-1150.
- Berahmani, S., D. Janssen, and N. Verdonschot, Experimental and computational analysis of micromotions of an uncemented femoral knee implant using elastic and plastic bone material models. J Biomech, 2017. 61: p. 137-143.
- 18. Engh, C.A., et al., Quantification of Implant Micromotion, Strain Shielding, and Bone Resorption With Porous-Coated Anatomic Medullary Locking Femoral Prostheses. Clinical Orthopaedics and Related Research, 1992. 285: p. 13-29.
- 19. Jasty, M., et al., In Vivo Skeletal Responses to Porous-Surfaced Implants Subjected to Small Induced Motions. The Journal of Bone and Joint Surgery, 1997. 79(5): p. 707-714.
- 20. Ryu, D.J., et al., Osteo-Compatibility of 3D Titanium Porous Coating Applied by Direct Energy Deposition (DED) for a Cementless Total Knee Arthroplasty Implant: in Vitro and in Vivo Study. J Clin Med, 2020. 9(2).



Chapter 4

The primary stability of a cementless PEEK femoral component is sensitive to BMI: a population-based FE study

Corine Post, Thom Bitter, Adam Briscoe, René Fluit, Nico Verdonschot, Dennis Janssen

Published in Journal of Biomechanics: https://doi.org/10.1016/j.jbiomech.2024.112061

Abstract

The use of polyetheretherketone (PEEK) for cementless femoral total knee arthroplasty (TKA) components is of interest due to several potential advantages, e.g., the use in patients with metal hypersensitivity. Additionally, the stiffness of PEEK closer resembles the stiffness of bone, and therefore, peri-prosthetic stressshielding may be avoided. When introducing a new implant material for cementless TKA designs, it is important to study its effect on the primary fixation, which is required for the long-term fixation. Finite element (FE) studies can be used to study the effect of PEEK as implant material on the primary fixation, which may be dependent on patient factors such as age, gender and body weight index (BMI). Therefore, the research objectives of this study were to investigate the effect of PEEK vs cobalt-chrome (CoCr) and patient characteristics on the primary fixation of a cementless femoral component. 280 FE models of 70 femora were created with varying implant material and gait and squat activity. Overall, the PEEK models generated larger peak micromotions than the CoCr models. Distinct differences were seen in the micromotion distributions between the PEEK and CoCr models for both the gait and squat models. The micromotions of all femoral models significantly increased with BMI. Neither gender nor age of the patients had a significant effect on the micromotions. This population study gives insights into the primary fixation of a cementless femoral component in a cohort of FE models with varying implant material and patient characteristics.

Introduction

Primary fixation of the cementless femoral component is essential for bone ingrowth on and into the implant surface, which occurs a few weeks to months after total knee arthroplasty (TKA) procedure [1]. This primary fixation is established by the compressive and shearing forces that are generated during the implantation of the press-fit components. Apart from the frictional properties of the implant surface, the primary fixation depends on the design and material of the femoral component. When introducing a new implant material for TKA designs, it is therefore important to study its effect on the primary fixation.

While cobalt-chrome (CoCr) alloy currently is the default material for cementless femoral TKA components, polyetheretherketone (PEEK-OPTIMA™) is of interest as the material has several potential advantages. One of the advantages of PEEK is that it can be used in patients with metal hypersensitivity. Moreover, the use of a non-metal TKA allows for easier analysis of the peri-prosthetic tissue with modalities such as MRI and CT in case of implant failure as metal artefacts will be avoided [2]. From a mechanical perspective, the stiffness of PEEK (3.7 GPa) closer resembles the stiffness of human bone that is replaced during the surgery compared to CoCr (210 GPa). Therefore, the potential peri-prosthetic stress-shielding may be reduced [3, 4].

To study the effect of PEEK as an implant material on the primary fixation, finite element (FE) studies can be adopted to simulate micromotions at the implant – bone interface, which can be used to evaluate the ingrowth potential of press-fit implants. Previous FE studies on the cementless PEEK femoral component mainly focused on the analysis of a single femoral model with parametric variations [5], while in clinical practice the outcome depends on patient factors such as age, gender and body weight index (BMI). For instance, several studies have investigated the influence of BMI on the outcomes of TKA [6-8]. While there has been controversy on whether or not a high BMI negatively affects the primary fixation, a recent study has shown that a high BMI causes larger micromotions in reconstructions with metal implants [7]. However, the influence of a high BMI on the primary fixation of a cementless PEEK femoral component is currently unknown. By adopting a population-based approach more insight can be gained into potential risk factors in patient populations.

Therefore, the research questions of this study were 1) What is the effect of simulated implant material change (PEEK vs. CoCr) on femoral micromotions within a population? 2) Is the primary fixation of a cementless femoral component influenced by patient characteristics (gender, age and BMI), and is there a difference in response as quantified by micromotions between PEEK and CoCr material?

Materials and methods

CT database

An anonymized CT database was created with approval from the ethical committee (reference number METC Oost-Nederland: 2021 - 13277). The patients were initially diagnosed with Kahler's disease. This patient category was selected as these patients undergo high resolution CT scans. The CT scans were checked and confirmed for not containing any pathologies in the knee joint. Gender, age, weight and height were known of these patients. As a result, 35 patients, and subsequently 70 femora, were included with the patient characteristics as listed in Table 4-1.

Gender, n (%)	
M	15 (43%)
F	20 (57%)
Age in years, mean (range)	62 (46 – 75)
Height in m, mean (range)	1.72 (1.55 – 1.90)
Weight in kg, mean (range)	78 (52 – 170)
BMI in kg/m², mean (range)	26 (19 – 49)

Table 4-1. Patient characteristics (n = 35)

Workflow FE model

FE models were created of femoral TKA reconstructions, based on 70 femora. The models were analysed with femoral components simulating either PEEK or CoCr material properties, and were subjected to a gait and squat activity, resulting in 280 simulations. All models were analysed using MSC.Marc FE software (MSC.Marc2020, MSC. Software Corporation, Santa Ana, CA, USA). The models were created using an automated workflow, which is explained below in further detail.

Segmentation

The left and right femur of all patients were segmented and labelled from the CT scans using a convolutional neural network (https://grand-challenge.org/algorithms/ femur-segmentation-in-ct/). The .mha files coming out of the segmentation algorithm were consecutively converted into surface meshes (.stl files).

Orientation of the femur and implant alignment

An anatomical reference frame was assigned to the surface meshes of the femur [9]. The femora were then aligned with the musculoskeletal model that was used to determine the implant-specific contact forces and centres of pressure of the loading conditions (see also "Boundary conditions, loads and contact interactions"). The CAD models of a generic cementless femoral component were available. At first, all implant sizes were rotated to replicate the implant orientation in the musculoskeletal model using a point cloud registration. The size of the femoral component for each specific femur was chosen based on the distance between the femoral anterior flange and the posterior condyles. The femur was then positioned such that overhang at the anterior flange and the posterior condyles was avoided. The implant was placed according to the mechanical alignment strategy.

Bone cuts

The simulated bone cuts were made based on the inner surface of the femoral component using modelling software (HyperMesh 2020, Altair Engineering, Troy, MI, USA). Additionally, the femur was cut on the proximal side at 120 mm from the joint line.

Volume meshing

The surface meshes of the femur and femoral component were converted into volume meshes consisting of tetrahedral elements (HyperMesh 2020, Altair Engineering, Troy, MI, USA). An edge length of 2.0 – 2.5 mm was used for both the femur and implant meshes, according to a previously performed mesh convergence study [10].

Bone material properties assignment

CT values were converted to bone mineral density values for of each bone element using a previously published calibration method that uses the known Hounsfield unit intensities for air, fat and muscle [11]. To allow for simulating permanent deformation of the bone during the virtual implantation, the bone was modelled as an elastic-plastic material, using a Von Mises yield material model [12]. The femoral component was modelled as an elastic isotropic material and assigned with the material properties of either PEEK (3.7 GPa) or CoCr (210 GPa).

Boundary conditions, loads and contact interactions

A single-sided touching algorithm was used to model the interaction between the femoral component and the femur. The friction between the femoral component and femur was modelled using a bilinear coulomb friction model. A coefficient of friction of 0.5 and an interference fit of 500 µm was applied at the anterior, posterior, distal and chamfer regions of the bone-implant interface and defined via the contact algorithm for material conditions [5]. The interference fit was linearly increased during a virtual implantation phase using ten simulation increments until the maximum value of 500 µm was reached, during which plastic deformation of the bone was allowed. Subsequently, the interference fit was kept constant at its maximum value during the loading phase.

Implant-specific tibiofemoral and patellofemoral contact forces and centres of pressure of gait and squat activities were derived from a previously developed musculoskeletal model that was based on the Grand Challenge dataset [13]. The musculoskeletal model was modified by incorporating the femoral and tibial implant design of the current study in the model (Figure 4-1). The patella was included in the musculoskeletal model without a patellar button. The contact forces were scaled based on the patient's bodyweight and applied during four loading cycles to allow for (numerical) settling of the implant. One loading cycle consisted of 73 increments for the gait activity and 67 increments for the squat activity. Furthermore, the femur was fixated on the proximal side in all directions. An example of a model including femur and femoral component is showed in figure 4-2.

Outcome measures

The micromotions were defined as the relative displacements between the bone and the implant in the shearing direction using the same technique as Van der Ploeg et al. [14]. More specifically, the motions of the contact nodes on the implant surface were tracked relative to the contact faces of the bone surface. Each contact node on the implant surface was projected onto the closest contact face on the bone surface. The relative displacement of the contact node on the projected surface was calculated incrementally during the whole simulation. Regions with a large normal gap, for example due to overhang at the anterior flange, and regions of the pegs were excluded from the results. For each model, the resulting micromotions were defined as the largest distance during the full fourth loading cycle. The maximum resulting micromotion value was the maximum value of the contact nodes on the implant interface at a specific moment in time. The 99th percentile of the maximum resulting micromotions was taken to remove the nodes which potentially represented outliers. We analysed the 99th percentile of the maximum resulting micromotions visually via the distributions on the interface of the femoral component and quantitively using violin plots. A violin plot shows the same information as boxplots (median, interquartile range and outliers), but also visualises the distribution of the data. Therefore, violin plots were used to visualize the difference in micromotions between the PEEK and CoCr models and to visualize the micromotions per patient characteristic.

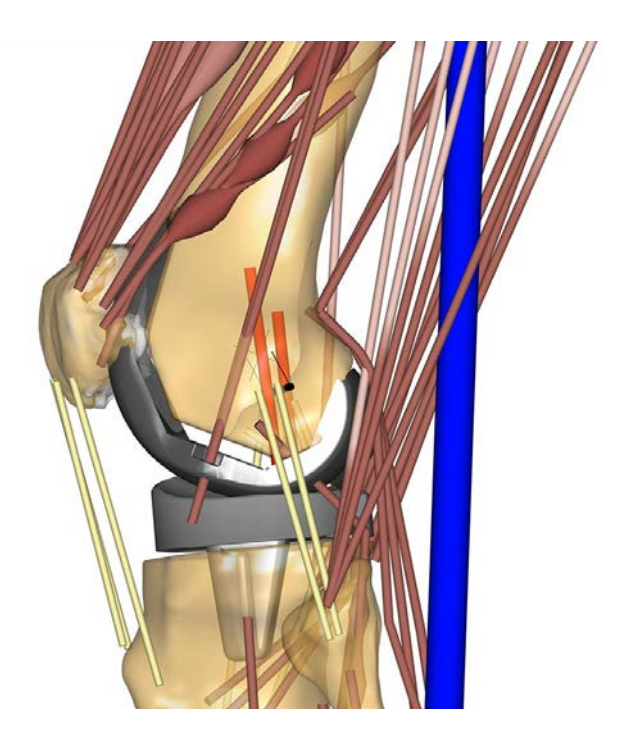


Figure 4-1. Musculoskeletal model including femoral and tibial implant design of the current study.

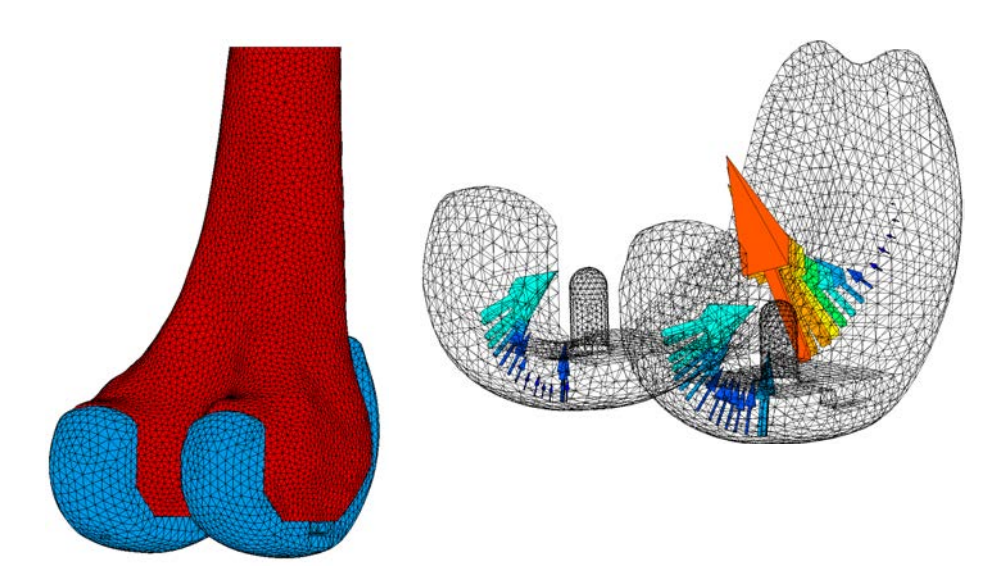


Figure 4-2. Left: model of a right femur including femoral component. The model was fixated on the proximal side in all directions. Right: the medial and lateral tibiofemoral forces and the patellofemoral forces of a squat cycle are represented by the arrows. Larger arrows represent larger forces.

Statistics

A linear mixed model was performed to evaluate statistical significance of the interactions between the micromotions, and the gender, age and BMI of the patients included in the population. Micromotion was taken as the dependent variable, and the fixed effects in our model included gender, age and BMI. The analysis was conducted using IBM SPSS Statistics 27. The results were presented as regression coefficient (β) and its 95% confidence interval.

Results

16 simulations numerically failed to converge due to meshing errors that caused excessive deformations or inside-out elements and were therefore excluded from the data set. Subsequently, 264 of the 280 simulations (132 PEEK simulations and 132 CoCr simulations) were included in the analyses.

Overall, the PEEK models generated larger peak micromotions than the CoCr models (94.7 vs. 75.2 µm on average). For PEEK, the range of peak micromotions varied from 25.5 to 465.6 µm within the simulated cases, whereas for CoCr a range of 19.0 to 234.2 µm was found. Under the gait and squat load, some PEEK models generated slightly smaller peak micromotions than the CoCr models (Figure 4-3).

Distinct differences were seen in the micromotion distributions between the PEEK and CoCr models for both the gait and squat models (Figure 4-3). For the CoCr models, the largest micromotions were concentrated around the tip of the anterior flange, both during gait and squat loads (Figure 4-4 B, D, F, H, J and L). The micromotions in the CoCr models were slightly larger during a squat load than during gait. In the PEEK models the largest resulting micromotions during gait were found at the anterior flange, medial distal region, chamfer regions and the posterior condyles (Figure 4-4 A, C and E). Under a squat load the largest resulting micromotions were found at the anterior flange, lateral regions of the chamfer and distal side and the posterior condyles (Figure 4-4 G, I and K). Hence, micromotions were greater at the tip of the anterior flange in the CoCr models, while the PEEK models displayed greater micromotions in other regions. While the distribution of the micromotions over the implant surfaces was quite consistent for the PEEK and CoCr models, there were distinct differences between specific cases. Figure 4-4 shows micromotion distributions for three cases with a PEEK and CoCr implant with various maximum micromotion values, illustrating the inter-specimen variations seen within the population of models. These results show relatively high

micromotions in the notch area for the PEEK models and at the flange area for the CoCr models (Figure 4-4).

The micromotions of all femoral models significantly increased with BMI: $3.843 \pm 0.600 \, \mu m$ (95% CI: 2.662, 5.024) (P<0.001). Neither gender nor age of the patients had a significant effect on the micromotions of all femoral models. There was no clinically relevant difference in response to BMI between the PEEK and CoCr material properties (Figure 4-5).

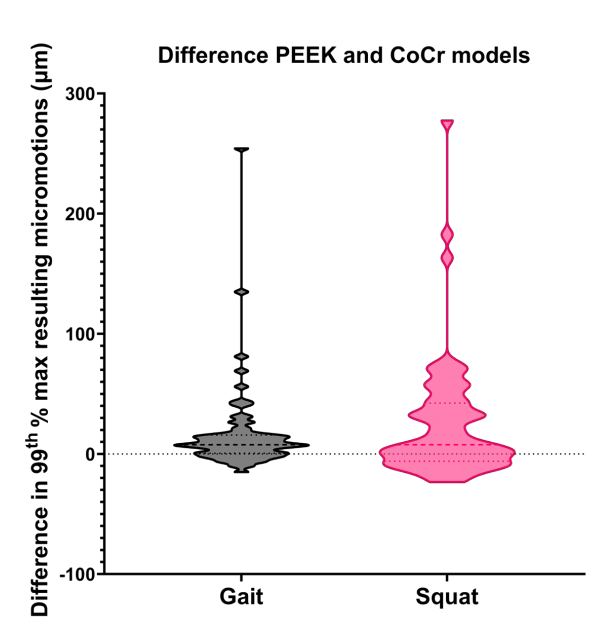
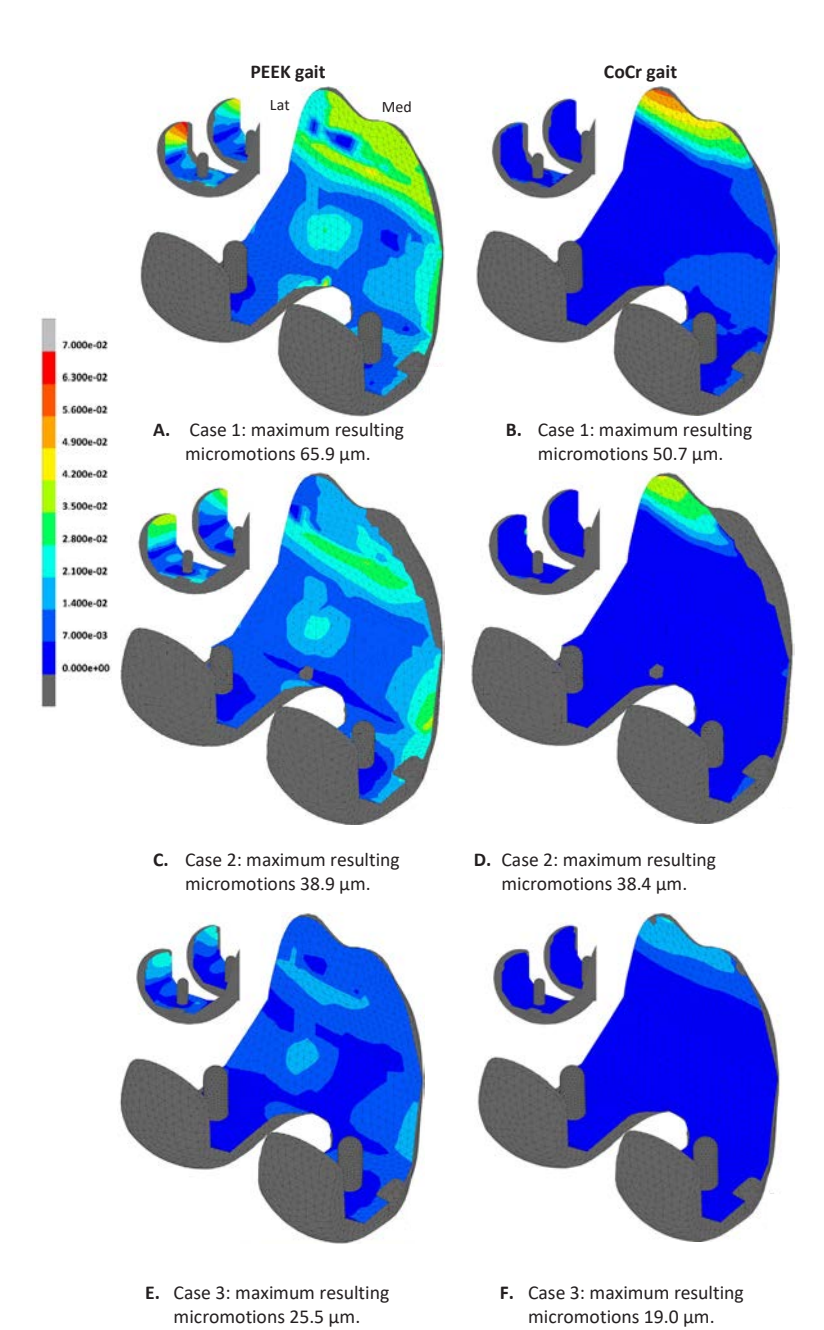


Figure 4-3. Difference in the 99th percentile of the maximum resulting micromotions between the PEEK and CoCr models within all individual subjects of the population for the gait and squat models. Micromotion values for CoCr models were subtracted from PEEK model values for each specific model.



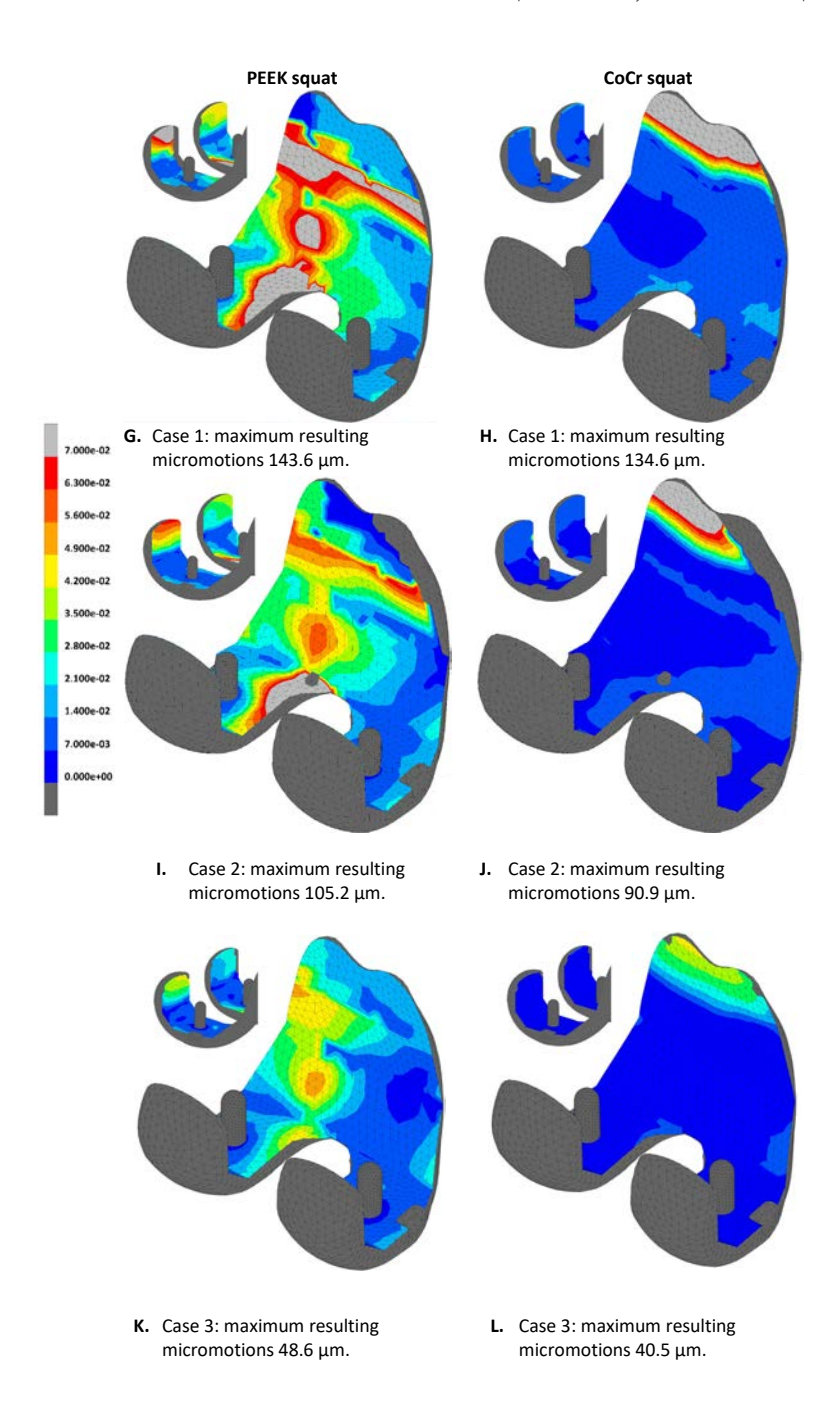


Figure 4-4. Resulting micromotion distribution (mm) at the implant interface of the femoral component after the 4th loading cycle of a gait and squat activity. Case 1: Case with large maximum resulting micromotions within the population (man, left, 56 years, BMI 28.1 kg/m²). Case 2: Case with average maximum resulting micromotions within the population (man, left, 73 years, BMI 26.6 kg/m²). Case 3: Case with small maximum resulting micromotions within the population (woman, left, 54 years, BMI 18.6 kg/m²).

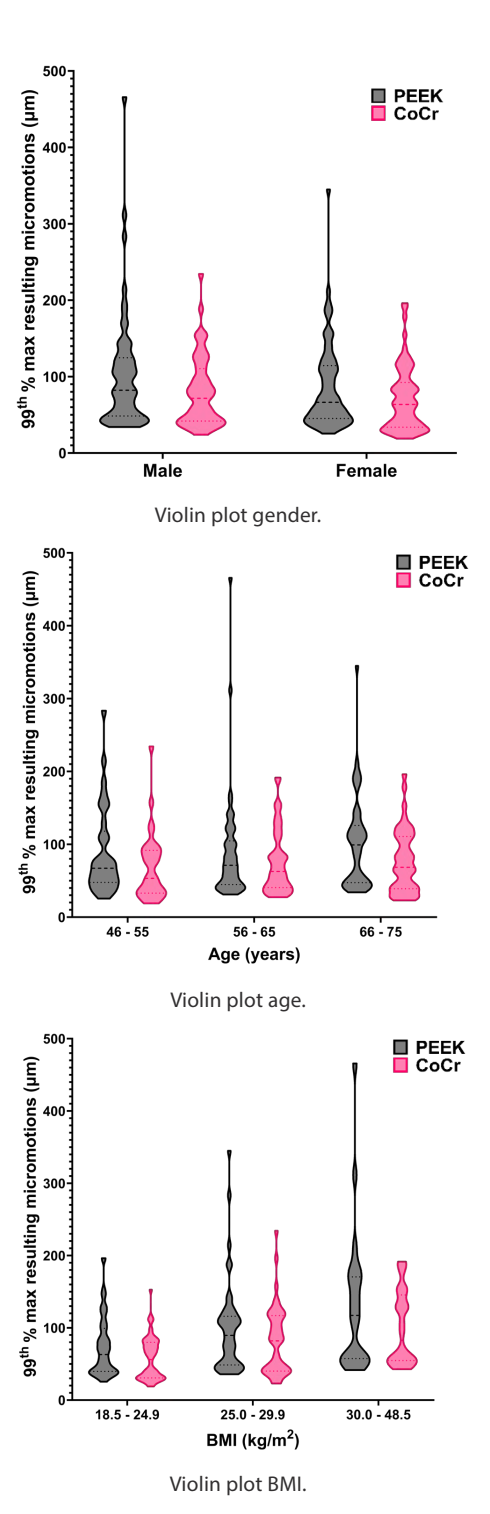


Figure 4-5. Violin plots of gender, age and BMI.

Discussion

In this study we studied the effect of implant material (PEEK vs. CoCr) on femoral micromotions within a population, and investigated the effect of patient characteristics (gender, age and BMI) on these micromotions. The current results show that, within the studied population, the micromotions of a cementless component generally increased when changing the material properties from CoCr to PEEK. Furthermore, the locations of peak micromotions were clearly different between the PEEK and CoCr models. Although the magnitudes of the micromotions were affected by specific bone cases, the distributions of the micromotion patterns were similar and consistent among the cases included in this study showing relatively high micromotions in the notch area for the PEEK models and at the flange area for the CoCr models. Of the included patient characteristics, only BMI had a significant effect on micromotions in both the CoCr and PEEK models.

The overall current finding that PEEK material led to larger micromotions is in agreement with an earlier study in which the effect of material properties (simulating either PEEK or CoCr) of a cementless femoral component were compared in a single model, with parametric variations [5]. In that single model study, the maximum micromotion was 70.1 µm and 15.2 µm for a PEEK and CoCr material, respectively, compared to a median maximum micromotion of 94.7 vs. 75.2 µm in the current study. However, the current study also found some gait and squat models with larger values for the CoCr component than the PEEK component, which emphasizes the importance of including a larger patient population, with more variability, to obtain a more robust outcome of a computational study. Additionally, this study found that the distributions of the micromotions were different for the PEEK models as compared to the CoCr models, which is in contrast with the single-model study. This can be explained by the differences in the loading configurations between the two studies (Orthoload vs. a dedicated musculoskeletal model) and type of activity (jogging vs. gait and squat) that were modelled. The use of implant-specific loading conditions including the patellofemoral forces is therefore important in the investigation of the primary fixation of a cementless PEEK femoral component. Although the maximum micromotions were somewhat higher in the PEEK models, the majority of the implant surface displayed micromotions that were below the threshold of 40 µm for bone ingrowth [15]. Moreover, the actual threshold for osseointegration has been subject of debate, and has been suggested to possibly be as high as 112 µm, based on a systematic review by Kohli et al. [16]. This suggests that also for a PEEK femoral component a large portion of the implant-bone interface has favourable conditions for osseointegration and long-term implant fixation. In addition, while it is obvious from clinical practice that fixation of CoCr femoral components is quite successful, the optimal conditions for implant osseointegration are largely unknown, which makes extending the current computational results to clinical practice challenging.

The optimal circumstances for osseointegration include both biomechanical and biological circumstances. From a biological point of view parameters of importance are good vascularisation, availability of stem cells and appropriate surface properties (porosity and coatings) that stimulate bone apposition. From a mechanobiological point of view biomechanical stimuli such as suggested by Prendergast et al. suggest that 1) low fluid flow and 2) low shearing strains of the newly formed bone, stimulate bone formation [17]. It is likely that these two quantities are related to micromotions as determined in this study, i.e., high micromotions are likely to increase fluid flow and shearing stresses at the interface.

Furthermore, ingrowth of a prosthetic component after implantation is a gradual biological process and bony ingrowth will progressively fixate the implant. Retrieved specimens show that ingrowth can be quite regional and incomplete [18, 19]. Hence, it may be that it is more important to assess whether there are regions of the implant where bone ingrowth will be initiated rather than focussing on peak micromotions as done in this study. Considering the micromotion distributions found in the population cases, low-micromotion areas were found in all cases, independent of the simulated implant material, suggesting appropriate biomechanical conditions to initiate the bone ingrowth process.

The current study furthermore investigated the effect of patient characteristics on primary fixation. From all characteristics, only BMI had a significant effect on the micromotions, with micromotions increasing with BMI. In line with our study, Wan et al. concluded that a high BMI causes higher micromotions in both a gait and deep knee bend activity [7]. On the influence of gender and age on the primary fixation of cementless femoral components is currently not much known. Gibbons et al. studied the risk of implant subsidence in elderly women who are more at risk for osteoporosis [20], and found no increased risk in this patient population. In our study, we also did not find a relation with elderly women and higher risk of large micromotions. However, it is expected that the reduced bone quality in this patient group would have an influence on the primary fixation of cementless femoral components. A more extensive population-based study including information on the bone quality of the femurs would therefore be required. Additional research is furthermore required to elucidate the relation between implant stiffness and primary

4

fixation, and whether there is an optimal stiffness that provides a good balance between primary fixation and long-term effects such as stress shielding.

It should be noted that there are a number of limitations of this study that affect interpretation of the results. As described above, the first limitation is related to the description of the bone quality in this study. While the patient-specific bone density distribution was incorporated in the FE models, a single parameter describing the overall bone quality, that can be used as a comparison within the studied population, was lacking, restricting statistical analysis of the effect of the overall bone quality on primary fixation. A second limitation is related to the missing values due to simulations that did not converge. Numerical none-convergence could be related to the (numerical) instability at the bone-implant interface, suggesting that circumstances that decrease stability would lead to more none-converged cases. However, we could not find any clear indications (e.g., like lower elastic moduli of bone or implant) that could explain the numerical instability of the cases. Another limitation of this study is the limited number of cases included. While this population study is a first start in the analysis of the influence of patient characteristics on the primary fixation of cementless femoral components, a larger study is required for the analysis of the outliers which may provide more detailed information on specific risk factors for patients receiving a TKA. Additionally, although we did incorporate plasticity of the bone during implant insertion, we did not include viscoelastic behaviour of the bone, while this may have an influence on the compressive forces generated by the interference fit. Another point to raise is the fact that this FE study was a parametric study; the material properties of the simulated component geometry were allocated with either CoCr or PEEK elastic properties and the effect on initial fixation assessed. In reality, a PEEK component will be provided with an ingrowth surface, typically made by titanium, which could increase overall stiffness. This could have an effect on the initial fixation of the component, but was not taken into account in the current study. Also, a single implant alignment strategy was adopted, while variations in alignment may lead to differences in the loading configuration, possibly affecting micromotions at the implant-bone interface. Lastly, the models simulated in our study were generated with a nominal implant-bone interface, while surgical cuts that can occur in clinical practice may influence the primary fixation of cementless femoral components, leaving gaps at the interface and creating less optimal conditions for bone ingrowth.

In conclusion, the current population study gives insights into the primary fixation and its variation of a cementless femoral component in a cohort of computational models with varying patient characteristics. Although the distributions of the micromotions were similar within this population, the differences in micromotion magnitudes were observed amongst the cases. PEEK models generated larger maximum micromotions than the CoCr models (94.7 vs. 75.2 μm, respectively) except for a few squat models. BMI was a significant parameter in the primary fixation of cementless femoral components. The results indicate that implant-specific loading conditions, including the patellofemoral forces, are essential for testing a cementless PEEK femoral component.

Future work will focus on a more in-depth multivariate analysis to investigate the effect of interactions of patient characteristics, including bone quality, and implant fixation. Moreover, an outlier analysis of a larger population may provide more insights in potential risk factors in patient characteristics for the primary fixation of cementless femoral components.

References

- 1 Hofmann, A.A., R.D. Bloebaum, and K.N. Bachus, Progression of human bone ingrowth into porouscoated implants. Rate of bone ingrowth in humans. Acta Orthop Scand, 1997. 68(2): p. 161-6.
- Nishio, F., et al., Radiopaque properties of polyetheretherketone crown at laboratory study. J Oral 2 Biosci, 2023. 65(3): p. 253-258.
- 3 de Ruiter, L., et al., A preclinical numerical assessment of a polyetheretherketone femoral component in total knee arthroplasty during gait. J Exp Orthop, 2017. 4(1): p. 3.
- Rankin, K.E., et al., Does a PEEK Femoral TKA Implant Preserve Intact Femoral Surface Strains 4. Compared With CoCr? A Preliminary Laboratory Study. Clin Orthop Relat Res, 2016. 474(11): p. 2405-2413.
- Post, C.E., et al., A FE study on the effect of interference fit and coefficient of friction on the micromotions and interface gaps of a cementless PEEK femoral component. J Biomech, 2022. 137: p. 111057.
- Basdelioğlu, K., Effects of body mass index on outcomes of total knee arthroplasty. Eur J Orthop Sur & Tra, 2020. 31(3): p. 595-600.
- 7. Wan, Q., et al., The influence of body weight index on initial stability of uncemented femoral knee protheses: A finite element study. Heliyon, 2023. 9(3): p. e13819.
- 8. Daniilidis, K., et al., Does BMI influence clinical outcomes after total knee arthroplasty? Technol Health Care, 2016. 24(3): p. 367-75.
- Miranda, D.L., et al., Automatic determination of anatomical coordinate systems for threedimensional bone models of the isolated human knee. J Biomech, 2010. 43(8): p. 1623-6.
- 10. Berahmani, S., et al., FE analysis of the effects of simplifications in experimental testing on micromotions of uncemented femoral knee implants. J Orthop Res, 2016. 34(5): p. 812-9.
- 11. Eggermont, F., et al., Calibration with or without phantom for fracture risk prediction in cancer patients with femoral bone metastases using CT-based finite element models. PLoS One, 2019. 14(7): p. e0220564.
- 12. Keyak, J.H., et al., Predicting proximal femoral strength using structural engineering models. Clin Orthop Relat Res, 2005(437): p. 219-28.
- 13. Marra, M.A., et al., Evaluation of a Surrogate Contact Model in Force-Dependent Kinematic Simulations of Total Knee Replacement. J Biomech Eng, 2017. 139(8).
- 14. van der Ploeg, B., et al., Toward a more realistic prediction of peri-prosthetic micromotions. J Orthop Res, 2012. 30(7): p. 1147-54.
- 15. Engh, C.A., et al., Quantification of Implant Micromotion, Strain Shielding, and Bone Resorption With Porous-Coated Anatomic Medullary Locking Femoral Prostheses. Clin Orthop Relat Res, 1992. 285: p. 13-29.
- 16. Kohli, N., J.C. Stoddart, and R.J. van Arkel, The limit of tolerable micromotion for implant osseointegration: a systematic review. Sci Rep, 2021. 11(1): p. 10797.
- 17. Prendergast, P.J., R. Huiskes, and K. Soballe, BIOPHY SICAL STIMULI ON CELLS DURING TISSUE DIFFERENTIATION AT IMPLANT INTERFACES. Journal of Biomechanics, 1997. 30: p. 539-548.
- 18. Hanzlik, J.A., J.S. Day, and G. Acknowledged Contributors: Ingrowth Retrieval Study, Bone ingrowth in well-fixed retrieved porous tantalum implants. J Arthroplasty, 2013. 28(6): p. 922-7.
- 19. Hanzlik, J.A., et al., Is There A Difference in Bone Ingrowth in Modular Versus Monoblock Porous Tantalum Tibial Trays? J Arthroplasty, 2015. 30(6): p. 1073-8.
- 20. Gibbons, J.P., et al., Is Cementless Total Knee Arthroplasty Safe in Women Over 75 Y of Age? J Arthroplasty, 2023. 38(4): p. 691-699.



Chapter 5

The sensitivity of the micromotions of a cementless PEEK tibial component to the interface characteristics

Corine Post, Thom Bitter, Adam Briscoe, Nico Verdonschot, Dennis Janssen

Submitted to Medical Engineering & Physics

Abstract

Total knee arthroplasty (TKA) components from a material with stiffness properties similar to the human bone, such as polyetheretherketone (PEEK), can be used to reduce peri-prosthetic stress-shielding. In cementless fixation, a proper primary fixation is a requirement for the long-term fixation. The primary fixation may be dependent on both the interference fit and coefficient of friction. Therefore, this finite element (FE) study investigated the effect of interference fit and coefficient of friction on the primary fixation of a cementless PEEK tibial component, compared with a cementless titanium tibial component which served as clinical default component. 144 FE models of the tibia, tibial tray and insert were created with variations in implant material, interference fit and coefficient of friction. No distinct differences were seen in the micromotion values and distributions between the PEEK and titanium models. Neither the interference fit nor the coefficient of friction had a major impact on the micromotions. Additionally, the majority of the cases remained below the ingrowth threshold of 40 µm. This study provides insights in the application of cementless PEEK tibial components.

Introduction

Tibial peri-prosthetic stress-shielding is the phenomenon that the physiological loading situation in the tibia is disturbed due to the insertion of an implant from a material stiffer than the human bone [1]. Due to this disturbance, bone resorption can take place which may result in aseptic loosening of the implant or even peri-prosthetic fractures of the tibia [2]. To overcome this problem, total knee arthroplasty (TKA) components from a material with stiffness properties similar to the human bone can be used. Polyetheretherketone (PEEK) has stiffness properties in the range of human bone and is already clinically implemented in craniomaxillofacial and spine surgery due to its favourable durability and biocompatibility [3]. Furthermore, the lack of any metal in TKA components gives the opportunity of helping patients who suffer from metal hypersensitivity and allows for easier analysis of the peri-prosthetic tissue with modalities such as MRI and CT in case of implant failure [4].

Although cemented fixation of the TKA is considered as the golden standard, cementless fixation is gaining popularity, especially among specific patient categories (i.e., young, physically active and obese patients) in which cemented fixation has a high failure rate [5]. In cementless fixation, an adequate primary fixation is a requirement for the long-term fixation through growth of bone onand into the implant surface. Primary fixation is achieved through compressive and shearing forces acting at the bone-implant interface, which are dependent on the interference fit and the coefficient of friction. The interference fit is determined by the dimensional difference between the bone cuts and the internal implant surface, leading to compressive forces at the interface during the implantation process. The shearing forces are influenced by the coefficient of friction, which amongst others depends on the roughness of the implant surface [6].

Several studies have investigated the effect of interference fit and coefficient of friction on the primary fixation of cementless knee components [7-10]. However, it is currently unknown how the primary fixation of a cementless PEEK tibial component is affected by the interference fit and coefficient of friction. Additionally, there are studies on the use of an isoelastic material for the stem of the total hip arthroplasty to avoid stress-shielding [11, 12]. However, these studies reported that these more flexible stems produced high stem/ bone interface stresses and consequently large micromotions. The question becomes whether this is also a consequence of using more flexible materials for the cementless tibial component. The two aims of this finite element (FE) study were therefore to determine whether a cementless PEEK tibial component generates larger micromotions than a cementless titanium tibial component and subsequently to determine the effect of interference fit and coefficient of friction on the primary stability of a cementless PEEK tibial component, both by simulating the micromotions at the bone-implant interface. A cementless titanium tibial component served as a clinically relevant control component.

Materials and methods

3D models of five left and four right tibiae of five fully anonymized cardiovascular patients were created based on their CT scans, resulting in nine tibial models. These tibial models were converted into FE models using a previously developed workflow [13]. Consecutively, the following steps were executed: (1) Segmentation of the tibia, (2) Implant alignment, (3) Preparation of bone cuts and mesh, (4) Material properties assignment, and (5) Assignment of boundary conditions, loads and contact interactions.

Seamentation

In the first step of the workflow, the nine knees were segmented based on graphcut segmentation and a bone boundary enhancement filter [14]. Subsequently, surface meshes of the tibial bones were made based on the binary voxel masks. The tibial bones were then aligned according to their anatomical reference frame [15].

Implant alignment

The alignment of the tibial tray and polyethylene insert was performed relative to the anatomical reference frame. The CAD model of a cementless cruciateretaining tibial tray and insert were provided by the manufacturer (Freedom knee, Maxx Orthopedics, Norristown, PA, USA). The mechanical alignment technique was applied consisting of a 3° varus rotation and 3° posterior slope. The internalexternal rotation of the implant was applied by aligning the centre of the tray with the medial third of the tibial tubercle as reference point. All tibiae were implanted with a well-matching size six implant, representing an average implant size.

Bone cuts and mesh preparation

The proximal tibial bone cuts were created using a cutting plane based on the internal implant surface, while the tibiae were cut distally at a length of 150 mm. The surface meshes of the tibia, tibial tray and insert were then converted into solid meshes with tetrahedral elements (HyperMesh 2020, Altair Engineering, Troy, MI, USA). An element size of 2.0 mm was chosen based on a previous convergence study [16].

Material properties assignment

The bone was modelled as an elastic-plastic material [16]. A previously published calibration method was used for converting the Hounsfield units of the CT scan into the bone mineral density values for each bone element [17]. This calibration method uses the Hounsfield unit intensities of air, fat and muscle tissues to define the bone density properties of the bone elements. A Young's modulus of either PEEK (PEEK-OPTIMA™ - 3700 MPa), or titanium (109,000 MPa) was assigned to the tibial tray. The insert was modelled with the material properties for ultra high molecular weight polyethylene (UHMWPE - 974 MPa).

Boundary conditions, loads and contact interactions

A touching contact was defined between the tibial tray and the bone. The friction was applied with a Coulomb bilinear displacement friction model. Two different values of coefficient of friction were analysed representing a more commonly used coefficient of friction of 0.5, and a more extreme value of 1.5 [18].

Two values of interference fit were investigated, 500 and 750 µm, representing an average and high interference fit value [10]. The interference fit was applied through the contact algorithm and applied on the whole implant surface that was in contact with the bone. The interference fit was applied over the whole tibial tray surface continuously to avoid any numerical errors. An initial displacement with a magnitude of the interference fit value was applied to the tibial tray and the insert to prevent unrealistic pushing-out of the tibial implant. An implantation phase was simulated in which the interference fit was linearly increased, followed by a loading phase in which the forces were applied.

Sampled tibiofemoral forces and moments from a gait and squat activity of the Orthoload database for an extreme case with a bodyweight of 100 kg were applied to the medial and lateral articulating surfaces of the tibial insert [19]. The forces and moments were incrementally applied, with 25 increments representing one loading cycle. Four loading cycles were simulated to allow for (numerical) settling of the implant [16]. The final results were taken from the fourth loading cycle.

The nine tibial bones were modelled with all variations of tibial tray material, interference fit, coefficient of friction and loading condition, resulting in 144 FE models in total (MSC.Marc2021.4, MSC. Software Corporation, Santa Ana, CA, USA).

Outcome measures

For all 144 simulations, the micromotions were determined. These micromotions were determined by considering the contact nodes on the implant interface and the corresponding closest contact faces on the bone interface. The relative motions in the shearing direction between the contact node on the implant interface and the closest contact face on the bone interface were calculated as the micromotions. The largest possible distance between the contact node and contact face during the fourth loading cycle was taken and defined as the maximum resulting micromotion value [20]. The micromotions on both the tray and the stem were included in the analysis. However, the areas having a large normal gap, for instance due to overhang, were removed from the results. Micromotion values lower than 40 µm were assumed to be favourable for long-term osseointegration [21].

For each simulation, the 95th percentile of the maximum resulting micromotions was taken to remove the nodes with any potential numerical outliers. Moreover, the distributions of the micromotions were visualized on the interface of the tibial tray.

Results

One simulation of a left tibia failed to converge and was therefore left out of the analysis (titanium, squat, interference fit = $500 \mu m$, coefficient of friction = 0.5). Subsequently, 143 of the 144 simulations were included in the analyses.

No distinct differences were seen in the micromotion distributions between the PEEK and titanium models on both the tray and the stem. For both implant materials the largest micromotions were located at the posterior lateral side of the tibial tray (Figure 5-1 A-D). When increasing the interference fit from 500 to 750 µm the largest micromotions were seen at the posterior lateral side and the anterior side of the tibial tray (Figure 5-1 E-H). No substantial differences were seen in the micromotion distributions on the stem between the models with varying interference fit and coefficient of friction

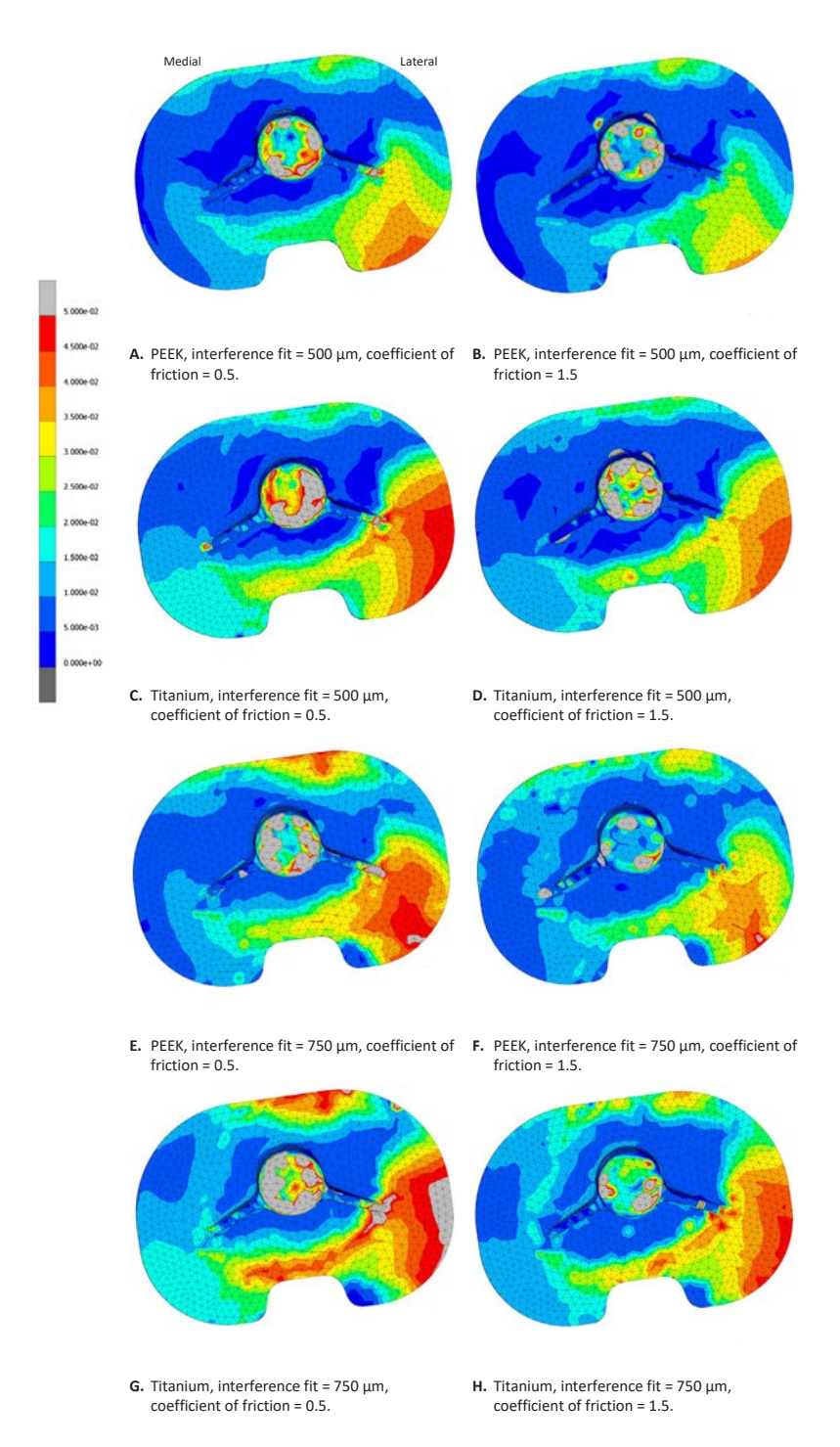


Figure 5-1. Resulting micromotion (mm) distribution at the implant interface of a left model after the 4th loading cycle of a gait activity.

The gait load resulted in larger micromotions than the squat load (Figure 5-2). Neither the interference fit nor the coefficient of friction had a major impact on the peak micromotions of the cementless PEEK tibial component (Figure 5-2). Additionally, the 95th percentile of micromotions were similar between the PEEK and titanium tibial component (Figure 5-2). In none of the cases micromotions exceeded 150 µm, and in the majority of the cases micromotions remained below the ingrowth threshold of 40 µm.

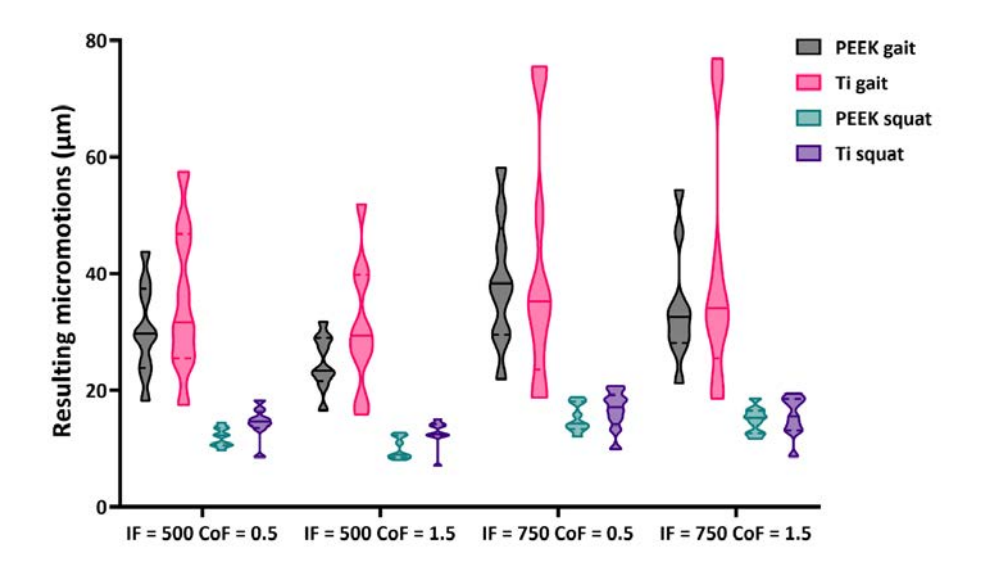


Figure 5-2. 95th percentile of the resulting micromotions (µm) of all models. These values were calculated for the whole interface including the tray and the stem. IF = Interference Fit, CoF = Coefficient of Friction.

Discussion

The two aims of this study were to determine whether a cementless PEEK tibial component generates larger micromotions than a cementless titanium tibial component and subsequently to determine the effect of interference fit and coefficient of friction on the micromotions of a cementless PEEK tibial component, relative to a cementless titanium tibial component that served as a control. The current results show that the micromotions for the PEEK and titanium tibial components were similar, and that variations in interference fit and coefficient of friction only had a minor effect on the primary fixation.

The fact that interference fit only had a negligible effect on micromotions in the current tibial simulations for both the PEEK and titanium models, is in contradiction with earlier findings with a PEEK femoral TKA component, where increasing the interference fit led to a reduction in micromotion values [22]. These findings are, however, similar to previous findings of Sanchez et al., who investigated the effect of interference fit on the primary fixation of a cementless tibial component in experiments with tibial cadaver reconstructions [10]. Although an increase in interference fit leads to an increase in compressive forces at the implant-bone interface, this study and the experiments of Sanchez et al. found that this does not notably influence the primary fixation. However, the optimal interference fit value may differ between specific implant designs; a too large interference fit may result in excessive compressive forces and consequently tibial fractures. More research with implant designs with different fixation features is required to obtain better insights in optimal interference fit values.

The coefficient of friction, similarly to the interference fit, only had a moderate effect on the micromotions in the current tibial simulations. Friction at the boneimplant interface is important for achieving implant stability as this is dependent on both the compressive and shearing, frictional, forces [6]. The friction of the bone-implant interface can be adjusted by changing the roughness of the implant surface for example by the addition of a coating. While on the one hand a large friction coefficient may increase the shear stresses at the implant-bone interface, it also makes it more difficult to fully seat the tibial component, and may therefore affect the implantation process.

While the primary fixation of cementless PEEK tibial components has not been studied previously, there are studies that investigated the primary fixation of cementless titanium tibial components. The study of Gonzalez et al. found micromotion values ranging from 20 to 80 µm in their tibial models [7]. Awadalla et al. found 95th percentiles of the peak micromotions in the range of 10 to 40 µm [8]. While these values are in a similar range as the micromotion values found in the current study, there are some differences in the specific definition of the micromotions. Most studies define micromotions as an absolute point-to-point displacement between nodes on the implant and bone interface, while the current study reported the shearing component of this displacement as micromotions, as defined by the study of Van der Ploeg et al. [20]. Other differences include the material model used to represent the bone. In our simulations bone was modelled as an elastic-plastic material, representing the non-linear yielding processes occurring in the bone during implant insertion, while using a linear elastic material model for bone may lead to an underestimation of the micromotions [23]. The finding of similar micromotion values for the PEEK and titanium models are in contradiction with earlier findings of a cementless PEEK femoral component in which larger micromotions were reported for the PEEK model compared to the cobalt-chrome model [22]. An explanation on this could be that the bending stiffness around the tibial tray is of less importance than the bending stiffness around the hip stems and femoral knee component [12].

The distributions of the micromotions at the implant-bone interface are slightly different from the micromotion distributions presented by Gonzalez et al., who found that the largest micromotions at the anterior lateral side of the tibial tray [7]. Our models also presented large micromotions on the posterior side of the tibial tray. This difference may be explained by a different way in applying the loads on the tibial models. Gonzalez et al. found the specific loading locations on the lateral and medial condyles for their specific implant design, while we used the loading location derived from the Orthoload database.

There are several limitations in this study that could be improved in future research. A first limitation is related to the validation of the FE models. The, in this study, used mesh size for the FE models are based on a mesh convergence study of the study of Berahmani et al. [16]. However, that was a study on the femoral side. In this study we assume that this method should be reliable on the tibial side as well. However, experimental testing needs to be performed to validate the results of the current FE study. A second limitation is related to the loading conditions that were applied to the models. The loading conditions used in this study were derived from the Orthoload database and based on a knee implant including an ultra-congruent tibial insert. In that design both cruciate ligaments were sacrificed, with loads that normally are transferred through the posterior cruciate ligament are transferred through the implant. The ultra-congruent design furthermore results in a limited femoral rollback. The application of more physiological loading conditions including the centres of pressure is therefore recommended for future research. Another limitation that needs to be discussed is associated with the bone models used in this study. Since the patient characteristics were unknown, the micromotion values could not be related to variations specific patient characteristics such as gender, age or weight. Furthermore, one simulation of a left tibia failed to converge and was therefore left out of the analysis (titanium, squat, interference fit = 500 μm, coefficient of friction = 0.5). Although we did incorporate plasticity of the bone during implant insertion, we did not include viscoelastic behaviour of the bone, while this may have an influence on the compressive forces generated by the

interference fit. Lastly, the models simulated in our study are generated with an optimal implant alignment. Variations in surgical cuts may influence the primary fixation of cementless tibial components.

In conclusion, the cementless PEEK tibial component generated similar resulting micromotions as the cementless titanium tibial component. Micromotions were hardly sensitive to variations of interference fit and coefficient of friction. This FE study provides insights in the application of cementless PEEK tibial components. Future work includes assessment of a larger population of models to investigate the influence of patient-related parameters and surgical cutting variations on micromotion outliers.

References

- Au, A.G., et al., Contribution of loading conditions and material properties to stress shielding near the tibial component of total knee replacements. Journal of Biomechanics, 2007. 40(6): p. 1410-1416.
- Lachiewicz, P.F., J.R. Steele, and S.S. Wellman, Unexpected high rate of revision of a modern 2. cemented fixed bearing modular posterior-stabilized knee arthroplasty. Bone Joint J, 2021. 103-B(6 Supple A): p. 137-144.
- 3. Kurtz, S.M. and J.N. Devine, PEEK biomaterials in trauma, orthopedic, and spinal implants. Biomaterials, 2007. 28(32): p. 4845-69.
- Nishio, F., et al., Radiopaque properties of polyetheretherketone crown at laboratory study. J Oral Biosci, 2023, 65(3); p. 253-258.
- Uivaraseanu, B., et al., Highlighting the advantages and benefits of cementless total knee 5. arthroplasty (Review). Exp Ther Med, 2022. 23(1): p. 58.
- 6. de Vries, E., et al., Predicting friction at the bone - Implant interface in cementless total knee arthroplasty, J Mech Behav Biomed Mater, 2022. 128: p. 105103.
- Quevedo Gonzalez, F.J., et al., Mechanical performance of cementless total knee replacements: It 7. is not all about the maximum loads. J Orthop Res, 2019. 37(2): p. 350-357.
- Awadalla, M., et al., Influence of varying stem and metaphyseal sleeve size on the primary stability of cementless revision tibial trays used to reconstruct AORI IIA defects. A simulation study. J Orthop Res, 2018. 36(7): p. 1876-1886.
- Navacchia, A., et al., Validation of model-predicted tibial tray-synthetic bone relative motion in cementless total knee replacement during activities of daily living. J Biomech, 2018. 77: p. 115-123.
- 10. Sanchez, E., et al., No effect in primary stability after increasing interference fit in cementless TKA tibial components. J Mech Behav Biomed Mater, 2021. 118: p. 104435.
- 11. Trebse, R., et al., Poor results from the isoelastic total hip replacement: 14-17-year follow-up of 149 cementless prostheses. Acta Orthop, 2005. 76(2): p. 169-76.
- 12. Huiskes, R., H. Weinans, and B. van Rietbergen, The Relationship Between Stress Shielding and Bone Resorption Around Total Hip Stems and the Effects of Flexible Materials. Clin Orthop Relat Res, 1992. 274: p. 124 - 134.
- 13. Anijs, T., et al., Population-based effect of total knee arthroplasty alignment on simulated tibial bone remodeling. J Mech Behav Biomed Mater, 2020. 111: p. 104014.
- 14. Krcah, M., G. Szekely, and R. Blanc, Fully automatic and fast segmentation of the femur bone from 3D-CT images with no shape prior. Proceedings - International Symposium on Biomedical Imaging, 2011: p. 2087-2090.
- 15. Miranda, D.L., et al., Automatic determination of anatomical coordinate systems for threedimensional bone models of the isolated human knee. J Biomech, 2010. 43(8): p. 1623-6.
- 16. Berahmani, S., et al., FE analysis of the effects of simplifications in experimental testing on micromotions of uncemented femoral knee implants. J Orthop Res, 2016. 34(5): p. 812-9.
- 17. Eggermont, F., et al., Calibration with or without phantom for fracture risk prediction in cancer patients with femoral bone metastases using CT-based finite element models. PLoS One, 2019. 14(7): p. e0220564.
- 18. Berahmani, S., et al., An experimental study to investigate biomechanical aspects of the initial stability of press-fit implants. J Mech Behav Biomed Mater, 2015. 42: p. 177-85.
- 19. Bergmann, G., et al., Standardized loads acting in knee implants. PLoS One, 2014. 9(1): p. e86035.

- 20. van der Ploeg, B., et al., Toward a more realistic prediction of peri-prosthetic micromotions. J Orthop Res, 2012. 30(7): p. 1147-54.
- 21. Engh, C.A., et al., Quantification of Implant Micromotion, Strain Shielding, and Bone Resorption With Porous-Coated Anatomic Medullary Locking Femoral Prostheses. Clinical Orthopaedics and Related Research, 1992. 285: p. 13-29.
- 22. Post, C.E., et al., A FE study on the effect of interference fit and coefficient of friction on the micromotions and interface gaps of a cementless PEEK femoral component. J Biomech, 2022. 137: p. 111057.
- 23. Berahmani, S., D. Janssen, and N. Verdonschot, Experimental and computational analysis of micromotions of an uncemented femoral knee implant using elastic and plastic bone material models. J Biomech, 2017. 61: p. 137-143.



Chapter 6

The effect of patient related factors on the primary fixation of PEEK and titanium tibial components: a population-based FE study

Corine Post, Thom Bitter, Adam Briscoe, Inger van Langen, René Fluit, Nico Verdonschot, Dennis Janssen

Published in Bioengineering: https://doi.org/10.3390/bioengineering11020116

Abstract

Polyetheretherketone (PEEK) is of interest as implant material for cementless tibial total knee arthroplasty (TKA) components due its potential advantages. One main advantage is that the stiffness of PEEK closer resembles the stiffness of bone, potentially avoiding peri-prosthetic stress-shielding. When introducing a new implant material for cementless TKA designs, it is essential to study its effect on the primary fixation. The primary fixation may be influenced by patient factors such as age, gender and body mass index (BMI). Therefore, the research objectives of this finite element (FE) study were to investigate the effect of material (PEEK vs. titanium alloy) and patient characteristics on the primary fixation (i.e., micromotions) of a cementless tibial tray component. 296 FE models of 74 tibiae were created with either PEEK or titanium material properties, under gait and squat loading conditions. Overall, the PEEK models generated larger peak micromotions than the titanium models. Differences were seen in the micromotion distributions between the PEEK and titanium models for both the gait and squat models. The micromotions of all tibial models significantly increased with BMI, while gender and age did not influence micromotions.

Introduction

While titanium currently is the default material for cementless tibial total knee arthroplasty (TKA) components, polyetheretherketone (PEEK-OPTIMA™) is of interest as an alternative implant material due to its potential advantages. First, PEEK can be used as implant material in patients with metal hypersensitivity [1]. Second, metal artefacts on MRI and CT images are avoided during the analysis of the peri-prosthetic tissue with a non-metal TKA [2]. Lastly, from a biomechanical perspective and with a potentially even larger effect. PEEK has a stiffness similar to human bone, which may contribute to avoiding peri-prosthetic stress-shielding [3, 4]. However, this difference in stiffness between PEEK and titanium may also influence the primary fixation.

The primary fixation of the cementless tibial component is essential for bone growth on- and into the implant surface, which occurs during the first few weeks to months after the TKA procedure [5]. This primary fixation (before ingrowth has occurred) is governed by the compressive and shearing forces that are generated during the implantation of the press-fit components, and retained to some extent during dynamic loading. Apart from the frictional properties of the implant surface, the primary fixation depends on the design and material of the titanium component. When introducing a new implant material for TKA designs, it is therefore important to study its effect on the primary fixation.

The primary fixation can be evaluated by studying micromotions between the tibial bone and tray. A systematic review of Kohli et al. reported a micromotion threshold of 112 µm for osseointegration [6]. Such micromotions can be studied using computational tools such as finite element (FE) analysis. Earlier FE studies on the cementless PEEK tibial component focused on the analysis of a tibial model with parametric variations on the interface characteristics [7]. However, in clinical practice the outcome may be influenced by patient factors such as age, gender and body mass index (BMI). For instance, several studies have investigated the influence of BMI on the outcomes of TKA [8-10]. While there has been controversy on whether or not a high BMI negatively affects the primary fixation, a recent study has shown that a high BMI causes larger micromotions in reconstructions with metal implants [9]. The influence of a high BMI on the primary fixation of a cementless PEEK tibial component, however, is currently unknown. We hypothesize that BMI may jeopardize the primary fixation of cementless tibial implants and that this effect may be more pronounced in cementless PEEK implants than cementless titanium implants. By adopting a population-based approach we aim to gain more insight into potential risk factors in patient populations.

The research questions of this study were 1) What is the effect of simulated implant material (PEEK vs. titanium) on tibial micromotions within a population? 2) Is the primary fixation of a cementless tibial tray influenced by patient characteristics (gender, age and BMI), and 3) is there a difference in response as quantified by micromotions between PEEK and titanium material?

Materials and Methods

CT database

An anonymized CT database was created with ethical committee approval (reference number METC Oost-Nederland: 2021 – 13277). The patients included in this CT database were originally diagnosed with Kahler's disease. This diagnosis was chosen as these patients undergo high resolution CT scans with a field of view that includes both knee joints. All CT scans were checked for not having pathologies in the knee joint. Additionally, gender, age, weight and height were collected. In total 74 tibiae (37 left) of 41 patients were included in the study (Table 6-1).

Gender, n (%)	
M	15 (37%)
F	26 (63%)
Age in years, mean (range)	63 (46 – 75)
Height in m, mean (range)	1.71 (1.55 – 1.99)
Weight in kg, mean (range)	79 (52 – 170)
BMI in kg/m², mean (range)	26 (18 – 49)

Table 6-1. Patient characteristics (n = 41)

Workflow FE model

74 FE models were created of tibial TKA reconstructions with a tibial tray and a polyethylene insert. The models were analysed with tibial trays with either PEEK or titanium material properties, and were subjected to a gait and squat activity, resulting in 296 simulations in total. The models were created using an automated workflow, which is explained below in further detail.

Segmentation

The left and right tibia of all patients were segmented from the CT scans using a convolutional neural network (https://grand-challenge.org/algorithms/tibiasegmentation-in-ct/) [11]. The .mha segmentation files produced by the algorithm were subsequently converted into surface meshes (.stl files) using Matlab (Mathworks Inc. 2021b, Natick, MA, USA).

Orientation of the tibia and implant alignment

An anatomical reference frame was assigned to the surface meshes of the tibia based on a previously defined coordinate system [12]. The tibiae were then aligned according to the orientation of the musculoskeletal model that was used to determine the implant-specific contact forces and centres of pressure of the loading conditions (see also "Boundary conditions, loads and contact interactions"). A coherent point drift registration was performed to find the rotation and translation for aligning the tibiae with the musculoskeletal model. CAD models of a generic cementless tibial tray and tibial insert were used. The size of the tibial tray and insert were chosen by inspecting the overlap of the contact area of the tibial tray with the cutting area of the proximal tibia. The proximal tibia was cut 8.9 mm distally from the articulating surface, such that the tibia including tibial tray and tibial insert were the same length as the length of the original tibia. The tibial tray size was chosen such that the bone surface was covered optimally with a maximum allowed overhang of 2 mm.

Bone cuts

The simulated bone cuts were made based on the distal surface of the tibial component using modelling software (HyperMesh 2020, Altair Engineering, Troy, MI, USA), achieving an ideal implant-bone interface. Additionally, the tibia was cut distally at 100 mm from the joint line.

Volume meshing

The surface meshes of the tibia, tibial tray and tibial insert were converted into volume meshes consisting of tetrahedral elements (HyperMesh 2020, Altair Engineering, Troy, MI, USA). An edge length of 2.0 – 2.5 mm was used for both the tibia, tibial tray and tibial insert meshes, according to a previously performed mesh convergence study [13].

Bone material properties assignment

CT values were converted to bone mineral density values for of each bone element using a calibration method that uses the known Hounsfield unit intensities for air, fat and muscle [14]. Typical Young's modulus values for trabecular and cortical bone are in a range of 5.0 – 20.5 GPa [15]. To allow for simulating permanent deformation of the bone during the virtual implantation, the bone was modelled as an elasticplastic material using a Von Mises yield material model [16]. The tibial tray and tibial insert were modelled as an elastic isotropic material. The tibial tray was assigned with the material properties of either PEEK (3.7 GPa) or titanium (109 GPa). The tibial insert was modelled with the material properties for ultra high molecular weight polyethylene (0.974 GPa) (Table 6-2).

Component	Material	Stiffness (GPa)
Tibia	Bone	5.0-20.5
Tibial tray	PEEK Titanium	3.7 109
Tibial insert	Ultra high molecular weight polyethylene	0.974

Table 6-2. Material properties FE model

Boundary conditions, loads and contact interactions

A single-sided touching algorithm was used to model the interaction between the tibial tray and the tibial bone. Friction between the tibial tray and tibia was modelled using a bilinear coulomb friction model. A coefficient of friction of 0.5 and an interference fit of 500 um were applied through the contact algorithm on the whole implant surface that was in contact with the bone [17]. To obtain the desired interference fit of 500 µm, the interference fit was linearly increased during a virtual implantation phase. During the virtual implantation phase, typically, elastic and plastic deformations would occur in the bone, near the interface with the implant. The interference fit was kept constant at its maximum value during the loading phase.

Implant-specific tibiofemoral contact forces and centres of pressure of gait and squat activities were derived from a musculoskeletal model that was modified by incorporating the current femoral and tibial implant design in the model [18]. The forces varied during the activities, with a maximum value of 1514 N. The centres of pressure were adapted according to the implant size. The contact forces were scaled based on the patient's bodyweight and applied during four loading cycles to allow for (numerical) settling of the implant. One loading cycle consisted of 73 increments for the gait activity and 67 increments for the squat activity. The tibia was fixated at the distal end in all directions. An example of a model including tibia, tibial tray and tibial insert is shown in figure 6-1.

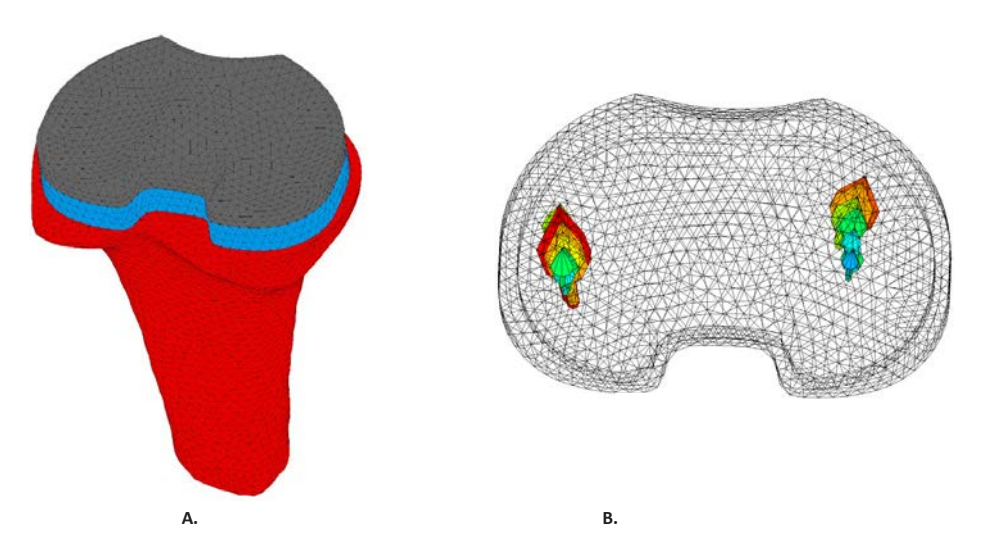


Figure 6-1. A. Model of a right tibia (red) including tibial tray (blue) and tibial insert (grey). The model was fixated distally in all directions. B. The medial and lateral tibiofemoral forces of a squat cycle are represented by the arrows. Larger arrows represent larger forces.

Outcome measures

The micromotions were defined as the relative displacements between the bone and the implant in the shearing direction using the same technique as Van der Ploeg et al. [19]. More specifically, the motions of the contact nodes on the implant surface were tracked relative to the contact faces of the bone surface. Each contact node on the implant surface was projected onto the closest contact face on the bone surface. The relative displacement of the contact node on the projected surface was calculated during the whole simulation. Regions with a large normal gap, for example due to overhang, were excluded from the results. For each model, the resulting micromotions were defined as the largest distance during the full fourth loading cycle. The maximum resulting micromotion value was the maximum value of the contact nodes on the implant interface at a specific moment in time. The 95th percentile of the maximum resulting micromotions was taken to remove the nodes which potentially represented outliers. We analysed the 95th percentile of the maximum resulting micromotions visually via the distributions on the interface of the tibial tray and quantitatively using violin plots. A violin plot shows the median, interquartile range and outliers (similar to a boxplot), but also visualises the distribution of the data.

Statistics

A linear mixed model was performed to evaluate statistical significance of the interactions between micromotions, and gender, age and BMI of the patients included in the population. Micromotion was taken as the dependent variable, and the fixed effects included gender, age and BMI. The analysis was conducted using IBM SPSS Statistics 27. The results were presented as regression coefficient (β) and its 95% confidence interval.

Results

Overall, the PEEK models generated larger peak micromotions than the titanium models (68 vs. 39 µm on average). For PEEK, the range of peak micromotions varied from 32.7 to 210.4 µm, while for titanium a range of 6.8 to 90.3 µm was found. Under the squat load the PEEK models generated larger peak micromotions than the titanium models, while under the gait load some PEEK models generated slightly smaller peak micromotions than the titanium models (Figure 6-2).

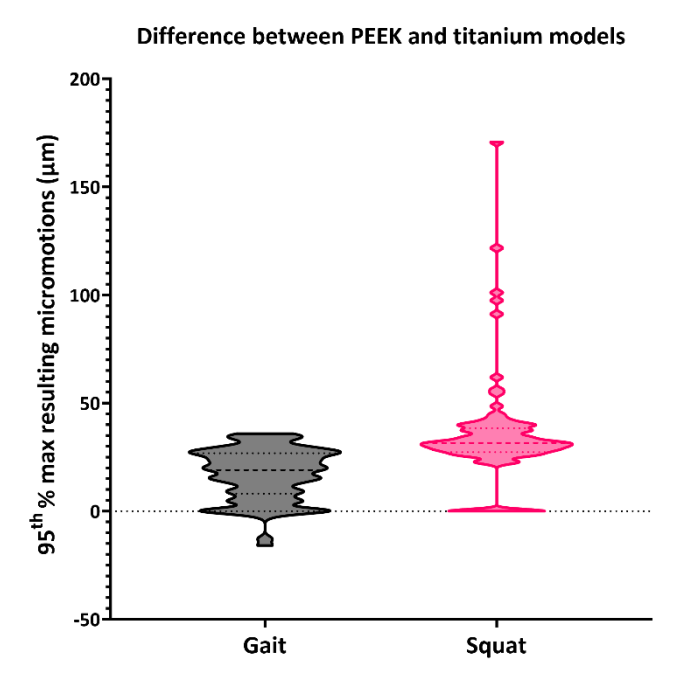
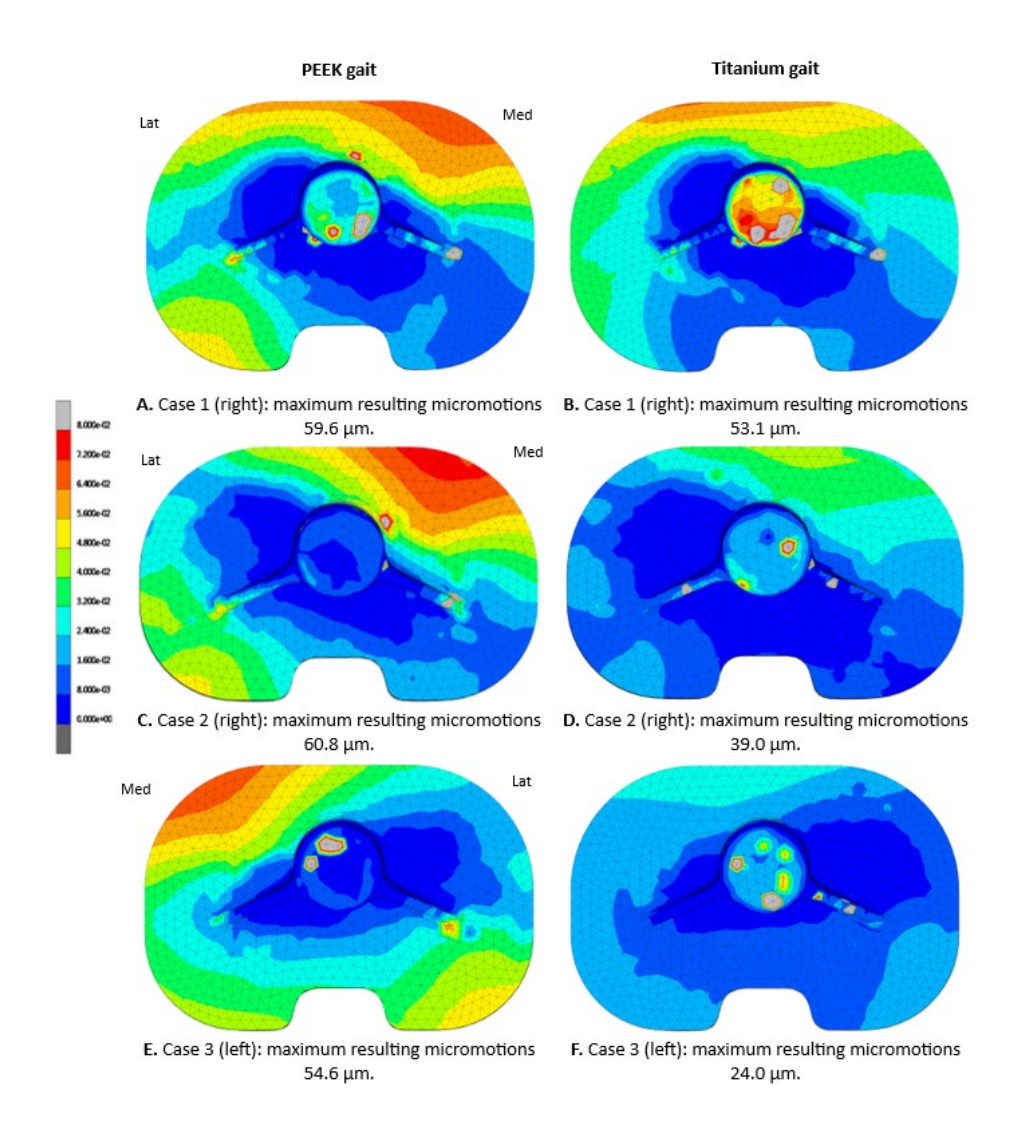


Figure 6-2. Difference in the 95th percentile of the maximum resulting micromotions between the PEEK and titanium models within all individual subjects of the population for the gait and squat models. Micromotion values for titanium models were subtracted from PEEK model values for each specific model.

Differences were seen in the distribution of the micromotions between the PEEK and titanium models for both the gait and squat models. Figure 6-3 shows the micromotion distributions for three specific cases within the population, with a PEEK and titanium tibial tray with relatively large (case 1), average (case 2) and small (case 3) maximum resulting micromotions, emphasizing the variations seen within this population of tibial models. For the titanium models, the largest resulting micromotions were concentrated around the anterior side of the tibial tray, both during the gait (Figure 6-3 B, D and F) and squat activity (Figure 6-3 H, J and L). The micromotions seen in the titanium models were comparable under squat and gait loads. In the PEEK models, the largest resulting micromotions under gait load were found at the anterior medial side and posterior lateral side (Figure 6-3 A, C and E). During the squat activity, the largest resulting micromotions were concentrated on the lateral side both anteriorly and posteriorly (Figure 6-3 G, I and K).

The micromotions of all tibial models significantly increased with BMI: $1.563 \pm 0.254 \, \mu m$ (95% CI: 1.064, 2.063) (P<0.001) (Figure 6-4). This was independent on the implant material. Neither gender (P=0.639) nor age (P=0.251) of the patients had a significant effect on the micromotions.



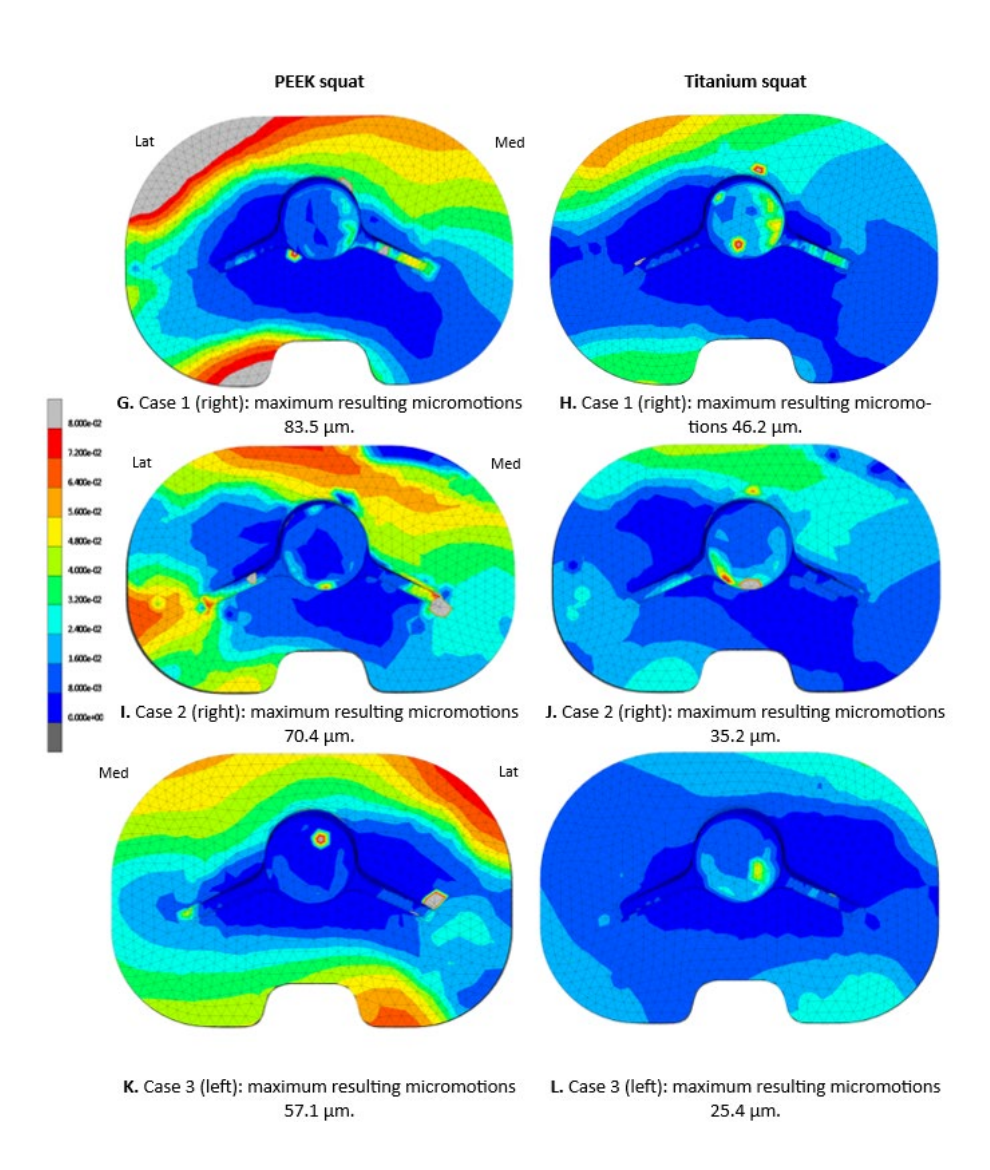
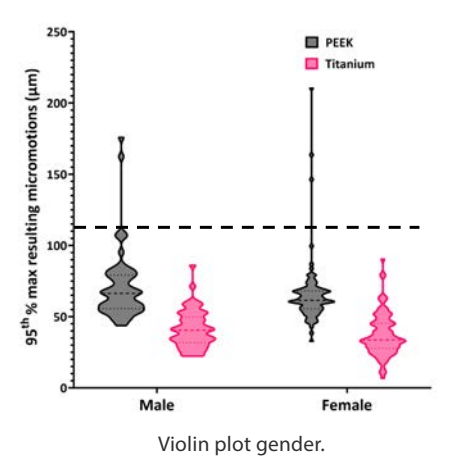


Figure 6-3. Resulting micromotion distribution (mm) at the implant interface of the tibial tray after the 4th loading cycle of a gait and squat activity. Case 1: Case with large maximum resulting micromotions within the population (man, right, 70 years, BMI 19.2 kg/m²). Case 2: Case with average maximum resulting micromotions within the population (woman, right, 62 years, BMI 31.2 kg/m2). Case 3: Case with small maximum resulting micromotions within the population (woman, left, 62 years, BMI 24.0 kg/m²).



250 PEEK Titanium 200 Titanium

Violin plot age (years).

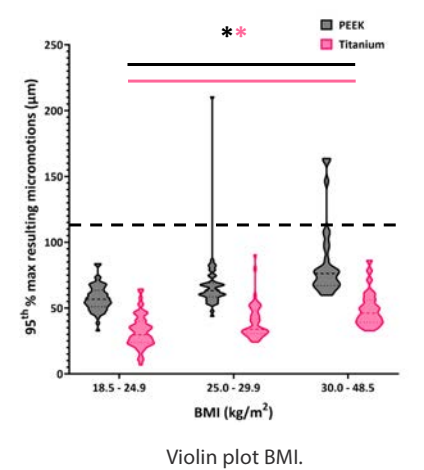


Figure 6-4. Violin plots of gender, age and BMI. Statistically significant interactions are indicated with an asterisk. The dotted line represents the osseointegration threshold of 112 μ m [6].

Discussion

In this study, we assessed the effect of tibial tray material (PEEK vs. titanium) on tibial micromotions within a population and studied the influence of the patient characteristics gender, age and BMI on these micromotions. The results of the current FE study indicate that, within the current cohort of models, peak tibial micromotions were larger for the tibial trays with PEEK material properties than for the tibial trays with titanium material properties. However, only relatively small differences were seen in the distributions of the peak micromotions on the tibial tray between the PEEK and titanium models. Additionally, the locations of the micromotions were similar among the cases included in this cohort, with in general higher micromotions on the anterolateral and medial side and the posterolateral side. The magnitude of the micromotions, however, were clearly different among the cases. In this cohort only BMI had a significant influence on micromotions in both the PFFK and titanium models.

The overall current finding that PEEK material led to larger micromotions is not in agreement with an earlier study in which the effect of material properties (simulating either PEEK or titanium) of a cementless tibial component were compared with parametric variations of the interface characteristics [7]. In that study, no distinct differences were seen in the micromotion values and distributions between the PEEK and titanium models. In addition to the fact that only a limited number of cases was studied, this may be due to the fact loads were applied in a different way (using Orthoload data with a single load application point vs. the application of more physiological loading conditions including shifting centres of pressure in the current study). The application of implant-specific loading conditions that include the shift of the centres of pressure seems essential when investigating the primary fixation of a cementless PEEK tibial component. This is also in agreement with a study of Gonzalez et al., who also used implant-specific loading locations and found similar micromotion distributions as in the current study, with the largest micromotions at the anterolateral side of the tibial tray [20].

The average maximum micromotion value in our previous study was around 40 µm for both a PEEK and titanium material, while in the current study the average maximum micromotion was 68 µm and 39 µm for PEEK and titanium implants, respectively. In the current study we also found gait models with larger micromotion values for the titanium component than the PEEK component, which emphasizes the importance of including a larger patient population with inherently a wider range of patient variations, to obtain more robust results.

While the maximum resulting micromotions were higher in the PEEK models, the micromotions were below the threshold of 112 µm for bone ingrowth at the vast majority of the implant surface [6, 21]. However, as indicated by the systematic review of Kohli et al. the threshold for osseointegration has been subject to debate. A threshold of 112 µm would, however, indicate that also for a PEEK tibial component a large portion of the implant-bone interface has favourable conditions for osseointegration and long-term implant fixation. Nonetheless, extending the current computational results to clinical practice is challenging. In the current study we focused on the peak micromotions to assess the primary fixation, while there may be regions on the tibial tray surface that are more important for the primary fixation than others. Such knowledge, either from animal studies or clinical retrieval studies, may provide valuable additional information for the interpretation of the current results.

In the current study, only BMI had a significant effect on the micromotions, with a higher BMI leading to higher micromotions. In line with this result, Wan et al. concluded that a high BMI causes higher micromotions in both a gait and deep knee bend activity [9]. We also considered the effect of weight instead of BMI, which also was a statistically significant parameter in the linear mixed model. However, as BMI is a widely accepted parameter that also takes into account the body composition, we chose BMI over bodyweight as a primary patient factor. Currently, not much is known on the influence of gender or age on the primary fixation of cementless tibial components. Gibbons et al. studied the risk of implant subsidence in elderly women who are more at risk for osteoporosis, and found no increased risk in this patient population [22]. In our study, we did not find a correlation between elderly women and large micromotions, either. However, it is expected that the reduced bone quality influences the primary fixation, as a good bone quality is a prerequisite. A larger population with a more in-depth analysis of BMD may be required to further elucidate this relation.

There are several limitations to the current study that may affect the interpretation of the results. As mentioned earlier, the first limitation refers to the bone quality of the models in this study. The analysis of a single parameter describing the overall bone quality of the models would have been useful for analysing the effect of bone quality on micromotions. The second limitation relates to the number of cases included in this study. Although this is the first simulation study on the effect of patient characteristics on the primary fixation of cementless tibial components, a study including more cases is required for the analysis of the outliers, which may provide more detailed information on specific risk factors for patients receiving

a TKA. Additionally, although we did incorporate plasticity of the bone during implant insertion, we did not include viscoelastic behaviour of the bone, while this may influence the compressive forces generated by the interference fit. Only a single implant alignment strategy was adopted, while variations in alignment may lead to differences in the loading configuration, possibly affecting micromotions at the implant-bone interface. Similarly, ligament and muscles were not included in the current loading configuration. Another point refers to the implementation of BMI in the models by using a bodyweight correction of the applied forces. A larger bodyweight led to higher forces and therefore larger micromotions. However, a similar correction was not made for gender, age, or related changes in activity levels. Lastly, the models simulated in our study were generated with an idealized implant-bone interface, while cutting errors that occur in clinical practice may influence the primary fixation, leaving gaps at the interface and creating less optimal conditions for bone ingrowth.

Conclusions

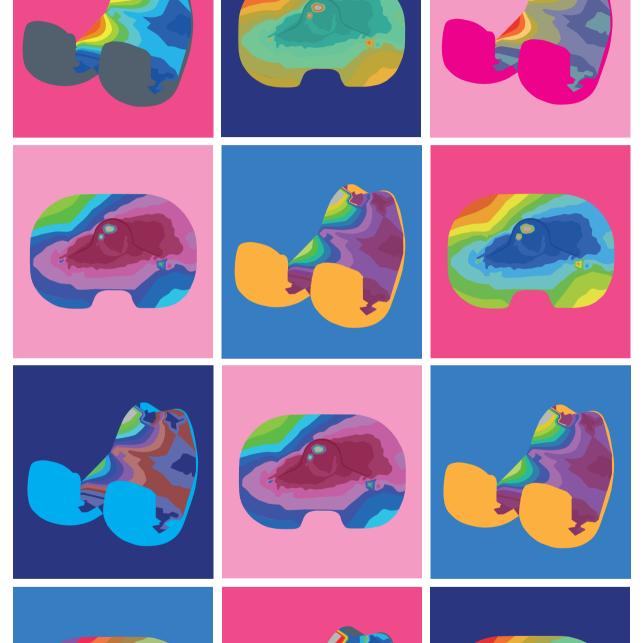
In conclusion, the current population study provides insights into the variation in primary fixation of a cementless tibial component in a cohort of computational models with varying patient characteristics. Although the distributions of the micromotions were comparable within this population, large differences in micromotion values were observed amongst the cases. PEEK models generated larger maximum micromotions than the titanium models except for a few gait models. BMI was a significant affecting parameter in the primary fixation of cementless tibial components.

Future research should focus on further elucidating the association between implant stiffness and primary fixation, and whether there is an optimal stiffness that provides a good balance between primary fixation and long-term effects such as stress shielding. In addition, a more in-depth multivariate analysis is required to highlight the effects of interactions of patient characteristics, including bone quality, bone geometry, bone density and implant fixation. Finally, an outlier analysis of a larger population may provide more insights into potential risk factors in patient characteristics for the primary fixation of cementless femoral components.

References

- 1 Innocenti, M., et al., Metal hypersensitivity after knee arthroplasty: fact or fiction? Acta Biomed, 2017. 88: p. 78-83.
- Nishio, F., et al., Radiopaque properties of polyetheretherketone crown at laboratory study. J Oral 2. Biosci, 2023. 65(3): p. 253-258.
- 3. de Ruiter, L., et al., A preclinical numerical assessment of a polyetheretherketone femoral component in total knee arthroplasty during gait. J Exp Orthop, 2017. 4(1): p. 3.
- Rankin, K.E., et al., Does a PEEK Femoral TKA Implant Preserve Intact Femoral Surface Strains 4. Compared With CoCr? A Preliminary Laboratory Study. Clin Orthop Relat Res, 2016. 474(11): p. 2405-2413.
- Hofmann, A.A., R.D. Bloebaum, and K.N. Bachus, Progression of human bone ingrowth into porous-coated implants. Rate of bone ingrowth in humans. Acta Orthop Scand, 1997. 68(2): p. 161-6.
- Kohli, N., J.C. Stoddart, and R.J. van Arkel, The limit of tolerable micromotion for implant osseointegration: a systematic review. Sci Rep, 2021. 11(1): p. 10797.
- Post, C.E., et al., The sensitivity of the micromotions of a cementless PEEK tibial component to the interface characteristics SSRN, 2023.
- Başdelioğlu, K., Effects of body mass index on outcomes of total knee arthroplasty. Eur J Orthop Sur & Tra, 2020. 31(3): p. 595-600.
- Wan, Q., et al., The influence of body weight index on initial stability of uncemented femoral knee protheses: A finite element study. Heliyon, 2023. 9(3): p. e13819.
- 10. Daniilidis, K., et al., Does BMI influence clinical outcomes after total knee arthroplasty? Technol Health Care, 2016. 24(3): p. 367-75.
- 11. Sendak, M.P., et al., Presenting machine learning model information to clinical end users with model facts labels. NPJ Digit Med, 2020. 3: p. 41.
- 12. Miranda, D.L., et al., Automatic determination of anatomical coordinate systems for threedimensional bone models of the isolated human knee. J Biomech, 2010. 43(8): p. 1623-6.
- 13. Berahmani, S., et al., FE analysis of the effects of simplifications in experimental testing on micromotions of uncemented femoral knee implants. J Orthop Res, 2016. 34(5): p. 812-9.
- 14. Eggermont, F., et al., Calibration with or without phantom for fracture risk prediction in cancer patients with femoral bone metastases using CT-based finite element models. PLoS One, 2019. 14(7): p. e0220564.
- 15. Keyak, J.H. and Y. Falkinstein, Comparison of in situ and in vitro CT scan-based finite element model predictions of proximal femoral fracture load. Medical Engineering & Physics, 2003. 25(9): p. 781-787.
- 16. Keyak, J.H., et al., Predicting proximal femoral strength using structural engineering models. Clin Orthop Relat Res, 2005(437): p. 219-28.
- 17. Post, C.E., et al., A FE study on the effect of interference fit and coefficient of friction on the micromotions and interface gaps of a cementless PEEK femoral component. J Biomech, 2022. 137: p. 111057.
- 18. Marra, M.A., et al., Evaluation of a Surrogate Contact Model in Force-Dependent Kinematic Simulations of Total Knee Replacement. J Biomech Eng, 2017. 139(8).

- 19. van der Ploeg, B., et al., Toward a more realistic prediction of peri-prosthetic micromotions. J Orthop Res, 2012. 30(7): p. 1147-54.
- 20. Quevedo Gonzalez, F.J., et al., Mechanical performance of cementless total knee replacements: It is not all about the maximum loads. J Orthop Res, 2019. 37(2): p. 350-357.
- 21. Engh, C.A., et al., Quantification of Implant Micromotion, Strain Shielding, and Bone Resorption With Porous-Coated Anatomic Medullary Locking Femoral Prostheses. Clin Orthop Relat Res, 1992. 285: p. 13-29.
- 22. Gibbons, J.P., et al., Is Cementless Total Knee Arthroplasty Safe in Women Over 75 Y of Age? J Arthroplasty, 2023. 38(4): p. 691-699.



Chapter 7

Summary and general discussion

Summary and general findings

The main goal of this thesis was to investigate the feasibility of using polyethere-therketone (PEEK) as a material for cementless total knee arthroplasty (TKA) implants. Finite element (FE) studies were performed to gain knowledge on the effect of PEEK on the primary fixation of femoral and tibial TKA implants. These findings were compared against implants made of metal alloys that currently are being used for TKA implants, such as cobalt-chrome (CoCr) for femoral and titanium alloy for tibial components. Since the primary fixation may be influenced by variations of the implant interface characteristics and patient characteristics, these were both investigated in our studies.

The effect of interference fit and coefficient of friction was investigated both in **chapter 2** on the femoral side and **chapter 5** on the tibial side. In **chapter 2** four different values of interference fit (250, 500, 750 and 1000 µm) and three different values of coefficient of friction (0.5, 1.0 and 1.5) were simulated in a single femoral FE model including femur and femoral component with either PEEK or CoCr material properties. Peak loads of a jogging activity were applied as loading conditions. In this study, we found that the micromotions and interface gaps were both sensitive to the interference fit, coefficient of friction and implant material. It was concluded that the PEEK femoral component generated higher micromotions and interface gaps compared to the CoCr femoral component. Furthermore, the highest interference fit value led to micromotion values in the PEEK models that were similar to the CoCr models with an interference fit that is common in current implant systems.

On the other hand, the micromotions of a tibial component were quite insensitive to variations in interference fit and coefficient of friction as concluded by **chapter 5**, in which interference fit values of 500 and 750 µm and coefficient of friction values of 0.5 and 1.5 were investigated. In this study, 144 FE models of the tibia, tibial tray and insert were created with variations in implant material (PEEK and titanium), interference fit and coefficient of friction. Additionally, both gait and squat activities were modelled. No distinct differences were seen in the micromotion values between the PEEK and titanium tibial models. And, as aforementioned, neither the interference fit nor the coefficient of friction had a major impact on the micromotions.

In **chapter 3** the PEEK femoral implant design was modified by adding a titanium inlay on the inner implant interface as this may improve the primary fixation while

maintaining the favourable stiffness properties. That study investigated the effect of inlay thickness and stiffness variations on primary fixation and peri-prosthetic bone strains. Therefore, the FE model of the femur including femoral component of chapter 2 was created including five variations of titanium inlay. As outcome measures, we quantified the micromotions and the strain energy density. Adding an inlay led to an overall decrease in micromotions when compared to a PEEK component without an inlay. Furthermore, the inlay variations all only had a minor effect on bone strains. It was therefore concluded that the addition of a titanium inlay could lead to a reduction of the micromotions without substantially affecting the favourable properties of PEEK with regard to bone stress-shielding.

Chapters 4 and 6 describe the results of population studies of the femoral and tibial model, respectively. Both studies gave insight into the primary fixation of PEEK implants in a cohort of computational models with varying patient characteristics. In chapter 4, 280 FE models of 70 femora were created with varying implant material (PEEK and CoCr) and loading conditions. Implant-specific tibiofemoral and patellofemoral contact forces and centres of pressure of a gait and squat activity derived from a musculoskeletal model were applied to the models. Overall, the PEEK models generated larger peak micromotions than the CoCr models. Additionally, the conclusion was that the micromotions of all models significantly increased with BMI and not with gender and age. Moreover, the variation in micromotion magnitudes amongst the cases within the simulated population confirm the need for population-based modelling.

In chapter 6, a total of 296 FE models of 74 tibiae were created with either PEEK or titanium material properties and either gait or squat implant-specific loading conditions derived from a musculoskeletal model. Same as in chapter 4 on the femoral side, it was concluded that the PEEK models overall generated larger peak micromotions than the titanium models. The micromotions of all tibial models significantly increased with BMI, while gender and age did not influence the micromotions.

Clinical implementation

The findings of the research presented in this thesis provides valuable input for the design process of PEEK femoral and tibial TKA implants, but also give insights into fixation principles of current metal TKA designs. For PEEK implants specifically, the FE tools developed here can be used to optimize the implant design, for instance by investigating the optimal interplay of material thickness, inlay characteristics, interference fit, and the required frictional properties. Prior to clinical evaluation physical testing is recommended to confirm the computational findings in stability tests. Subsequently, clinical safety studies can confirm the actual functionality and survival in patients.

The PEEK prosthesis is currently tested in a clinical setting in its cemented form. Currently 14 patients are included with signs of metal allergy and received an all-poly total knee replacement consisting of a cemented polyethylene tibial component and a cemented PEEK femoral component. The near future will show whether the PEEK component fulfils the pre-clinical expectations.

While the population-based models in chapters 4 and 6 already provided some insights into the effect of clinical variations on the primary stability, patient characteristics such as age, gender, and BMI may influence clinical outcomes to a broader extent than studied in the current thesis.

One of the factors influenced by age and gender is the level of osteoporosis in a patient. Osteoporosis is a condition that is mainly observed in older patients, and even more pronounced in post-menopausal women. The reduced bone mineral density may affect the primary stability, and therefore is an important factor to take into account. On the long term, osteoporotic patients may be more susceptible to bone loss induced by stress shielding. PEEK has been demonstrated to produce a more physiological transfer of forces through the bones [1, 2], and therefore may aid in reducing or preventing peri-prosthetic bone adaptation in patients that are more at risk. However, PEEK also requires a relatively high initial bone quality for obtaining proper primary stability which could be a reason why the use of PEEK may not be recommended in these patients. It is therefore logical to first test the functioning of the PEEK component in patients with a relatively high bone quality before expanding the clinical studies to osteoporotic patients.

An additional risk of osteoporosis is that it can impede metabolic processes in the bone, and may therefore affect the osseointegration of the implant. Osseointegration occurs over a period of weeks to months after surgery, during which the bone grows on- and into the porous surface of the implant. A study of Aro et al. [3] observed that patients with low bone mineral density (osteopenia or osteoporosis) exhibited increased migration of a cementless femoral stem within the initial three postoperative months, attributed to the lack of osseointegration. Osteoporosis obviously is less pronounced in younger patients, which means this patient category generally has a better bone stock at the primary surgery. However, considering their longer life expectancy, also for these patients maintaining bone

stock is important, to ensure an extended survival of the TKA reconstruction. However, results from arthroplasty registries indicate that younger patients currently have a much higher revision rate than older patients [4]. This elevated risk of revision is often attributed to the fact that young patients are more active, and therefore require more from their joint replacement. On the one hand, using PEEK as material for TKA components may reduce stress-shielding and help maintaining better bone quality on the long term, supported by the favourable initial bone stock. On the other hand, a more flexible implant may be more susceptible to the elevated loads of more demanding patients. Further fundamental and clinical research is required to determine the optimal configuration of a PEEK TKA design that adequately addresses these aspects, particularly considering that TKA is becoming more and more popular under an increasingly younger patient group.

Our population studies indicated that a high BMI leads to significantly higher micromotions both in metal and PEEK TKA implants. There is an ongoing debate in the orthopaedic community on whether or not there is a limit to BMI beyond which TKA should not be considered. Besides comorbidities and elevated infection risks associated with obesity, our simulations indicated larger micromotions for PEEK TKA implants compared to metal TKA implants. It is therefore important to closely monitor the effect of BMI on survival in clinical trials to identify whether or not obesity causes an elevated risk for PEEK TKA components.

Future perspectives

Early failure of the TKA may be prevented by achieving a robust primary fixation. The computational results in this thesis provide an initial understanding of the primary fixation of a cementless PEEK TKA implant. Supplementary in vitro testing is required to further expand this understanding. After extensive pre-clinical testing, clinical trials and follow-up studies are essential to demonstrate the functionality of a PEEK TKA implant in the patient. In such a clinical trial dual x-ray absorptiometry analysis (DEXA) scanning may be useful to confirm the bone maintenance in the patient. Moreover, roentgen stereophotogrammetric analysis (RSA) may provide insights in primary fixation, by comparing measurements in loaded and unloaded condition (cyclic inducible motions), and can demonstrate long term fixation in follow-up studies.

In the current thesis, we mainly focused on the analysis of micromotions as a measure for primary stability of TKA reconstructions with PEEK and metal implants. As already discussed in several chapters, the interpretation of the current findings is subject to debate, as it is currently unknown which micromotion values are optimal for bone ingrowth. Moreover, the exact definition of micromotions is guite variable. In experimental studies micromotions are often measured as changes in point-to-point distances between locations on the implant and bone, typically at a certain distance from the exact interface. These experimental micromotions may be subject to elastic deformations of the bone near and at the actual interface, as shown by detailed tribological analyses [5]. In computational models micromotions are generally quantified at the actual interface, by tracking motions between the bone and implant at the contact surface. However, even in computational studies the exact definition may vary: some models (such as the current thesis) make a distinction between in-plane motions and out-of-plane gaps, while others report complete motions. Also, the simulation of an activity (e.g., gait or squat) that is subdivided in multiple increments requires following the complete motion path during a cycle, which is different from quasi-static simulations that consist of a single loading instance. These differences complicate the interpretation of micromotions, but also the comparison against thresholds that may use different metrics. It is therefore necessary to, also in future studies, clearly describe the definition of the metrics used. Moreover, introducing a uniform definition of micromotions within the biomechanical research field would improve the comparison of the outcomes of research in this research area. Additionally, the question remains whether the micromotion thresholds known from the current literature could be used. Therefore, studies may be performed in which similar fixation metrics are compared between a new PEEK TKA design and an already proven TKA design.

Additionally, with respect to the micromotions, this thesis mainly focused on the peak micromotions, generally ignoring the distribution of micromotions. The process of bone ingrowth may be initiated on a surface where micromotions are small. Subsequently, the implant will be stabilised which will decrease the micromotions. Then, a larger region of bone ingrowth will follow. A more indepth analysis on the micromotion distributions may therefore provide additional information on regions that have favourable conditions for osseointegration, that potentially could provide secondary stabilization on the long term with progression of bone ingrowth. In addition, there may be specific areas that may be less prone to ingrowth, such as the high-density (cortical) femoral bone underneath the anterior flange, which may impede bone ingrowth due to its limited vascularity and bone turnover. Further research is required to investigate whether bone ingrowth will take place in inert regions with a low biological ingrowth potential such as the anterior flange region.

Another subject of debate in TKA surgeries is the alignment strategy of the components. In the studies included in this thesis, we used loading conditions that

were based on mechanical alignment for all FE models. This results in one similar alignment being investigated in all models. Alternatively, kinematic alignment has gained popularity in the last decade. Kinematic alignment is a more patientspecific alignment strategy, more adhering to the patient's anatomy compared with mechanical alignment. It is, however, currently unknown what the effect of alignment is on the fixation of (PEEK) implants. Particularly in patients with excessive varus/valgus angles, the alignment strategy may have a significant effect on the resulting joint loads that act on the TKA reconstruction. This effect may be even more pronounced in patients with a high BMI. Musculoskeletal patientspecific simulations in combination with FE-based fixation analyses may give a better understanding into the effects of alignment strategy on implant survival.

The main focus of the current thesis was on the primary fixation of cementless PEEK TKA components, while other mechanical failure mechanisms obviously also play a role, such as material failure and material wear. Tribological research on the PEEKpolyethylene articulation performed by the research group of Leeds [6] showed wear results that are comparable to CoCr, indicating PEEK is a suitable material for TKA articulating surfaces. Again, clinical trials are required to further confirm these findings in actual clinical practice.

While the current thesis investigated TKA, other knee implant designs such as a PEEK unicondylar knee arthroplasty (UKA) may be of interest in patients with clear unicompartmental osteoarthritis in the knee. Additionally, multi-compartmental arthroplasty is gaining popularity among orthopaedic surgeons, since it only replaces the part(s) of the knee joint that are damaged due to osteoarthritis. Thorough evaluation of the primary fixation of such reconstructions is required, as aseptic loosening currently is one of the main causes of UKA failure [7]. The computational methods presented here are suitable to explore the biomechanical response of such a novel design to determine whether an all-polymer or metalbacked PEEK component can be used to avoid UKA loosening.

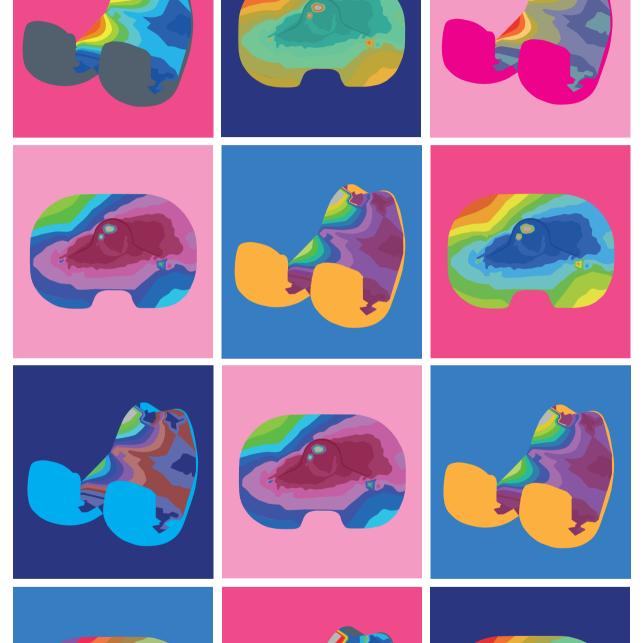
Another development in orthopaedics is the use of additive manufacturing for the production of joint replacement components. While current 3D-printed implants generally are made of titanium alloys, PEEK can be possibly made suitable for 3D printing as well in the near future, although this is a challenging process. The use of 3D printed moulds during the injection moulding process may be a more feasible solution for creating patient-specific PEEK implants. Additive manufacturing of PEEK provides flexibility in the design process, enabling the production of custom or patient-specific implant designs.

General conclusion

This thesis evaluated the effect of design- and patient-related factors on the primary fixation of a cementless PEEK implant, performing in silico preclinical testing approaches. The micromotions of PEEK femoral and tibial components generally were higher than those of CoCr femoral and titanium tibial components. However, the majority of PEEK models remained below the critical threshold values as reported in the literature that allow adequate bone ingrowth. The findings of this thesis emphasized the complicated interplay between design- and patient-related factors that affect primary fixation. Clarification of these factors will aid in the adequate design of cementless PEEK TKA components and may serve orthopaedic companies, surgeons and patients suffering from knee osteoarthritis with a new generation of total knee replacement components.

References

- Rankin, K.E., et al., Does a PEEK Femoral TKA Implant Preserve Intact Femoral Surface Strains Compared With CoCr? A Preliminary Laboratory Study. Clin Orthop Relat Res, 2016. 474(11): p. 2405-2413.
- de Ruiter, L., et al., Decreased stress shielding with a PEEK femoral total knee prosthesis measured in validated computational models. J Biomech, 2021. 118: p. 110270.
- Aro, H.T., et al., Low BMD affects initial stability and delays stem osseointegration in cementless total hip arthroplasty in women: a 2-year RSA study of 39 patients. Acta Orthop, 2012. 83(2): p. 107-14.
- Australian Orthopaedic Association National Joint Replacement Registry Hip, Knee & Shoulder Arthroplasty 2022 Annual Report. 2022.
- Sanchez, E., et al., The effect of coating characteristics on implant-bone interface mechanics. Journal of Biomechanics, 2024. 163.
- Cowie, R.M., A. Briscoe, and L.M. Jennings, The influence of cross shear and contact pressure on the wear of UHMWPE-on-PEEK-OPTIMA for use in total knee replacement. J Mech Behav Biomed Mater, 2023. 148: p. 106196.
- Montilla, F.J., et al., Unicompartmental knee arthroplasties: does the type of tibial component selected influence implant survival? Arch Orthop Trauma Surg, 2024. 144(1): p. 347-355.



Chapter 8

Nederlandse samenvatting

Het hoofddoel van deze thesis was het onderzoeken van de haalbaarheid van het gebruik van polyetheretherketone (PEEK) als materiaal voor cementloze totale knieprothese (TKP) implantaten. Eindige elementen (EE) studies zijn uitgevoerd om inzicht te krijgen in het effect van PEEK op de primaire fixatie van femorale en tibiale TKP-implantaten. Deze bevindingen zijn vergeleken met implantaten gemaakt van metaallegeringen die momenteel worden gebruikt voor TKP-implantaten, zoals kobalt-chroom (KoCr) voor femorale en titaniumlegering voor tibiale componenten. Aangezien de primaire fixatie kan worden beïnvloed door variaties in de kenmerken van het implantaatoppervlak en variaties in de kenmerken van patiënten, zijn deze beiden onderzocht in onze studies.

Het effect van interference fit en wrijvingscoëfficiënt is zowel in **hoofdstuk 2** aan de femorale zijde als in **hoofdstuk 5** aan de tibiale zijde onderzocht. In **hoofdstuk 2** werden vier verschillende waarden van interference fit (250, 500, 750 en 1000 µm) en drie verschillende waarden van wrijvingscoëfficiënt (0,5, 1,0 en 1,5) gesimuleerd in een enkel femoraal EE model, inclusief femur en femorale component met PEEK of KoCr materiaaleigenschappen. Piekkrachten die optreden tijdens joggen werden toegepast als belasting. In dit onderzoek vonden we dat de microbewegingen en interface openingen beiden gevoelig waren voor de interference fit, wrijvingscoëfficiënt en implantaatmateriaal. Er werd geconcludeerd dat de PEEK femorale component hogere microbewegingen en interface openingen genereerde in vergelijking met de KoCr femorale component. Toepassing van de hoogste interference fit in de PEEK modellen leidden tot microbewegingen die vergelijkbaar waren met de KoCr modellen met een interference fit die gangbaar is in huidige implantaat systemen.

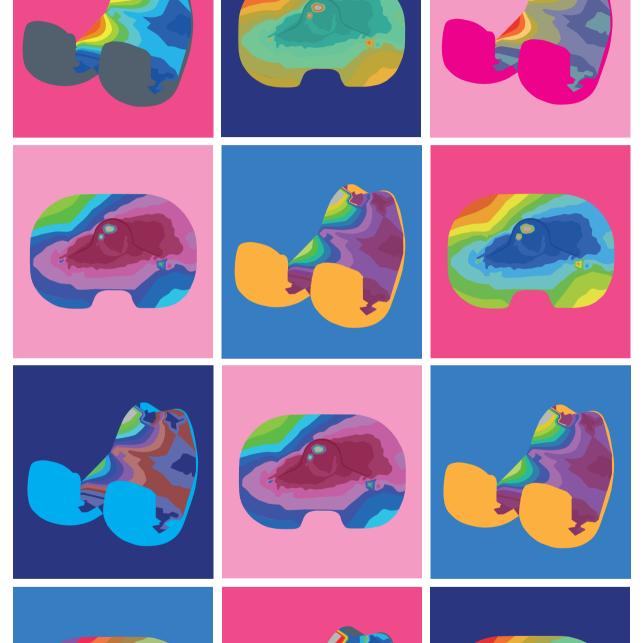
Anders dan bij de femorale component bleken de microbewegingen van het tibiale component vrij ongevoelig voor variaties in interference fit en wrijvingscoëfficiënt, zoals geconcludeerd in **hoofdstuk 5**. In dit hoofdstuk werden interference fit waarden van 500 en 750 µm en wrijvingscoëfficiënt waarden van 0,5 en 1,5 onderzocht. In dit onderzoek werden 144 EE modellen van de tibia, tibiale tray en de insert gemaakt met variaties in implantaatmateriaal (PEEK en titanium), interference fit en wrijvingscoëfficiënt. Verder werden zowel loop- als squatactiviteiten gemodelleerd. Er waren geen duidelijke verschillen te zien in de microbewegingen tussen de PEEK en titanium tibiale modellen. En, zoals eerder vermeld, hadden noch de interference fit noch de wrijvingscoëfficiënt een grote invloed op de microbewegingen.

In hoofdstuk 3 werd het ontwerp van het PEEK femorale implantaat aangepast door een titanium inlay toe te voegen aan de binnenzijde van het implantaatoppervlak, aangezien dit de primaire fixatie zou kunnen verbeteren terwijl de gunstige stijfheidseigenschappen behouden blijven. Dat onderzoek onderzocht het effect van de dikte van de inlay en variaties in stijfheid op de primaire fixatie en de periprothetische botspanningen. Daarom werd het EE model van het femur inclusief femorale component van hoofdstuk 2 gebruikt, inclusief vijf variaties in titanium inlay. Als uitkomstmaten hebben we de microbewegingen en de spanningsenergiedichtheid gekwantificeerd. Het toevoegen van een inlav leidde tot een algemene afname van microbewegingen in vergelijking met een PEEK component zonder inlay. Bovendien hadden de inlay varianten allemaal slechts een gering effect op de botspanningen. Er werd daarom geconcludeerd dat de toevoeging van een titanium inlay zou kunnen leiden tot een vermindering van de microbewegingen zonder dat dit aanzienlijke invloed heeft op de gunstige eigenschappen van PEEK met betrekking tot stress-shielding.

Hoofdstukken 4 en 6 beschrijven de resultaten van populatiestudies van respectievelijk het femorale en tibiale model. Beide studies gaven inzicht in de primaire fixatie van PEEK implantaten in een cohort van computationele modellen met variërende patiëntkenmerken. In hoofdstuk 4 werden 280 EE-modellen van 70 femurs gemaakt met variërend implantaatmateriaal (PEEK en KoCr) en variërende opgelegde belastingen. Implantaat-specifieke tibiofemorale en patellofemorale contactkrachten en aangrijpingspunten van een loop- en squatactiviteit afgeleid van een musculoskeletaal model werden toegepast op de modellen. Over het algemeen genereerden de PEEK modellen grotere piek microbewegingen dan de KoCr modellen. Bovendien werd geconcludeerd dat de microbewegingen van alle modellen significant toenamen met BMI, terwijl geslacht en leeftijd geen effect leken te hebben. Daarnaast bevestigden de variaties in grootte van de microbewegingen tussen de onderzochte patiënt-cases binnen de gesimuleerde populatie de noodzaak van op populatie gebaseerde modellering.

In **hoofdstuk 6** werden in totaal 296 EE modellen van 74 tibiae gemaakt met PEEK of titanium materiaaleigenschappen en implantaat-specifieke belastingen voor loop- of squatbelastingen die berekend werden middels een spierskeletmodel. Net als in hoofdstuk 4 aan de femorale zijde werd geconcludeerd dat de PEEK modellen over het algemeen hogere piek-microbewegingen genereerden dan de titaniummodellen. De microbewegingen van alle tibiale modellen namen significant toe met BMI, terwijl geslacht en leeftijd de microbewegingen nauwelijks beïnvloedden.

Deze thesis evalueerde het effect van ontwerp en patiënt gerelateerde factoren op de primaire fixatie van een cementloos PEEK implantaat door in silico preklinische testen uit te voeren. De microbewegingen van femorale en tibiale PEEK componenten waren over het algemeen hoger dan die van KoCr femorale en titanium tibiale componenten. De microbewegingen van de meerderheid van de PEEK modellen bleef echter onder de kritische drempelwaarden zoals gerapporteerd in de literatuur die voldoende botingroei mogelijk maken. De bevindingen van dit proefschrift benadrukten de gecompliceerde wisselwerking tussen ontwerp en patiënt gerelateerde factoren die van invloed kunnen zijn op de primaire fixatie. In kaart brengen van deze factoren zal helpen bij het adequaat ontwerpen van cementloze PEEK TKP componenten wat ten goede komt aan orthopedische bedrijven, chirurgen en patiënten met knieartrose.



Appendix

Research Data Management
PhD Portfolio
Curriculum Vitae
Dankwoord

Research Data Management

The research data and a regularly made back-up of the research data have been archived on a secured department-specific network drive of the Radboud University Medical Centre (O:\Projects\R1681-Invibio). Meta files have been added to the data sets to make the data interpretable. The network drive is only accessible by selected staff members of the Orthopaedic Research Laboratory and will be available upon reasonable request by contacting the staff secretary of the Orthopaedic Research Laboratory at the Radboud University Medical Centre (secretariaatstaf.orthop@radboudumc.nl) or the corresponding author. The data will be saved for at least 15 years after termination of the study concerned and can therefore be reused in this time period. Published data is available upon request to the corresponding author. Furthermore, the scientific articles in this thesis have been published open access, in line with the institutional preference.

PhD Portfolio

Department: Orthopaedic Research Laboratory PhD period: **01/01/2019 – 31/12/2022** PhD Supervisor(s): **Prof. N. Verdonschot** PhD Co-supervisor(s): **Dr. D. Janssen, Dr. T. Bitter**

Training activities	Hours
Courses	
- RIHS - Introduction course for PhD candidates (2019)	15.00
- HyperMesh Modelling for Finite Element Simulation (2019)	8.40
- Radboudumc - Introduction day (2019)	6.00
- Projectmanagement for PhD candidates (2019)	56.00
- Radboudumc - Scientific integrity (2020)	20.00
- Scientific Integrity for PhD candidates (2020)	28.00
- Workshop Supervising your students (2020)	0.10
- RU - Statistics for PhD's by using SPSS (2022)	60.00
Conferences	
- RIHS PhD Retreat (2019)	20.00
- ISTA 2020 - Online (2020)	8.00
- European Society of Biomechanics 2022 - Porto (2022) (oral presentation)	40.00
- World Congress of Biomechanics (online) (2022) (oral presentation)	10.00
- International Society for Technology in Arthroplasty 2022 - Maui (2022) (poster presentation)	40.00
- Orthopaedic Research Society 2023 - Dallas (2023) (oral presentation)	40.00
- European Society of Biomechanics 2023 - Maastricht (2023) (oral presentation)	40.00
Other	
- Workshop committee member RIHS PhD council (2019)	0.50
- Secretary RIHS PhD council (2020)	1.00
Teaching activities	
Lecturing	
- Minor Moving Questions Journal Club (2019-2022)	40.00
- Orthopaedic Biomechanics in Motion (2020-2022)	90.00
- Bachelorcongres BMW (2021-2022)	8.00
- Belasting & Belastbaarheid (2021-2022)	28.00
Supervision of internships	
- MSc Biomedical Engineering Internship - Evi van den Kieboom - 3 months (2020)	28.00
- MSc Biomedical Engineering Internship and Graduation - Carlos Galdamez - 12 months (2021)	112.00
- MSc Biomedical Engineering Internship - Emma Roubaud - 3 months (2022)	28.00
- MSc Biomedical Engineering Internship - Inger van Langen - 4 months (2022)	37.00
Total	764.00

Curriculum Vitae



Corine Post was born on the 8th of June 1993 in Hilversum. She obtained in 2011 her VWO diploma from the Gemeentelijk Gymnasium in Hilversum. In 2015, she finished her bachelor's Degree in Life, Science & Technology, with a major in Biomedical Engineering at the University of Groningen. Hereafter, she started the master Biomedical Engineering at the University of Groningen. For her master thesis, she completed an internship at the Orthopaedic Research Laboratory in Radboudumc, working on a solution for improving trochleoplasty procedures.

In 2017, she started as a Junior Researcher at the University of Twente working on improving the diagnosis of the problematic knee prosthesis using low-field MRI. After this, in 2019, she started as a PhD candidate at the Orthopaedic Research Laboratory in Nijmegen focusing on the assessment of the primary fixation of a cementless PEEK knee prosthesis. Currently, she works as a postdoctoral researcher on personalized osteoarthritis knee models at Universitat Pompeu Fabra in Barcelona, Spain.

Dankwoord

Dit proefschrift was nooit tot stand gekomen zonder de aanwezigheid en hulp van alle lieve mensen om mij heen. Woorden doen eigenlijk altijd te kort, en er bestaat een risico dat ik iemand ga vergeten, maar toch ga ik een poging wagen om iedereen die om mij heen was afgelopen jaren te bedanken.

Beste Nico, nog heel goed weet ik de allereerste dag dat ik jouw kantoor binnenliep om de opties voor een afstudeeronderzoek bij het ORL te bespreken, zenuwachtig met mijn aantekeningenboek onder mijn arm. Wat ik toen niet wist, was dat ik de zeven opvolgende jaren nog met jou zou mogen samenwerken. Wat heb ik veel van jou mogen leren gedurende deze periode. Niet alleen over het kritisch blijven tijdens het onderzoeken, maar ook over het oog houden voor het leven buiten het onderzoek, want dat is wat jij altijd doet. De eerste vraag tijdens een overleg was vaak iets in de trant van "en, wordt er nog getoeterd komend weekend?". Na zo'n overleg voelde ik me altijd weer even gezien, maar ook uitgerust met een lading nieuwe ideeën om onze onderzoeksvragen te tackelen. Toen jij bij mijn concert kwam kijken zei ik tegen iedereen trots "mijn professor is er ook!" Ik had geen betere promotor aan mijn zijde kunnen wensen tijdens deze PhD. Bedankt voor alles!

Beste Dennis, nog steeds baal ik dat al onze pogingen jou uit te roepen tot supervisor van het jaar van het Radboudumc niet tot de daadwerkelijke nominatie hebben geleid. Wel zegt dit alles over hoe jij voor mij afgelopen jaren een begeleider bent geweest. Na twee stappen in de overlegruimte had jij al door hoe ik op dat moment in de strijd zat: helemaal vastgelopen met een eindige elementen simulatie, te kritisch over wat ik in een paper aan het opschrijven was, euforisch over een werkende simulatie of gewoon even klaar met onderzoeken. Jouw vraag "hoe gaat het?" beantwoordde ik in het begin vaak, heel serieus, over hoe het met het onderzoek gaat. "Nee, ik bedoel eigenlijk hoe het met jou gaat" zei jij dan. De overleggen met jou ga ik missen; vol (flauwe) grappen, goede adviezen (ook over films) en pragmatische oplossingen, precies afgemeten op wat ik nodig had, want jij kende mij al snel meer dan goed genoeg. De congressen waren altijd een feest, was de ene kroeg dicht, dan was er altijd plano B. Bedankt voor de, in alle opzichten, ontzettend goede tijd bij het ORL! Mahalo!

Beste Thom, tijdens mijn PhD kreeg jij een steeds belangrijkere rol in de begeleiding. Ik weet niet precies hoeveel uren wij samen hebben gestaard naar Marc Mentat errors en vreemde simulatie uitkomsten, maar dat zijn er veel. Toch zijn we er keer op keer weer uitgekomen en dat is vooral aan jou te danken. Daarnaast vond ik het ook wel prettig, als ik een nogal korte eerste versie van een paper naar jullie had opgestuurd, te bedenken dat jij het nog veel korter zou hebben opgeschreven. Als ik jou even nodig had, was je er altijd, en dat is heel waardevol, bedankt!

Dear Adam, what made this PhD very special, was the connection with industry via you. Our monthly meetings were not only very fruitful and informative, I also greatly enjoyed these meetings. Although an industrial-academic collaboration is sometimes challenging, we have always been able to take into consideration both interests. Besides this, I also received many recommendations from you and Dennis for good movies. We, unfortunately, only had the chance to eat a "broodje kip" together once, because it has been a true pleasure to work with you. Thank you for all our adequate meetings!:)

Leden van de manuscriptcommissie, Prof. Dr. Ir. Sander Leeuwenburgh, Prof. Dr. Paul Jutte en Prof. Dr. Ir. Bart Verkerke, dank voor het lezen en beoordelen van dit boekwerk.

Jasper, Erim en Jurre, een PhD op zichzelf is best leuk, maar het op kantoor zitten met zulke fijne vrienden, maakt het nog veel leuker. Lieve Jasper, een van de ORLmannen van de goede kant. Als het even te veel naar mijn bol steeg, was jij er (en nog steeds) met een goed gesprek, goede adviezen, een pakje roosvicee of een slaapplek. Lieve Erim, onze goede gesprekken en huppels over de gang zitten allemaal verwerkt in deze PhD. Lieve Jurre, keek ik naar rechts, dan zat jij daar, vaak in voor een echte Jurre grap. Ik wil jullie alle drie bedanken voor de ontzettend fijne tijd die ik nog zeer regelmatig mis. Ik ben blij dat we elkaar nu nog steeds regelmatig spreken en zien en hoop dat we dat ook in de toekomst zullen blijven doen!

Dan waren er natuurlijk ook nog de dames van "de andere kant"; onder andere Erin, Miriam, Mirthe en Dineke, dank voor alle etentjes, feestjes, (kokos)koffies, foto's van muhammara ongelukjes en heel veel gezelligheid!

Hans, jouw verdediging was een feestelijke dag, maar voor mij persoonlijk ook een sippe dag. Het was het officiële einde van onze samenwerking die we gehad hebben tijdens de studie, stages en PhD. In die tijd heb ik veel geleerd van jou; van jouw kordate aanpak, kritische blik, tot oog voor detail. Bedankt voor al onze goede gesprekken en wandelingetjes!

Florieke, na jouw aanmoediging bij de Vierdaagse samen met Jens en Marleen volgden de spraakberichten en de speelmomenten. Ik weet niet wie het leuker vond om van de glijbaan te gaan, Jens of ik. Ook voelde ik me vereerd toen jij vertelde dat Jens voor Spanje juichte met de EK finale, "omdat Corine in Spanje woont". Hiernaast wil ik je natuurlijk ook bedanken voor alle fijne gesprekken, onderwijsactiviteiten en BOS-samenwerkingen op werk!

Beste Richard, zo blij was ik toen ik even tussen het computeren door met jou in het lab de driepuntsbuigtesten mocht doen. Een geoliede machine waren we (ondanks dat de eerste paar stiften met 0.1 mm punt gelijk kapotgingen, dat was mijn fout en jij lachte mij uit...). Bedankt voor al jouw hulp en gezelligheid!

Beste Sebastiaan, tijdens de online meetings met Dennis sloot jij af en toe (vaak ongevraagd, maar zeker gewenst) aan om kritische, klinische vragen te stellen. Deze vragen en onze overleggen over de klinische kant van het onderzoek, hebben dit onderzoek naar een hoger level getild, bedankt!

Beste Max, als de matlabnood hoog was, was jij daar! Nog steeds, als ik een script verbeter naar een versie met een nauwkeurigere uitkomst, heb ik de neiging om het script "vervvervvervaccurate" te noemen. Naast de matlabhulp, was iji er ook voor een potje beachvolleybal en gesprekken over de zin van het leven, veel dank daarvoor!

Dear Evi, Carlos, Emma and Inger, thank you for your contribution to this thesis and the courage doing an internship under my supervision. I have learned a lot from you, thank you!

Ook alle andere ORL collega's wil ik graag bedanken voor alle hulp en ontzettend veel gezelligheid. De leuke BBQ's en uitjes zoals golfen, suppen, boulderen en curlen waren erg gezellig en mis ik nu al.

Lieve Neeke en Maaike, ik ben zo ontzettend blij deze dag te mogen beleven met jullie aan mijn zijde als paranimfen. Bedankt dat jullie dat voor mij willen doen! Lieve Neeke, wat ben ik dankbaar voor onze band en dat we altijd alles (maar dan ook écht alles) kunnen bespreken samen. Ik gloei van trots als ik denk aan hoe goede moeder jij bent voor Lauren. Lieve Maaike, begonnen als mijn BME-maatje, getransformeerd tot levensmaatie, door dik en dun. We hoeven elkaar maar aan te kijken en we weten hoe laat het is (vaak betekent dit tijd voor bier, of we hebben honger). Bedankt allebei voor jullie waardevolle vriendschap!

Lieve Esmee, Anne, Kirsten en Tineke, van woeste woensdag tot 's ochtends brak in de collegezaal zitten na 3 uur slaap. Een vriendschap die ruim 13 jaar geleden begonnen is en die we nog steeds in stand houden met onder andere onze dagjes en weekenden weg. Ik ben heel trots op hoe eenieder van jullie haar weg aan het vinden is en ik ben heel blij met onze waardevolle vriendschap!

En dan (een selectie van) alle muziekvrienden; Reinier, Lisa, Petra, Peter-Jos, Florance, Wendy en Sofanne. Wat allemaal is begonnen met toeteren en biertjes na afloop in verschillende orkesten, is uitgegroeid tot hele fijne vriendschappen, dankjulliewel!

Lieve meiden van Allez, en dan specifiek Mad, Mar, An en Twan, wat ben ik blij dat wij elkaar in alle hectiek gevonden hebben. Zodra ik jullie zie en spreek, is het gelijk weer als vanouds. Jullie kennen mij als geen ander en ik vind het een heel fijn idee dat ik altijd bij jullie terecht kan. Bedankt!

Lieve An, Veer, Tess en Kiek, ik durf het bijna niet te zeggen, maar wij kennen elkaar al bijna 20 jaar. We zien elkaar niet heel regelmatig, maar als we elkaar zien, voelt het weer als even terug naar de middelbare school. Het is absoluut door jullie, dat dit zo'n fijne tijd was.

Aan alle vrienden van Thomas: de carnavalsvieringen, festivals, avonden samen eten en andere uitjes met jullie zijn altijd een feestje! Ik heb mij nog nooit zo snel thuis gevoeld in een nieuwe groep, bedankt!

Lieve Xandra, Jaap, Isabelle en Rick, bedankt voor jullie warmte en dat ik zo welkom ben bij jullie.

Lieve Christiaan, goed voorbeeld doet volgen! Ik ben trots op hoe jij het leven aangaat en alles precies op jouw manier doet. Wel heb ik een wens, wanneer gaan we eindelijk een keer samen dat Mahler concertje geven? Dear Ingrid (and Marie), Christiaan must be really happy with you as girlfriend (and dog).

Lieve oma, vaak betrap ik mezelf erop dat ik mensen verbeter als ze een grammaticale fout maken, net zoals u dat vroeger bij mij deed: "Je kunt jezelf niet irriteren, wel ergeren". Als ik u een appje stuur, kijk ik altijd uit naar uw reactie vol grapjes, zelfspot en updates over de kippen, kat en vissen. En uw interesse in mijn "veel interessantere leven", want die blijft altijd. Bedankt!

Lieve papa en mama, we spreken elkaar niet altijd even veel, maar het weten dat jullie er altijd zijn, is onbetaalbaar. Bedankt voor alles wat jullie mij geleerd hebben en nog steeds leren.

En dan jij, lieve, lieve Thomas, het allermooiste dat deze PhD mij heeft gegeven is niet dit boekje, dat ben jij. Ik had nooit verwacht iemand te vinden die mij zoveel zou geven als dat jij doet en bij wie ik zo mezelf kan zijn. Bij jou zijn betekent een gevoel van vakantie, ook al zitten we midden in een drukke werkweek. Bedankt voor alle nerdgesprekken voor als een van ons weer een error heeft hoe de interference fit ook alweer werkt, maar ook voor alle avonturen, liefde en waardevolle gesprekken. Ik ben ontzettend trots op jou en ik kijk uit naar alles wat op ons pad gaat komen. I love you!



